

Gross N₂O emission and gross N₂O uptake in temperate cropland agroforestry and monoculture systems



Dissertation

to attain the doctoral degree Doctor of Philosophy (Ph.D.)

of the Faculty of Forest Sciences and Forest Ecology

Georg-August-Universität Göttingen

Submitted by

Jie Luo

Born on the 16th June, 1991, in Chongqing, China

Göttingen, February, 2022

1. Referee: Dr. Marife D. Corre
2. Referee: Prof. Dr. Klaus Dittert

Date of oral examination: 12.01.2021

Table of Contents

Summary	3
Zusammenfassung	5
Chapter 1: General Introduction	9
1.1. Gross N ₂ O emission and uptake in soils	9
1.2. Gross N ₂ O emission and uptake in cropland agroforestry and monoculture	11
1.3. Gross N ₂ O emission and uptake in contrasting agroforestry systems and at depths	13
1.4. Aims and hypothesis	14
1.5. References	15
Chapter 2: Reduced Soil Gross N₂O Emission driven by Substrates rather than Denitrification Gene Abundance in Cropland Agroforestry and Monoculture	29
2.1. Abstract	30
2.2. Introduction	30
2.3. Materials and Methods	34
2.3.1. Study sites and experimental design	34
2.3.2. Measurement of gross N ₂ O emission and uptake	38
2.3.3. Soil controlling factors	38
2.3.4. Quantification of denitrification genes in soil	41
2.3.5. Statistical analysis	42
2.4. Results	43
2.4.1. Gross N ₂ O fluxes	43
2.4.2. Soil variables	48
2.4.3. Denitrification gene abundance	51
2.4.4. Temporal relationships between gross N ₂ O fluxes and soil factors	54
2.5. Discussion	57
2.5.1. Gross N ₂ O emissions	57
2.5.2. Denitrification gene abundance	59
2.5.3. Gross N ₂ O uptake	60
2.5.4. Implications	60
2.6. Acknowledgments	61
2.7. References	61
2.8. Appendix	69
Chapter 3: Soil gross N₂O emission and uptake under two contrasting agroforestry systems (riparian tree buffer vs. trees of alley cropping)	77
3.1. Abstract	78
3.2. Introduction	79
3.3. Materials and methods	81
3.3.1. Site description and soil sampling	81
3.3.2. Measurement of gross N ₂ O emission and uptake	82
3.3.3. Soil characteristics	83
3.3.4. Quantification of bacteria, fungi, and denitrification genes in soil	85

3.3.5. Statistical analyses.....	86
3.4. Results.....	87
3.4.1. Soil N ₂ O flux dynamics.....	87
3.4.2. Soil controlling factors.....	89
3.4.3. Microbial community and denitrification gene abundance.....	91
3.4.4. Factors controlling gross N ₂ O fluxes.....	94
3.5. Discussion.....	97
3.5.1. Gross N ₂ O fluxes in different agroforestry systems.....	97
3.5.2. Gross N ₂ O fluxes at depths.....	99
3.5.3. Coupling between gross N ₂ O fluxes and microbial population size.....	100
3.6. Acknowledgments.....	101
3.7. References.....	101
3.8. Appendix.....	105
Chapter 4: Synthesis	111
4.1. Key findings of this thesis.....	111
4.1.1. Gross N ₂ O fluxes in temperate cropland agroforestry and monoculture.....	111
4.1.2. Gross N ₂ O fluxes in contrasting agroforestry systems.....	111
4.2. Linking gross N ₂ O fluxes with functional gene abundance.....	112
4.3. The relationships among gross N ₂ O emission, gross N ₂ O uptake, and net N ₂ O flux.....	113
4.4. Net N ₂ O flux.....	113
4.5. Outlook.....	114
4.6. References.....	115
Acknowledgment	117

Summary

Nitrous oxide (N₂O) is a powerful greenhouse gas and also the remaining threat to the ozone layer. N₂O emission is mainly from cropland accounting for 82% of the global N₂O increase, which is of great concern for policymakers making strategies of mitigating N₂O emissions. One of such strategies is agroforestry systems which integrate trees into cropland and are considered as environmentally-friendly ecosystems, in particular in greenhouse gas mitigation (e.g. N₂O emissions). The net balance of N₂O flux is constrained by gross N₂O emissions and uptake. However, we are still struggling to fully understand the complexity of gross N₂O emissions and uptake due to its spatial- and temporal variation. No systematic comparison of gross N₂O fluxes was conducted between cropland agroforestry and monoculture. Besides, N₂O produced and consumed are not only in topsoil but also in subsoil and there is lacking information about how gross N₂O emissions and uptake vary at depths in different types of agroforestry systems.

The first study aimed to assess the impact of land-use change on gross N₂O emissions and uptake and their associated controls between cropland agroforestry and monoculture. The study was conducted at three sites in Germany, of which two sites had paired cropland agroforestry and monoculture on a loam Calcaric Phaeozem soil and a clay Vertic Cambisol soil, and one site was a cropland monoculture on a sandy Arenosol soil. Gross N₂O emissions and uptake were monthly measured by using the ¹⁵N₂O pool dilution technique over two growing seasons (2018 - 2019). Our results showed that soil gross N₂O emissions from the area-weighted tree and crop rows in the agroforestry did not differ from monoculture. Nonetheless, the unfertilized tree rows showed the lowest gross N₂O emissions. Although tree rows only occupied 20% in the agroforestry, annual gross N₂O emissions in the top 5-cm soil decreased by 6% to 36% in the agroforestry compared to monoculture. Gross N₂O emissions were influenced by soil mineral N, available C, and moisture content rather than by denitrification gene abundance. Soil gross N₂O uptake was highest in the tree row and decreased with distance into crop rows. The agroforestry tree row increased annual gross N₂O uptake in the top 5-cm soil by 27% to 42% compared to monoculture. In the tree row, soil gross N₂O uptake correlated with *nirK* gene abundance which, in turn, was correlated with *nosZ* clade II that was related to low mineral N-to-available C ratios.

The second study aimed to compare gross N₂O emissions and uptake between riparian tree buffer and tree row of alley cropping system, and between depths (0 – 5 vs. 40 – 60 cm), and to elucidate their associated abiotic and biotic controls. This study was conducted at two contrasting agroforestry systems in Germany: riparian tree buffer and tree row of the alley cropping system. We quantified gross N₂O emissions and uptake using the ¹⁵N₂O pool dilution technique in early spring (April), spring (June), summer (August), and fall (October). Our results showed that riparian tree buffer had higher gross N₂O emissions and uptake in topsoil (0 – 5 cm) than the tree row of alley cropping but such differences were not observed in subsoil (40 – 60 cm). Although gross N₂O emissions and uptake did not differ between the two depths in each agroforestry system, we observed a hot moment, i.e. early spring, for gross N₂O emissions in topsoil of riparian tree buffer, with a large source of N₂O observed. Gross N₂O emissions were mainly controlled by mineral N, biodegradable organic carbon, and water-filled pore space rather than microbial population size between the two agroforestry systems and depths. Gross N₂O uptake in topsoil was driven by available carbon and *nirK* gene abundance across agroforestry systems. But subsoil showed a sink of N₂O due to low mineral N. Gross N₂O uptake in subsoil was affected by soil temperature in each agroforestry system, indicating positive feedback of global warming.

Overall, this research provides new insights into mitigation of N₂O emissions from soil to atmosphere after conversion of cropland monoculture to agroforestry and also provides field-based rates of gross N₂O fluxes at depths in contrasting agroforestry systems. Our research provides the first year-round quantification of gross N₂O emission and uptake using ¹⁵N₂O pool dilution for cropland agroforestry and monoculture, with key implications for support on greenhouse gas regulation function for policy implementation of agroforestry. Our findings emphasize that adjusting the tree and crop areal coverages of agroforestry can further optimize the benefits of agroforestry in reducing emissions and increasing uptake of N₂O in soils. As discussed in the synthesis chapter, future studies should increase the measurement frequency of gross N₂O fluxes at depths to capture hot moments and spots especially in the riparian tree buffer, and further better constrain the contribution of subsoil to the ecosystem N loss although this area is relatively small.

Zusammenfassung

Distickstoffoxid (N_2O) ist ein starkes Treibhausgas und auch die verbleibende Gefahr für die Ozonschicht. Die N_2O -Emissionen stammen hauptsächlich von Ackerflächen, auf die 82 % des weltweiten N_2O -Anstiegs entfallen, was für politische Entscheidungsträger, die Strategien zur Eindämmung der N_2O -Emissionen entwickeln, von großer Bedeutung ist. Eine dieser Strategien ist die Agroforstwirtschaft, bei der Bäume in Ackerflächen integriert werden und die als umweltfreundliches Ökosystem angesehen wird, insbesondere im Hinblick auf die Eindämmung von Treibhausgasen (z.B. N_2O -Emissionen). Die Nettobilanz des N_2O -Flusses wird durch die Brutto- N_2O -Emissionen und N_2O -Aufnahme eingeschränkt. Jedoch haben wir immer noch Mühe, die Komplexität der Brutto- N_2O -Emissionen und -Aufnahme aufgrund ihrer räumlichen und zeitlichen Variation vollständig zu erfassen. Es wurde kein systematischer Vergleich der Brutto- N_2O -Flüsse zwischen Ackerland-Agroforst und Monokultur durchgeführt. Außerdem wird N_2O nicht nur im Oberboden, sondern auch im Unterboden produziert und verbraucht, und es fehlen Informationen darüber wie die Brutto- N_2O -Emissionen und -Aufnahme in den verschiedenen agroforstwirtschaftlichen Systemen in der Tiefe variieren.

Die erste Studie hatte zum Ziel, die Auswirkungen von Landnutzungsänderungen auf die Brutto- N_2O -Emissionen und N_2O -Aufnahme sowie die damit verbundenen Regulierungen zwischen Ackerland-Agroforst und Monokultur zu bewerten. Die Studie wurde an drei Standorten in Deutschland durchgeführt, wobei an zwei Standorten Ackerland-Agroforst und Monokultur auf einem lehmigen Calcaric Phaeozem-Boden und einem lehmigen Vertic Cambisol-Boden angesiedelt waren und an einem Standort eine Monokultur auf einem sandigen Arenosol-Boden betrieben wurde. Die Brutto- N_2O -Emissionen und die Aufnahme wurden monatlich mit der $^{15}N_2O$ -Pool-Verdünnungstechnik über zwei Vegetationsperioden (2018 - 2019) gemessen. Unsere Ergebnisse zeigten, dass sich die Brutto- N_2O -Emissionen des Bodens der flächengewichteten Baum- und Ackerstreifen im Agroforst nicht von der Monokultur unterschieden. Dennoch wiesen die ungedüngten Baumstreifen die niedrigsten Brutto- N_2O -Emissionen auf. Obwohl der Anteil der Baumstreifen im Agroforstsystem nur 20 % betrug, gingen die jährlichen Brutto- N_2O -Emissionen in den obersten 5 cm des Bodens im Agroforst im Vergleich zur Monokultur um 6 % bis 36 % zurück. Die Brutto- N_2O -Emissionen wurden eher

durch den mineralischen Stickstoff, den verfügbaren Kohlenstoff und den Feuchtigkeitsgehalt des Bodens als durch die Häufigkeit der Denitrifikationsgene beeinflusst. Die Brutto-N₂O-Aufnahme des Bodens war im Baumstreifen am höchsten und nahm mit dem Abstand vom Baumstreifen in den Ackerstreifen ab. Der agroforstliche Baumstreifen erhöhte die jährliche Brutto-N₂O-Aufnahme in den obersten 5 cm des Bodens um 27 % bis 42 % im Vergleich zur Monokultur. Im Baumstreifen korrelierte die Brutto-N₂O-Aufnahme des Bodens mit der Häufigkeit des nirK-Gens, das wiederum mit der nosZ-Klade II korreliert war, die mit einem niedrigen Verhältnis von mineralischem N zu verfügbarem C zusammenhängte.

Die zweite Studie zielte darauf ab, die Brutto-N₂O-Emissionen und N₂O-Aufnahme zwischen Baum-Uferrandstreifen und Baumstreifen des Alley cropping Systems sowie zwischen den Tiefen (0 – 5 vs. 40 – 60 cm) zu vergleichen und die damit verbundene abiotische und biotische Regulation zu klären. Diese Studie wurde an zwei unterschiedlichen Agroforstsystemen in Deutschland durchgeführt: Baum-Uferrandstreifen und Baumstreifen des Alley cropping Systems. Wir quantifizierten die Brutto-N₂O-Emissionen und -Aufnahme mithilfe der ¹⁵N₂O-Pool-Verdünnungstechnik im zeitigen Frühjahr (April), im Frühjahr (Juni), im Sommer (August) und im Herbst (Oktober). Unsere Ergebnisse zeigten, dass die Uferrandstreifen im Oberboden (0 – 5 cm) höhere Brutto-N₂O-Emissionen und -Aufnahme aufwiesen als die Baumstreifen im Alley cropping. Im Unterboden (40 – 60 cm) wurden solche Unterschiede jedoch nicht beobachtet. Obwohl sich die Brutto-N₂O-Emissionen und -Aufnahme zwischen den beiden Tiefen in jedem Agroforstsystem nicht unterschieden, beobachteten wir einen kritischen Moment, d.h. das frühe Frühjahr, für die Brutto-N₂O-Emissionen im Oberboden des Uferrandstreifens, wobei eine große N₂O-Quelle beobachtet wurde. Die Brutto-N₂O-Emissionen wurden hauptsächlich durch mineralischen Stickstoff, biologisch abbaubaren organischen Kohlenstoff und den mit Wasser gefüllten Porenraum gesteuert und nicht durch die Größe der mikrobiellen Populationen in den beiden Agroforstsystemen und Tiefen. Die Brutto-N₂O-Aufnahme im Oberboden wurde durch den verfügbaren Kohlenstoff und die Häufigkeit von nirK-Genen über die Agroforstsysteme bestimmt. Der Unterboden war jedoch aufgrund des geringen mineralischen Stickstoffs eine N₂O-Senke. Die Brutto-N₂O-Aufnahme im Unterboden wurde in jedem Agroforstsystem durch die Bodentemperatur beeinflusst, was auf eine positive Rückkopplung der globalen Erwärmung hindeutet.

Insgesamt bietet diese Forschungsarbeit neue Einblicke in die Verringerung der N₂O-Emissionen aus dem Boden in die Atmosphäre nach der Umstellung von Ackerbau-Monokulturen auf Agroforstwirtschaft und liefert auch feldbasierte Raten der Brutto-N₂O-Flüsse in der Tiefe in unterschiedlichen Agroforstsystemen. Unsere Forschung liefert die erste ganzjährige Quantifizierung von Brutto-N₂O-Emissionen und -Aufnahme unter Verwendung von ¹⁵N₂O-Pool-Verdünnungstechnik für Agroforst und Monokulturen auf Ackerland, mit wichtigen Implikationen für die Unterstützung der Treibhausgasregulierungsfunktion für die politische Umsetzung von Agroforstwirtschaft. Unsere Ergebnisse unterstreichen, dass eine Anpassung der Baum- und Ackerflächen in der Agroforstwirtschaft die Vorteile der Agroforstwirtschaft bei der Verringerung der Emissionen und der Erhöhung der N₂O-Aufnahme in den Böden weiter optimieren kann. Wie im zusammenfassenden Kapitel erörtert, sollten künftige Studien die Messhäufigkeit der Brutto-N₂O-Flüsse in der Tiefe erhöhen, um kritische Momente und Flecken vor allem im Ufergehölzstreifen zu erfassen und den Beitrag des Unterbodens zum Stickstoff-Verlust des Ökosystems besser einzugrenzen, auch wenn dieser Bereich relativ klein ist.

Chapter 1

General Introduction

1.1. Gross N₂O emission and uptake in soils

Nitrous oxide (N₂O) is the third most important anthropogenic greenhouse gas after carbon dioxide (CO₂) and methane, resulting in the radiative forcing of Earth's climate. It is also a long-lived stratospheric ozone-depleting substance with a current atmospheric lifetime of 116 ± 9 years (Prather et al., 2015), which contributes to a global warming potential 298 times greater than a CO₂-equivalent basis (Montzka et al., 2011). The atmospheric N₂O concentration has increased by over 20% from 270 ppb in 1750, to 331 ppb in 2018, with a current rate of increase estimated at 2% per decade (Tian et al., 2020). In the coming decades, N₂O emissions are predicted to continue to increase due to the growing population with a greater demand for food (Godfray et al., 2010). Furthermore, the recent growth in N₂O emissions exceeds some of the highest projected emission scenarios (Davidson, 2012), emphasizing the importance to mitigate N₂O emissions. Although the measurements of net N₂O flux have been intensively investigated, there's little information about gross N₂O production and consumption, and their associated controls in terrestrial ecosystems.

Soils are the predominant sources of N₂O emissions, with 6.6 (3.3 – 9.0) Tg N yr⁻¹ from natural soils and 4.1 (1.7 – 4.8) Tg N yr⁻¹ from agricultural soils (Ciais et al., 2013). Primary sources of N₂O come from processes of microbial denitrification and nitrification, however, the only known sink of N₂O is the final step of denitrification, i.e., the reduction of N₂O to N₂. Denitrification is of outstanding importance for closing the nitrogen (N) cycle, and agricultural soils are hotspots for denitrification, of which rates in agricultural soils are likely to be about one order of magnitude larger than in natural soils (Butterbach-Bahl and Dannenmann, 2011). However, simultaneously measuring N₂O and N₂ is challenging as it is difficult to quantify the N₂ production because of its high background concentration in the atmosphere and the high spatiotemporal variability (Groffman et al., 2006). There are available methods for measuring

N_2O and N_2 , like acetylene (C_2H_2) inhibition and ^{15}N tracer but these methods have their limitations. For example, the C_2H_2 inhibition method has been documented by underestimation of denitrification caused by disturbance of the physical setting of the process while the ^{15}N tracer technique did not show such bias but appeared relatively limited in their adoption (Groffman et al., 2006). Additionally, these methods are all predominantly laboratory-based. Given these weaknesses of measuring denitrification, Yang et al. (2011) proposed the $^{15}\text{N}_2\text{O}$ pool dilution ($^{15}\text{N}_2\text{O}$ PD) technique, referring to adding $^{15}\text{N}_2\text{O}$ into the intact static chamber headspace and measuring the changes in $^{14}\text{N}_2\text{O}$ and $^{15}\text{N}_2\text{O}$ with time. Currently, this is the only method that provides much-needed field measurements of gross N_2O emission and uptake without intensive soil disturbance (Wen et al., 2017; Yang and Silver, 2016a; Yang et al., 2011). Nonetheless, this technique may not capture the total N_2 production, like in anaerobic soil microsites (Wen et al., 2016; Yang et al., 2011) and thus Wen et al. (2016) change the terms ‘gross N_2O production’ and ‘gross N_2O consumption’ into ‘gross N_2O emission’ and ‘gross N_2O uptake’, respectively. Gross N_2O emission elucidates that both the N_2O emitted from the soil to the atmosphere and the N_2O reduction to N_2 within soil pores (Wen et al., 2016). Gross N_2O uptake elucidates both reductions of N_2O from the atmosphere diffusing into the soil and within soil pores (Wen et al., 2016). Thus, their relative flux rates decide the magnitude and direction of net N_2O flux at the soil-atmosphere interface.

Understanding factors driving biogeochemical processes, e.g., denitrification, and their rates over space and time is critical to quantify the impacts of human activity on the N cycle and to manage and mitigate the severe environmental problems associated with N pollution (Boyer et al., 2006). The conceptual model of ‘hole-in-the-pipe’ speculated two levels of controls regulating the emissions of N_2O from the soil to the atmosphere. These were to control the rates of denitrification and nitrification and to control the proportions between the gaseous end product of these processes (Firestone and Davidson, 1989). These two processes are primarily regulated by proximal factors, such as oxygen, N, and C availabilities. Soil moisture and temperature act as roles of regulating oxygen availability to soil microbes and coupling with the microbial N and C cycle (Butterbach-Bahl et al., 2013; Davidson et al., 2000). Substantial N_2O emissions occur under the range of 60 – 70% water-filled pore space (WFPS) while N_2O emissions tend to be decreased owing to the formation of N_2 instead of N_2O when WFPS is higher than 70% (Davidson et al., 2000). N_2O uptake mainly occurs at high WFPS, available C, and low NO_3^-

availability has been proved by many studies (Clayton et al., 1997; Senbayram et al., 2012). When soil NO_3^- concentrations are limited atmospheric and/or soil gaseous N_2O may be the only electron acceptor left for denitrification (Rosenkranz et al., 2006). Additionally, distal factors, like climate, soil type, or microbial community, can also indirectly affect soil N_2O production and consumption through regulating proximal factors. Denitrification is a respiratory microbial process involving four enzymatically catalyzed reductive steps: nitrate reduction controlled by nitrate reductases (encoded by *narG* and *napA*), nitrite reduction controlled by nitrite reductase (encoded by the *nos* gene cluster), nitric oxide reduction controlled by nitric oxide reductase (encoded by *nor* gene cluster) and N_2O reduction controlled by N_2O reductase (encoded by *nosZ* gene cluster) (Wallenstein et al., 2006). These functional genes may be affected by management practices, such as fertilization and land-use change (Hallin et al., 2009; Attard et al., 2011; Ding et al., 2021), thereby directly or indirectly influencing N_2O fluxes in soils. However, most of the studies are mainly focused on net N_2O fluxes by using the static chamber method in the natural and managed ecosystems. The $^{15}\text{N}_2\text{O}$ PD technique is rarely applied in terrestrial ecosystems, which hinders our understanding of the ecosystem N loss to characterize controls on processes.

1.2. Gross N_2O emission and uptake in cropland agroforestry and monoculture

Global anthropogenic N_2O emissions, which are dominated by N additions to cropland monocultures, increased by 30% in the past four decades to 7.3 (4.2–11.4) Tg N yr⁻¹ (Tian et al., 2020). Mitigating the increasing N_2O emissions and contributing to the Paris Agreement goal of constraining global warming to below 2 °C by 2100 the adoption of land-based mitigation strategies is urgently required. These strategies mostly involve the production of organic matter by plant photosynthesis coupled with C storage in living biomass and/or soil organic matter (Paustian et al., 2016). One of the strategies is the agroforestry system which integrates trees and crops in the same land-use unit and it is a globally practiced strategy for enhancing food production and ecosystem sustainability, and supplying other forms of long-term ecosystem services (Ma et al., 2020b). Agroforestry systems can optimize the utilization of light, water, and nutrients (Tsonkova et al., 2012), enhance C sequestration (Pardon et al., 2017; Baah-Acheamfour et al., 2014), conserve biodiversity (Beule et al., 2019a; Bainard et al., 2013), improve food security (Beule et al., 2019b) and water quality (Wolz et al., 2018a; Wolz et al., 2018b), and mitigate climate change (Chapman et al., 2020) while maintaining productivity that

cropland monocultures do not or minimally provide. Due to the provision of specific economic, environmental, and social solutions of agroforestry systems, they have become more promising land-management alternatives compared to conventional intensive cropland monoculture (Zhu et al., 2019). Although evidence points to decreases in N₂O emissions in temperate agroforestry systems (Wolz et al., 2018a; Amadi et al., 2016; Beaudette et al., 2010), soil-based N₂O mitigation in such ecosystems is at an early stage, especially for accurately quantifying gross N₂O emissions and uptake.

Conversion of cropland monoculture to cropland agroforestry is commonly associated with changes in soil substrate, soil microbial attributes, and chemical properties (Strickland et al., 2015; Rivest et al., 2013), which could directly/indirectly affect soil N₂O production and consumption. On the one hand, trees in the cropland are unfertilized as farmers commonly practiced, which can create microclimates decreasing ambient temperatures and heat stress, maintaining soil moisture, and supplying leaf litter (Thornton et al., 2017), therefore, likely to increase N₂O consumption. As low temperature and high soil moisture content hamper the diffusion of N₂O into the atmosphere, long residence time coupled with low mineral N (electron acceptor) and high organic C (electron donor) in soils facilitate N₂O reduction to N₂. However, some other studies have found that the lower soil moisture is the limiting factor for lowering N₂O emissions in agroforestry systems by possibly reducing heterotrophic denitrification (Beaudette et al., 2010; Amadi et al., 2016). The difference in soil moisture in the tree row of agroforestry systems may be attributed to evapotranspiration. Additionally, the commonly fertilized crop rows of agroforestry and monoculture lead to high N₂O emissions due to the high N input and low root biomass (Amadi et al., 2017). In addition to soil physical and chemical properties, agroforestry systems have a positive impact on microbial abundance and diversity (Beule et al., 2020; Beule et al., 2019a; Banerjee et al., 2016). Beule et al. (2020) reported that tree rows of agroforestry systems increase soil bacterial, fungal biomass, and denitrifier abundance possibly due to the high WFPS, indicating a greater genetic potential for denitrification. Similar findings are also found in agroforestry systems in Alberta (Banerjee et al., 2016). Additionally, the variation of soil N₂O emissions across the agricultural landscape has been well-documented due to other factors, like topography (Vilain et al., 2010; Izaurrealde et al., 2004; Corre et al., 1996), soil texture (Skiba and Ball, 2002; Corre et al., 1999), and crop types (Liu et al., 2021; Gelfand et al., 2015; Walter et al., 2015). It is well-known that fine-textured soils favor denitrification and

N₂O emissions relative to coarse-textured soils (Pelster et al., 2012), whereas Kaiser and Heinemeyer (1996) have found lower N₂O emissions in fine-textured soils due to lower gas diffusivity that supports N₂O reduction. However, there are no available data detailing the spatial and temporal effects of cropland agroforestry and monoculture on gross N₂O emission and uptake. Therefore, a combination of the relatively new technique i.e., ¹⁵N₂O PD and modern molecular technique applied in agroforestry systems could provide novel insights into making better management practices in the temperate region on climate change mitigation.

1.3. Gross N₂O emission and uptake in contrasting agroforestry systems and at depths

Another form of agroforestry system is riparian buffers located in a transitional area between terrestrial and aquatic ecosystems and an integral part of the terrestrial-aquatic ecotone (Baskerville et al., 2021). Some of these riparian buffers are planted with wooded species because of their economic value. Particularly, short-rotation forestry crops, like poplars and willow, are commonly planted in riparian zones in many European countries (e.g., Germany, Sweden) and the United States (Dimitriou et al., 2012; Schmidt-Walter and Lamersdorf, 2012; Caputo et al., 2014). The primary benefit of these crops is that the farmers can benefit from the economic value by frequently harvesting woody crops and immediately processing them for commercial use, and these crops do not commonly require fertilization and provide habitat for wildlife (Vidon et al., 2019). At the same time, the riparian tree buffers also deliver multiple ecosystem services, one of which is to decrease nutrient pollution deriving from agricultural practices (Weller and Baker, 2014). The ecological benefits of riparian tree buffers involve reducing N loading through plant uptake, favoring microbial denitrification, and enhancing retention in the soil and groundwater (Hill, 2019; King et al., 2016). Owing to the presence of shallow groundwater tables and high soil organic matter content in riparian zones, soil biogeochemical conditions in riparian zones are generally conducive to high N₂O emissions at the soil-atmosphere interface (Davis et al., 2019). However, Fisher et al. (2014) found relatively high soil organic C (SOC), dissolved organic C, and microbial biomass C in riparian buffers were in parallel with low N₂O emissions, indicating the reduction of N₂O to N₂. On the other hand, most denitrifiers are heterotrophic and use organic compounds as energy sources (Gift et al., 2010). Thus, these environmental factors can significantly affect the microbial activity and enzymatic pathways impacting N₂O emissions (Butterbach-Bahl et al., 2013).

In contrast, the trees planted in the cropland (i.e. cropland agroforestry) with well-drained soil are commonly unfertilized (Schmidt et al., 2021) and can capture and recycle subsoil inorganic N that have leached below the rooting zone of associated crops, resulting in more efficient interception of leached N (Lang et al., 2019). However, most studies focusing on N₂O emissions in riparian buffers are either surveyed on different types of riparian buffers (Baskerville et al., 2021) or the comparison of riparian buffers and their adjacent croplands (Fisher et al., 2014; Figueiredo et al., 2016). Little information is known about how different agroforestry systems with contrasting inherent soil properties (e.g., SOC, water table) affect gross N₂O emissions and uptake.

Additionally, large evidence points to subsurface N₂O production arose from sharp increases in N₂O concentrations with depth (Goldberg and Gebauer, 2009; van Groenigen et al., 2005). For example, Shcherbak and Robertson (2019) found N₂O concentrations below 20 cm up to 900 times those of atmospheric concentrations. Most studies have reported that N₂O emissions are mainly from the top few centimeters where substrate availability and microbial activity are generally higher (Tian et al., 2016; Yang and Silver, 2016a). However, little is known about the rates of subsoil N₂O fluxes measured in situ, especially for the two co-occurring processes: gross N₂O emission and uptake. Factors regulating gross N₂O emissions and uptake are likely co-limited by the availability of NO₃⁻, C, and WFPS (Wen et al., 2017; Yang and Silver, 2016a, 2016b), and these three limitations, as well as microbial communities and denitrification gene abundance, typically change with depth (Liu et al., 2020; Barrett et al., 2016; Tian et al., 2016). Depth variation in microbial population size including gene abundance of denitrifiers may result in differential controls on gross N₂O emission and uptake in topsoil vs. subsoil horizons. Therefore, understanding the relationships between environmental factors, the dynamics of soil microbial communities, denitrification gene abundance, and gross N₂O fluxes across different agroforestry systems and soil depths is crucial to gaining insights into gross N₂O emission and uptake in the context of global climate change.

1.4. Aims and hypothesis

The first study aimed to quantify gross N₂O emission and gross N₂O uptake in temperate cropland agroforestry and monoculture systems, and investigate the relationships of gross N₂O

fluxes with soil controlling factors, including a series of denitrification gene abundance (*nirK*, *nirS*, *nosZ* clade I, and *nosZ* clade II) over two growing seasons (2018-2019) at three study sites on different soils in Germany. We hypothesized that (1) cropland agroforestry will have lower gross N₂O emission and higher gross N₂O uptake than monocultures, and (2) this pattern of gross N₂O fluxes will reflect the changes in substrate levels, soil moisture, and temperature conditions as well as in denitrifier population size.

The second study aimed to compare tree rows of alley cropping with riparian tree buffer on their influence on gross N₂O emission and uptake and to compare two soil depths (0 – 5 cm vs. 40-60 cm) in both agroforestry systems for gross N₂O emission and uptake to elucidate the factors controlling their differences. We hypothesized that riparian tree buffer will have higher gross N₂O emission and uptake than tree row of alley cropping, and topsoil (0 – 5 cm) will have higher gross N₂O emission and uptake than subsoil (40 – 60 cm).

1.5. References

- Allen, M.R., 2015. Climate change 2014. Synthesis report. [IPCC, WMO], [Geneva].
- Allen, S.C., Jose, S., Nair, P., Brecke, B.J., Nkedi-Kizza, P., Ramsey, C.L., 2004. Safety-net role of tree roots: evidence from a pecan (*Carya illinoensis* K. Koch)–cotton (*Gossypium hirsutum* L.) alley cropping system in the southern United States. *Forest Ecology and Management* 192, 395–407.
- Almaraz, M., Wong, M.Y., Yang, W.H., 2020. Looking back to look ahead: a vision for soil denitrification research. *Ecology* 101, e02917.
- Amadi, C.C., Farrell, R.E., van Rees, K.C., 2017. Greenhouse gas emissions along a shelterbelt-cropped field transect. *Agriculture, Ecosystems & Environment* 241, 110–120.
- Amadi, C.C., van Rees, K.C., Farrell, R.E., 2016. Soil–atmosphere exchange of carbon dioxide, methane and nitrous oxide in shelterbelts compared with adjacent cropped fields. *Agriculture, Ecosystems & Environment* 223, 123–134.
- Attard, E., Recous, S., Chabbi, A., Berranger, C. de, Guillaumaud, N., Labreuche, J., Philippot, L., Schmid, B., Le Roux, X., 2011. Soil environmental conditions rather than denitrifier abundance and diversity drive potential denitrification after changes in land uses. *Global Change Biology* 17, 1975–1989.

- Baah-Acheamfour, M., Carlyle, C.N., Bork, E.W., Chang, S.X., 2014. Trees increase soil carbon and its stability in three agroforestry systems in central Alberta, Canada. *Forest Ecology and Management* 328, 131–139.
- Baah-Acheamfour, M., Carlyle, C.N., Bork, E.W., Chang, S.X., 2020. Forest and perennial herbland cover reduce microbial respiration but increase root respiration in agroforestry systems. *Agricultural and Forest Meteorology* 280, 107790.
- Bainard, L. d., Koch, A.M., Gordon, A.M., Klironomos, J.N., 2013. Growth response of crops to soil microbial communities from conventional monocropping and tree-based intercropping systems. *Plant and Soil* 363, 345–356.
- Banerjee, S., Baah-Acheamfour, M., Carlyle, C.N., Bissett, A., Richardson, A.E., Siddique, T., Bork, E.W., Chang, S.X., 2016. Determinants of bacterial communities in Canadian agroforestry systems. *Environmental microbiology* 18, 1805–1816.
- Barnes, A.D., Allen, K., Kreft, H., Corre, M.D., Jochum, M., Veldkamp, E., Clough, Y., Daniel, R., Darras, K., Denmead, L.H., Farikhah Haneda, N., Hertel, D., Knohl, A., Kotowska, M.M., Kurniawan, S., Meijide, A., Rembold, K., Edho Prabowo, W., Schneider, D., Tschardtke, T., Brose, U., 2017. Direct and cascading impacts of tropical land-use change on multi-trophic biodiversity. *Nature ecology & evolution* 1, 1511–1519.
- Barrett, M., Khalil, M.I., Jahangir, M.M.R., Lee, C., Cardenas, L.M., Collins, G., Richards, K.G., O'Flaherty, V., 2016. Carbon amendment and soil depth affect the distribution and abundance of denitrifiers in agricultural soils. *Environmental science and pollution research international* 23, 7899–7910.
- Bartels, R., 1982. The Rank Version of von Neumann's Ratio Test for Randomness. *Journal of the American Statistical Association* 77, 40–46.
- Baskerville, M., Reddy, N., Ofosu, E., Thevathasan, N.V., Oelbermann, M., 2021. Vegetation type does not affect nitrous oxide emissions from riparian zones in agricultural landscapes. *Environmental Management* 67, 371–383.
- Beaudette, C., Bradley, R.L., Whalen, J.K., McVetty, P., Vessey, K., Smith, D.L., 2010. Tree-based intercropping does not compromise canola (*Brassica napus* L.) seed oil yield and reduces soil nitrous oxide emissions. *Agriculture, Ecosystems & Environment* 139, 33–39.
- Beule, L., Arndt, M., Karlovsky, P., 2021. Relative abundances of species or sequence variants can be misleading: soil fungal communities as an example. *Microorganisms* 9.

- Beule, L., Corre, M.D., Schmidt, M., Göbel, L., Veldkamp, E., Karlovsky, P., 2019a. Conversion of monoculture cropland and open grassland to agroforestry alters the abundance of soil bacteria, fungi and soil-N-cycling genes. *PloS one* 14, 1-19.
- Beule, L., Karlovsky, P., 2021. Tree rows in temperate agroforestry croplands alter the composition of soil bacterial communities. *PloS one* 16, e0246919.
- Beule, L., Lehtsaar, E., Corre, M.D., Schmidt, M., Veldkamp, E., Karlovsky, P., 2020. Poplar rows in temperate agroforestry croplands promote bacteria, fungi, and denitrification genes in soils. *Frontiers in Microbiology* 10, 1–5.
- Beule, L., Lehtsaar, E., Rathgeb, A., Karlovsky, P., 2019b. Crop diseases and mycotoxin accumulation in temperate agroforestry systems. *Sustainability* 11, 2925.
- Bissett, A., Brown, M.V., Siciliano, S.D., Thrall, P.H., 2013. Microbial community responses to anthropogenically induced environmental change: towards a systems approach. *Ecology Letters* 16 Suppl 1, 128–139.
- Boleman, P., Jacobson, M., 2021. Nitrogen credit trading as an incentive for riparian buffer establishment on Pennsylvania farmland. *Agroforestry Systems*.
- Bowen, H., Maul, J.E., Poffenbarger, H., Mirsky, S., Cavigelli, M., Yarwood, S., 2018. Spatial patterns of microbial denitrification genes change in response to poultry litter placement and cover crop species in an agricultural soil. *Biology and Fertility of Soils* 54, 769–781.
- Boyer, E.W., Alexander, R.B., Parton, W.J., Li, C., Butterbach-Bahl, K., Donner, S.D., Skaggs, R.W., Del Grosso, S.J., 2006. Modeling denitrification in terrestrial and aquatic ecosystems at regional scales. *Ecological Applications* 16, 2123–2142.
- Brandfass, C., Karlovsky, P., 2008. Upscaled CTAB-based DNA extraction and real-time PCR assays for *Fusarium culmorum* and *F. graminearum* DNA in plant material with reduced sampling error. *International journal of molecular sciences* 9, 2306–2321.
- Brookes, P.C., Landman, A., Pruden, G., Jenkinson, D.S., 1985. Chloroform fumigation and the release of soil nitrogen: A rapid direct extraction method to microbial biomass nitrogen in soil. *Soil Biology and Biochemistry* 17, 837–842.
- Butterbach-Bahl, K., Baggs, E.M., Dannenmann, M., Kiese, R., Zechmeister-Boltenstern, S., 2013. Nitrous oxide emissions from soils: how well do we understand the processes and their controls? *Philosophical transactions of the Royal Society of London. Series B, Biological sciences* 368, 20130122.

- Butterbach-Bahl, K., Dannenmann, M., 2011. Denitrification and associated soil N₂O emissions due to agricultural activities in a changing climate. *Current Opinion in Environmental Sustainability* 3, 389–395.
- Butterbach-Bahl, K., Willibald, G., Papen, H., 2002. Soil core method for direct simultaneous determination of N₂ and N₂O emissions from forest soils. *Plant and Soil* 240, 105–116.
- Caputo, J., Balogh, S.B., Volk, T.A., Johnson, L., Puettmann, M., Lippke, B., Oneil, E., 2014. Incorporating uncertainty into a life cycle assessment (LCA) model of short-rotation willow biomass (*Salix spp.*) crops. *BioEnergy Research* 7, 48–59.
- Chapman, M., Walker, W.S., Cook-Patton, S.C., Ellis, P.W., Farina, M., Griscom, B.W., Baccini, A., 2020. Large climate mitigation potential from adding trees to agricultural lands. *Global Change Biology*, 4357–4365.
- Chapuis-Lardy, L., Wrage, N., Metay, A., Chotte, J.-L., Bernoux, M., 2007. Soils, a sink for N₂O? A review. *Global Change Biology* 13, 1–17.
- Chen, J., Strous, M., 2013. Denitrification and aerobic respiration, hybrid electron transport chains and co-evolution. *Biochimica et biophysica acta* 1827, 136–144.
- Chen, Y., Liu, F., Kang, L., Zhang, D., Kou, D., Mao, C., Qin, S., Zhang, Q., Yang, Y., 2020. Large-scale evidence for microbial response and associated carbon release after permafrost thaw. *Global Change Biology*, 1–12.
- Ciais, P., Sabine, C., Bala, G., Bopp, L., Brovkin, V., Canadell, J., Chhabra, A., DeFries, R., Galloway, J., Heimann, M., Jones, C., Le Quéré, C., Myneni, R. B., Piao, S., & Thornton, P. (2013). Carbon and Other Biogeochemical Cycles (Climate Change 2013: The Physical Science Basis. Contribution of Working Group I to the Fifth Assessment Report of the Intergovernmental Panel on Climate Change, Issue. C. U. Press.
- Clayton, H., McTaggart, I.P., Parker, J., Swan, L., Smith, K.A., 1997. Nitrous oxide emissions from fertilised grassland: A 2-year study of the effects of N fertiliser form and environmental conditions. *Biology and Fertility of Soils* 25, 252–260.
- Corre, M.D., Pennock, D.J., van Kessel, C., Kirkelliott, D., 1999. Estimation of annual nitrous oxide emissions from a transitional grassland-forest region in Saskatchewan, Canada. *Biogeochemistry* 44, 29–49.
- Corre, M.D., van Kessel, C., Pennock, D.J., 1996. Landscape and seasonal patterns of nitrous oxide emissions in a semiarid region. *Soil Science Society of America Journal* 60, 1806–1815.

- Dandie, C.E., Burton, D.L., Zebarth, B.J., Henderson, S.L., Trevors, J.T., Goyer, C., 2008. Changes in bacterial denitrifier community abundance over time in an agricultural field and their relationship with denitrification activity. *Applied and environmental microbiology* 74, 5997–6005.
- Davidson, E.A., 2012. Representative concentration pathways and mitigation scenarios for nitrous oxide. *Environmental Research Letters* 7, 24005.
- Davidson, E.A., Keller, M., Erickson, H.E., Verchot, L.V., Veldkamp, E., 2000. Testing a conceptual model of soil emissions of nitrous and nitric oxides. *BioScience* 50, 667.
- Davis, M.P., Groh, T.A., Jaynes, D.B., Parkin, T.B., Isenhardt, T.M., 2019. Nitrous oxide emissions from saturated riparian buffers: are we trading a water quality problem for an air quality problem? *Journal of Environment Quality* 48, 261.
- Dimitriou, I., Mola-Yudego, B., Aronsson, P., 2012. Impact of willow short rotation coppice on water quality. *BioEnergy Research* 5, 537–545.
- Ding, L., Zhou, J., Li, Q., Tang, J., Chen, X., 2021. Effects of land-use type and flooding on the soil microbial community and functional genes in reservoir riparian zones. *Microbial Ecology*.
- Figueiredo, v., Enrich-Prast, A., Rütting, T., 2016. Soil organic matter content controls gross nitrogen dynamics and N₂O production in riparian and upland boreal soil. *European Journal of Soil Science* 67, 782–791.
- Firestone, M.K., Davidson, E.A., 1989. Microbiological basis of NO and N₂O production and consumption in soil. *Exchange of Trace Gases between Terrestrial Ecosystems and the Atmosphere*. John Wiley & Sons, Ltd, New York.
- Fisher, K., Jacinthe, P.A., Vidon, P., Liu, X., Baker, M.E., 2014. Nitrous oxide emission from cropland and adjacent riparian buffers in contrasting hydrogeomorphic settings. *Journal of environmental quality* 43, 338–348.
- Foley, J.A., Ramankutty, N., Brauman, K.A., Cassidy, E.S., Gerber, J.S., Johnston, M., Mueller, N.D., O'Connell, C., Ray, D.K., West, P.C., Balzer, C., Bennett, E.M., Carpenter, S.R., Hill, J., Monfreda, C., Polasky, S., Rockström, J., Sheehan, J., Siebert, S., Tilman, D., Zaks, D.P.M., 2011. Solutions for a cultivated planet. *Nature* 478, 337–342.

- Gelfand, I., Cui, M., Tang, J., Robertson, G.P., 2015. Short-term drought response of N₂O and CO₂ emissions from mesic agricultural soils in the US Midwest. *Agriculture, Ecosystems & Environment* 212, 127–133.
- Gift, D.M., Groffman, P.M., Kaushal, S.S., Mayer, P.M., 2010. Denitrification potential, root biomass, and organic matter in degraded and restored urban riparian zones. *Restoration Ecology* 18, 113–120.
- Godfray, H.C.J., Beddington, J.R., Crute, I.R., Haddad, L., Lawrence, D., Muir, J.F., Pretty, J., Robinson, S., Thomas, S.M., Toulmin, C., 2010. Food security: the challenge of feeding 9 billion people. *Science (New York, N.Y.)* 327, 812–818.
- Goldberg, S.D., Gebauer, G., 2009. Drought turns a central European norway spruce forest soil from an N₂O source to a transient N₂O sink. *Global change biology* 15, 850–860.
- Graf, D.R.H., Jones, C.M., Hallin, S., 2014. Intergenomic comparisons highlight modularity of the denitrification pathway and underpin the importance of community structure for N₂O emissions. *PLoS one* 9, e114118.
- Groffman, P.M., Altabet, M.A., Böhlke, J.K., Butterbach-Bahl, K., David, M.B., Firestone, M.K., Giblin, A.E., Kana, T.M., Nielsen, L.P., Voytek, M.A., 2006. Methods for measuring denitrification: diverse approaches to a difficult problem. *Ecological Applications* 16, 2091–2122.
- Guerra, V., Beule, L., Lehtsaar, E., Liao, H.-L., Karlovsky, P., 2020. Improved protocol for DNA extraction from subsoils using phosphate lysis buffer. *Microorganisms* 8.
- Gundersen, P., Laurén, A., Finér, L., Ring, E., Koivusalo, H., Saetersdal, M., Weslien, J.-O., Sigurdsson, B.D., Högbom, L., Laine, J., Hansen, K., 2010. Environmental services provided from riparian forests in the Nordic countries. *AMBIO* 39, 555–566.
- Hallin, S., Jones, C.M., Schloter, M., Philippot, L., 2009. Relationship between N-cycling communities and ecosystem functioning in a 50-year-old fertilization experiment. *The ISME journal* 3, 597–605.
- Han, X., Huang, C., Khan, S., Zhang, Y., Chen, Y., Guo, J., 2020. nirS-type denitrifying bacterial communities in relation to soil physicochemical conditions and soil depths of two montane riparian meadows in North China. *Environmental Science and Pollution Research* 27, 28899–28911.

- Henry, S., Baudoin, E., López-Gutiérrez, J.C., Martin-Laurent, F., Brauman, A., Philippot, L., 2004. Quantification of denitrifying bacteria in soils by *nirK* gene targeted real-time PCR. *Journal of microbiological methods* 59, 327–335.
- Henry, S., Bru, D., Stres, B., Hallet, S., Philippot, L., 2006. Quantitative detection of the *nosZ* gene, encoding nitrous oxide reductase, and comparison of the abundances of 16S rRNA, *narG*, *nirK*, and *nosZ* genes in soils. *Applied and environmental microbiology* 72, 5181–5189.
- Hill, A.R., 2019. Groundwater nitrate removal in riparian buffer zones: a review of research progress in the past 20 years. *Biogeochemistry* 143, 347–369.
- Izaurrealde, R.C., Lemke, R.L., Goddard, T.W., McConkey, B., Zhang, Z., 2004. Nitrous oxide emissions from agricultural toposequences in Alberta and Saskatchewan. *Proceedings of the National Academy of Sciences* 68, 1285–1294.
- Jahangir, M., Khalil, M.I., Johnston, P., Cardenas, L.M., Hatch, D.J., Butler, M., Barrett, M., O’flaherty, V., Richards, K.G., 2012. Denitrification potential in subsoils: A mechanism to reduce nitrate leaching to groundwater. *Agriculture, Ecosystems & Environment* 147, 13–23.
- Jones, C.M., Graf, D.R.H., Bru, D., Philippot, L., Hallin, S., 2013. The unaccounted yet abundant nitrous oxide-reducing microbial community: a potential nitrous oxide sink. *The ISME journal* 7, 417–426.
- Jones, D., Willett, V., 2006. Experimental evaluation of methods to quantify dissolved organic nitrogen (DON) and dissolved organic carbon (DOC) in soil. *Soil Biology and Biochemistry* 38, 991–999.
- Juhanson, J., Hallin, S., Söderström, M., Stenberg, M., Jones, C.M., 2017. Spatial and phylogeographical analyses of *nosZ* genes underscore niche differentiation amongst terrestrial N₂O reducing communities. *BioScience* 115, 82–91.
- Kaiser, E.-A., Heinemeyer, O., 1996. Temporal changes in N₂O-losses from two arable soils. *Plant and Soil* 181, 57–63.
- Kanzler, M., Böhm, C., Mirck, J., Schmitt, D., Veste, M., 2019. Microclimate effects on evaporation and winter wheat (*Triticum aestivum* L.) yield within a temperate agroforestry system. *Agroforestry Systems* 93, 1821–1841.
- Kay, S., Graves, A., Palma, J.H., Moreno, G., Roces-Díaz, J.V., Aviron, S., Chouvardas, D., Crous-Duran, J., Ferreiro-Domínguez, N., García de Jalón, S., Măcicășan, V., Mosquera-Losada, M.R., Pantera, A., Santiago-Freijanes, J.J., Szerencsits, E., Torralba, M., Burgess,

- P.J., Herzog, F., 2019. Agroforestry is paying off – Economic evaluation of ecosystem services in European landscapes with and without agroforestry systems. *Ecosystem Services* 36, 100896.
- Kim, D.-G., Kirschbaum, M.U., Beedy, T.L., 2016. Carbon sequestration and net emissions of CH₄ and N₂O under agroforestry: Synthesizing available data and suggestions for future studies. *Agriculture, Ecosystems & Environment* 226, 65–78.
- King, S.E., Osmond, D.L., Smith, J., Burchell, M.R., Dukes, M., Evans, R.O., Knies, S., Kunickis, S., 2016. Effects of riparian buffer vegetation and width: A 12-Year longitudinal study. *Journal of environmental quality* 45, 1243–1251.
- Kline, R.B., 2014. Convergence of Structural Equation Modeling and Multilevel Modeling, in: Vogt, W.P., Williams, M. (Eds.), *The SAGE handbook of innovation in social research methods*. SAGE Publications, Los Angeles, pp. 562–589.
- Koehler, B., Corre, M.D., Veldkamp, E., Wullaert, H., Wright, S.J., 2009. Immediate and long-term nitrogen oxide emissions from tropical forest soils exposed to elevated nitrogen input. *Global change biology* 15, 2049–2066.
- Lang, M., Li, P., Ti, C., Zhu, S., Yan, X., Chang, S.X., 2019. Soil gross nitrogen transformations are related to land-uses in two agroforestry systems. *Ecological Engineering* 127, 431–439.
- Langenberg, J., Feldmann, M., Theuvsen, L., 2018. agroforestry systems: using Monte-Carlo simulation for a risk analysis in comparison with arable farming systems. *German Journal of Agricultural Economics* 67, 95–112.
- Liu, L., Knight, J.D., Lemke, R.L., Farrell, R.E., 2021. Type of pulse crop included in a 2-year rotation with wheat affects total N₂O loss and intensity. *Biology and Fertility of Soils* 57, 699–713.
- Liu, M., Zhang, W., Wang, X., Wang, F., Dong, W., Hu, C., Liu, B., Sun, R., 2020. Nitrogen leaching greatly impacts bacterial community and denitrifiers abundance in subsoil under long-term fertilization. *Agriculture, Ecosystems & Environment* 294, 106885.
- Liu, X., Chen, C., Wang, W., Hughes, J.M., Lewis, T., Hou, E., Shen, J., 2015. Vertical distribution of soil denitrifying communities in a wet Sclerophyll forest under long-term repeated burning. *Microbial Ecology* 70, 993–1003.

- Liu, X., Chen, C.R., Wang, W.J., Hughes, J.M., Lewis, T., Hou, E.Q., Shen, J., 2013. Soil environmental factors rather than denitrification gene abundance control N₂O fluxes in a wet sclerophyll forest with different burning frequency. *BioScience* 57, 292–300.
- Lutz, S.R., Trauth, N., Musolff, A., van Breukelen, B.M., Knöller, K., Fleckenstein, J.H., 2020. How important is denitrification in riparian zones? Combining end-member mixing and isotope modeling to quantify nitrate removal from riparian groundwater. *Water Resources Research* 56.
- Ma, L., Xiong, Z., Yao, L., Liu, G., Zhang, Q., Liu, W., 2020a. Soil properties alter plant and microbial communities to modulate denitrification rates in subtropical riparian wetlands. *Land Degradation & Development* 31, 1792–1802.
- Ma, Z., Chen, H.Y.H., Bork, E.W., Carlyle, C.N., Chang, S.X., 2020b. Carbon accumulation in agroforestry systems is affected by tree species diversity, age and regional climate: A global meta-analysis. *Global Ecology and Biogeography* 00, 1–12.
- Markwitz, C., Knohl, A., Siebicke, L., 2020. Evapotranspiration over agroforestry sites in Germany. *Biogeosciences* 17, 5183–5208.
- Matson, A.L., Corre, M.D., Langs, K., Veldkamp, E., 2017. Soil trace gas fluxes along orthogonal precipitation and soil fertility gradients in tropical lowland forests of Panama. *Biogeosciences* 14, 3509–3524.
- McCarty, G.W., Bremner, J.M., 1992. Availability of organic carbon for denitrification of nitrate in subsoils. *Biology and Fertility of Soils* 14, 219–222.
- McDowell, W.H., Zsolnay, A., Aitkenhead-Peterson, J.A., Gregorich, E.G., Jones, D.L., Jödemann, D., KALBITZ, K., Marschner, B., Schwesig, D., 2006. A comparison of methods to determine the biodegradable dissolved organic carbon from different terrestrial sources. *Soil Biology and Biochemistry* 38, 1933–1942.
- Michotey, V., Méjean, V., Bonin, P., 2000. Comparison of methods for quantification of cytochrome cd(1)-denitrifying bacteria in environmental marine samples. *Applied and environmental microbiology* 66, 1564–1571.
- Mitchell, E., Scheer, C., Rowlings, D., Cotrufo, M.F., Conant, R.T., Friedl, J., Grace, P., 2020. Trade-off between ‘new’ SOC stabilisation from above-ground inputs and priming of native C as determined by soil type and residue placement. *Biogeochemistry* 149, 221–236.

- Montzka, S.A., Dlugokencky, E.J., Butler, J.H., 2011. Non-CO₂ greenhouse gases and climate change. *Nature* 476, 43–50.
- Pardon, P., Reubens, B., Mertens, J., Verheyen, K., Frenne, P. de, Smet, G. de, van Waes, C., Reheul, D., 2018. Effects of temperate agroforestry on yield and quality of different arable intercrops. *Agricultural Systems* 166, 135–151.
- Pardon, P., Reubens, B., Reheul, D., Mertens, J., Frenne, P. de, Coussement, T., Janssens, P., Verheyen, K., 2017. Trees increase soil organic carbon and nutrient availability in temperate agroforestry systems. *Agriculture, Ecosystems & Environment* 247, 98–111.
- Paustian, K., Lehmann, J., Ogle, S., Reay, D., Robertson, G.P., Smith, P., 2016. Climate-smart soils. *Nature* 532, 49–57.
- Pelster, D.E., Chantigny, M.H., Rochette, P., Angers, D.A., Rieux, C., Vanasse, A., 2012. Nitrous oxide emissions respond differently to mineral and organic nitrogen sources in contrasting soil types. *Journal of environmental quality* 41, 427–435.
- Prather, M.J., Hsu, J., DeLuca, N.M., Jackman, C.H., Oman, L.D., Douglass, A.R., Fleming, E.L., Strahan, S.E., Steenrod, S.D., Søvde, O.A., Isaksen, I.S.A., Froidevaux, L., Funke, B., 2015. Measuring and modeling the lifetime of nitrous oxide including its variability. *Journal of Geophysical Research: Atmospheres* 120, 5693–5705.
- R Core Team, 2019. R: A language and environment for statistical computing, Vienna, Austria: R Foundation for Statistical Computing. Retrieved from <https://www.r-project.org/>.
- Rivest, D., Lorente, M., Olivier, A., Messier, C., 2013. Soil biochemical properties and microbial resilience in agroforestry systems: effects on wheat growth under controlled drought and flooding conditions. *The Science of the total environment* 463-464, 51–60.
- Rocca, J.D., Hall, E.K., Lennon, J.T., Evans, S.E., Waldrop, M.P., Cotner, J.B., Nemergut, D.R., Graham, E.B., Wallenstein, M.D., 2015. Relationships between protein-encoding gene abundance and corresponding process are commonly assumed yet rarely observed. *The ISME Journal* 9, 1693–1699.
- Rosenkranz, P., Brüggemann, N., Papen, H., Xu, Z., Seufert, G., Butterbach-Bahl, K., 2006. N₂O, NO and CH₄ exchange, and microbial N turnover over a Mediterranean pine forest soil. *Biogeosciences* 3, 121–133.

- Schmidt, M., Corre, M.D., Kim, B., Morley, J., Göbel, L., Sharma, A.S.I., Setriuc, S., Veldkamp, E., 2021. Nutrient saturation of crop monocultures and agroforestry indicated by nutrient response efficiency. *Nutrient Cycling in Agroecosystems* 119, 69–82.
- Schmidt-Walter, P., Lamersdorf, N.P., 2012. Biomass production with willow and poplar short rotation coppices on sensitive areas—the impact on nitrate leaching and groundwater recharge in a drinking water catchment near Hanover, Germany. *BioEnergy Research* 5, 546–562.
- Semedo, M., Wittorf, L., Hallin, S., Song, B., 2020. Differential expression of clade I and II N_2O reductase genes in denitrifying *Thauera linaloolentis* 47LoIT under different nitrogen conditions. *FEMS Microbiology Letters*.
- Senbayram, M., Chen, R., Budai, A., Bakken, L., Dittert, K., 2012. N_2O emission and the $N_2O/(N_2O+N_2)$ product ratio of denitrification as controlled by available carbon substrates and nitrate concentrations. *Agriculture, Ecosystems & Environment* 147, 4–12.
- Shcherbak, I., Robertson, G.P., 2019. Nitrous oxide (N_2O) emissions from subsurface soils of agricultural ecosystems. *Ecosystems* 22, 1650–1663.
- Shen, S.M., Pruden, G., Jenkinson, D.S., 1984. PII: Mineralization and immobilization of nitrogen in fumigated soil and the measurement of microbial biomass nitrogen. *Soil Biology and Biochemistry* 16, 437–444.
- Sihi, D., Davidson, E.A., Savage, K.E., Liang, D., 2020. Simultaneous numerical representation of soil microsite production and consumption of carbon dioxide, methane, and nitrous oxide using probability distribution functions. *Global Change Biology* 26, 200–218.
- Skiba, U., Ball, B., 2002. The effect of soil texture and soil drainage on emissions of nitric oxide and nitrous oxide. *Soil Use and Management* 18, 56–60.
- Smith, J., Pearce, B.D., Wolfe, M.S., 2013. Reconciling productivity with protection of the environment: Is temperate agroforestry the answer? *Renewable Agriculture and Food Systems* 28, 80–92.
- Song, K., Lee, S.-H., Kang, H., 2011. Denitrification rates and community structure of denitrifying bacteria in newly constructed wetland. *European Journal of Soil Biology* 47, 24–29.
- Stark, C.H., Richards, K.G., 2008. The continuing challenge of agricultural nitrogen loss to the environment in the context of global change and advancing research.

- Strickland, M.S., Lehmann, M.F., Sucre, E.B., Bradford, M.A., 2015. Biofuel intercropping effects on soil carbon and microbial activity. *Ecological Applications*, 140–150.
- Swieter, A., Langhof, M., Lamerre, J., Greef, J.M., 2019. Long-term yields of oilseed rape and winter wheat in a short rotation alley cropping agroforestry system. *Agroforestry Systems* 93, 1853–1864.
- Thornton, P.K., Rosenstock, T., Förch, W., Lamanna, C., Bell, P., Henderson, B., Herrero, M., 2017. A qualitative evaluation of CSA options in mixed crop-livestock systems in developing countries, in: *Climate Smart Agriculture*. Springer International Publishing, Cham, pp. 385–423.
- Throbäck, I.N., Enwall, K., Jarvis, A., Hallin, S., 2004. Reassessing PCR primers targeting *nirS*, *nirK* and *nosZ* genes for community surveys of denitrifying bacteria with DGGE. *FEMS microbiology ecology* 49, 401–417.
- Tian, H., Xu, R., Canadell, J.G., Thompson, R.L., Winiwarter, W., Suntharalingam, P., DAVIDSON, E.A., Ciais, P., Jackson, R.B., Janssens-Maenhout, G., Prather, M.J., Regnier, P., Pan, N., Pan, S., Peters, G.P., Shi, H., Tubiello, F.N., Zaehle, S., Zhou, F., Arneth, A., Battaglia, G., Berthet, S., Bopp, L., Bouwman, A.F., Buitenhuis, E.T., Chang, J., Chipperfield, M.P., Dangal, S.R.S., Dlugokencky, E., Elkins, J.W., Eyre, B.D., Fu, B., Hall, B., Ito, A., Joos, F., Krummel, P.B., Landolfi, A., Laruelle, G.G., Lauerwald, R., Li, W., Lienert, S., Maavara, T., MacLeod, M., Millet, D.B., Olin, S., Patra, P.K., Prinn, R.G., Raymond, P.A., Ruiz, D.J., van der Werf, G.R., Vuichard, N., Wang, J., Weiss, R.F., Wells, K.C., Wilson, C., Yang, J., Yao, Y., 2020. A comprehensive quantification of global nitrous oxide sources and sinks. *Nature* 586, 248–256.
- Tian, H., Yang, J., Xu, R., Lu, C., Canadell, J.G., Davidson, E.A., Jackson, R.B., Arneth, A., Chang, J., Ciais, P., Gerber, S., Ito, A., Joos, F., Lienert, S., Messina, P., Olin, S., Pan, S., Peng, C., Saikawa, E., Thompson, R.L., Vuichard, N., Winiwarter, W., Zaehle, S., Zhang, B., 2018. Global soil nitrous oxide emissions since the preindustrial era estimated by an ensemble of terrestrial biosphere models: Magnitude, attribution, and uncertainty. *Global change biology*, 1–12.
- Tian, Q., Yang, X., Wang, X., Liao, C., Li, Q., Wang, M., Wu, Y., Liu, F., 2016. Microbial community mediated response of organic carbon mineralization to labile carbon and nitrogen addition in topsoil and subsoil. *Biogeochemistry* 128, 125–139.

- Tomasek, A., Kozarek, J.L., Hondzo, M., Lurndahl, N., Sadowsky, M.J., Wang, P., Staley, C., 2017. Environmental drivers of denitrification rates and denitrifying gene abundances in channels and riparian areas. *Water Resources Research* 53, 6523–6538.
- Truax, B., Gagnon, D., Lambert, F., Fortier, J., 2017. Riparian buffer growth and soil nitrate supply are affected by tree species selection and black plastic mulching. *Ecological Engineering* 106, 82–93.
- Tsonkova, P., Böhm, C., Quinkenstein, A., Freese, D., 2012. Ecological benefits provided by alley cropping systems for production of woody biomass in the temperate region: a review. *Agroforestry Systems* 85, 133–152.
- van Groenigen, J.W., Georgius, P.J., van Kessel, C., Hummelink, E.W., Velthof, G.L., Zwart, K.B., 2005. Subsoil ^{15}N - N_2O concentrations in a sandy soil profile after application of ^{15}N -fertilizer. *Nutrient Cycling in Agroecosystems* 72, 13–25.
- Veldkamp, E., Koehler, B., Corre, M.D., 2013. Indications of nitrogen-limited methane uptake in tropical forest soils. *Biogeosciences* 10, 5367–5379.
- Vidon, P.G., Welsh, M.K., Hassanzadeh, Y.T., 2019. Twenty years of riparian zone research (1997–2017): Where to next? *Journal of Environment Quality* 48, 248.
- Vilain, G., Garnier, J., Tallec, G., Cellier, P., 2010. Effect of slope position and land use on nitrous oxide (N_2O) emissions (Seine Basin, France). *Agricultural and Forest Meteorology* 150, 1192–1202.
- Wallenstein, M.D., Myrold, D.D., Firestone, M., Voytek, M., 2006. Environmental controls on denitrifying communities and denitrification rates: insights from molecular methods. *Ecological Applications* 16, 2143–2152.
- Walter, K., Don, A., Flessa, H., 2015. Net N_2O and CH_4 soil fluxes of annual and perennial bioenergy crops in two central German regions. *Biomass and Bioenergy* 81, 556–567.
- Weier, K.L., Doran, J.W., Power, J.F., Walters, D.T., 1993. Denitrification and the dinitrogen/nitrous oxide ratio as affected by soil water, available carbon, and nitrate. *Proceedings of the National Academy of Sciences* 57, 66–72.
- Weller, D.E., Baker, M.E., 2014. Cropland riparian buffers throughout Chesapeake Bay watershed: spatial patterns and effects on nitrate loads delivered to streams. *JAWRA Journal of the American Water Resources Association* 50, 696–712.

- Wen, Y., Chen, Z., Dannenmann, M., Carminati, A., Willibald, G., Kiese, R., Wolf, B., Veldkamp, E., Butterbach-Bahl, K., Corre, M.D., 2016. Disentangling gross N₂O production and consumption in soil. *Scientific reports* 6, 36517.
- Wen, Y., Corre, M.D., Schrell, W., Veldkamp, E., 2017. Gross N₂O emission and gross N₂O uptake in soils under temperate spruce and beech forests. *Soil Biology and Biochemistry* 112, 228–236.
- Wolz, K.J., Branham, B.E., DeLucia, E.H., 2018a. Reduced nitrogen losses after conversion of row crop agriculture to alley cropping with mixed fruit and nut trees. *Agriculture, Ecosystems & Environment* 258, 172–181.
- Wolz, K.J., Lovell, S.T., Branham, B.E., Eddy, W.C., Keeley, K., Revord, R.S., Wander, M.M., Yang, W.H., DeLucia, E.H., 2018b. Frontiers in alley cropping: Transformative solutions for temperate agriculture. *Global change biology* 24, 883–894.
- Yang, W.H., Silver, W.L., 2016a. Gross nitrous oxide production drives net nitrous oxide fluxes across a salt marsh landscape. *Global change biology* 22, 2228–2237.
- Yang, W.H., Silver, W.L., 2016b. Net soil–atmosphere fluxes mask patterns in gross production and consumption of nitrous oxide and methane in a managed ecosystem. *Biogeosciences* 13, 1705–1715.
- Yang, W.H., Teh, Y.A., Silver, W.L., 2011. A test of a field-based ¹⁵N-nitrous oxide pool dilution technique to measure gross N₂O production in soil. *Global Change Biology* 17, 3577–3588.
- Zhu, X., Liu, W., Chen, J., Bruijnzeel, L.A., Mao, Z., Yang, X., Cardinael, R., Meng, F.-R., Sidle, R.C., Seitz, S., Nair, V.D., Nanko, K., Zou, X., Chen, C., Jiang, X.J., 2019. Reductions in water, soil and nutrient losses and pesticide pollution in agroforestry practices: a review of evidence and processes. *Plant and Soil*.
- Zuur, A.F., Ieno, E.N., Walker, N., Saveliev, A.A., Smith, G.M., 2009. *Mixed effects models and extensions in ecology with R*. Springer, New York.

Chapter 2

Reduced Soil Gross N₂O Emission driven by Substrates rather than Denitrification Gene Abundance in Cropland Agroforestry and Monoculture

Under review in JGR Biogeosciences

Jie Luo¹, Lukas Beule², Guodong Shao¹, Edzo Veldkamp¹, and Marife D. Corre¹

¹Soil Science of Tropical and Subtropical Ecosystems, Faculty of Forest Sciences and Forest Ecology, University of Goettingen, Goettingen, Büsgenweg 2 37077, Germany

²Julius Kühn Institute (JKI) – Federal Research Centre for Cultivated Plants, Institute for Ecological Chemistry, Plant Analysis and Stored Product Protection, Berlin, Germany

Key Points:

- The tree row in the agroforestry decreased annual gross N₂O emission and increased annual gross N₂O uptake compared to monoculture.
- Reduced gross N₂O emission was directly regulated by mineral N, C availability and WFPS rather than denitrification gene abundance.
- The increased gross N₂O uptake in the agroforestry was largely controlled by the low mineral N-to-CO₂-C ratio in the tree row.

2.1. Abstract

Conversion of monoculture to agroforestry (integrating trees with crops) is promoted as a promising management in reducing N₂O emissions from croplands. How agroforestry influences gross N₂O emission (N₂O+N₂ from N₂O reduction) and uptake (N₂O reduced to N₂) compared to monoculture is unknown. We used the ¹⁵N₂O pool dilution technique to quantify these processes using soil cores (top 5 cm) incubated in the field with monthly measurements over two growing seasons (2018–2019) at two sites (each with paired agroforestry and monoculture) and one site with monoculture only. The unfertilized tree rows showed the lowest gross N₂O emissions ($P \leq 0.002$). Although tree rows occupied only 20% in agroforestry, gross N₂O emissions tended to decrease by 6–36% in agroforestry (0.98–1.02 kg N₂O-N ha⁻¹ yr⁻¹) compared to monoculture (1.04–1.59 kg N₂O-N ha⁻¹ yr⁻¹). Gross N₂O emissions were influenced by soil mineral N, soil respiration and moisture content rather than by denitrification gene abundance. Soil gross N₂O uptake was highest in the tree row and decreased with distance into crop rows ($P = 0.012$). The agroforestry tended to increase gross N₂O uptake by 27–42% (0.38–0.44 kg N₂O-N ha⁻¹ yr⁻¹) compared to monoculture (0.30–0.31 kg N₂O-N ha⁻¹ yr⁻¹). In tree rows, soil gross N₂O uptake correlated with *nirK* gene abundance which was indirectly influenced by the low mineral N-to-soil CO₂-C ratio. Adjusting the tree and crop areal coverages of agroforestry and optimizing fertilization can further augment the benefits of agroforestry in reducing emission and increasing uptake of N₂O in soils.

Plain Language Summary

Nitrous oxide (N₂O) is a potent greenhouse gas and its largest anthropogenic source is from nitrogen fertilization in agriculture. Conversion of cropland monoculture to agroforestry (integrating trees with crops) is one promising mitigation practice to reduce soil N₂O emissions from agriculture. We quantified gross rates of N₂O emission (N₂O+N₂ from N₂O reduction) and uptake (N₂O reduced to N₂) in the soil to evaluate how agroforestry performs compared to monoculture. Our findings showed that agroforestry decreased gross N₂O emissions and increased gross N₂O uptake. These were due to the absence of nitrogen fertilization and increased soil respiration (which partly indicated increase in carbon availability to soil microbes) in the tree row. These findings suggest that if fertilizer inputs are optimized without sacrificing crop yield or profit, combined with the impact of tree rows on increasing soil N₂O uptake,

agroforestry will be an efficient mitigation strategy to curb N₂O emission from croplands. The benefits of agroforestry in reducing gross N₂O emission and increasing gross N₂O uptake in soils should be included in the economic valuation to support its policy implementation and adoption by farmers.

2.2. Introduction

Nitrous oxide (N₂O) is an important ozone-depleting substance and a potent greenhouse gas (GHG) with 298 times global warming potential relative to CO₂ in a 100-year time frame (IPCC, 2014). The main source of N₂O is croplands, which occupy about 12% of the Earth's ice-free land (Foley et al., 2011). Soil N₂O emissions from croplands have increased from 0.3 to 3.3 Tg N₂O-N yr⁻¹ in recent decades (2007 – 2016), accounting for 82% of the global N₂O increase (Tian et al., 2018), as a result of cropland expansion and increased fertilizer use to meet the food demand of the growing human population (IPCC, 2019). Therefore, meeting the goal of keeping global warming below 2 °C by 2100 requires the adoption of a set of strategies to reduce detrimental impacts of increasing N fertilizer use in agriculture on the environment (Galloway et al., 2008).

Agroforestry, i.e. simultaneous cultivation of trees and crops in arable land, is promoted as one of the promising strategies to mitigate climate change and reduce nutrient leaching losses while maintaining agricultural productivity (Smith et al., 2013). Modern agroforestry systems in the temperate zone include alley-cropping systems that alternate rows of trees with rows of crops, whereby fast-growing trees (e.g. *Populus nigra* × *P. maximowiczii*) are used for feedstock of bioenergy production (Schmidt et al., 2021). These systems have been shown to be profitable (Langenberg et al., 2018) and deliver ecosystem services such as carbon (C) sequestration (Ma et al., 2020b; Pardon et al., 2017), biodiversity improvement (Banerjee et al., 2016; Beule and Karlovsky, 2021), food production and security (Schmidt et al., 2021; Beule et al., 2019b; Beaudette et al., 2010), and climate mitigation (Chapman et al., 2020; Wolz et al., 2018b). Few studies in the temperate zone suggest that cropland agroforestry reduces soil N₂O emissions (Amadi et al., 2017; Amadi et al., 2016; Beaudette et al., 2010). These studies, however, focused mainly on net soil N₂O flux (e.g. using the static chamber method), which is the net balance of the simultaneously occurring processes of gross emission and gross uptake of N₂O in soils. Net N₂O flux measurement does not allow us to delve into the mechanisms driving N₂O emission

and uptake. The Intergovernmental Panel on Climate Change has included the net N₂O uptake by soils in the global N₂O budget in 2013, showing that this sink is possibly more important than previously assumed (Chapuis-Lardy et al., 2007). At present, only one-third of studies reported both N₂O and N₂ fluxes in the past decades (1975 – 2015) in terrestrial ecosystems (Almaraz et al., 2020). It is therefore imperative to quantify separately gross N₂O production and consumption for systematic comparison between cropland agroforestry and monoculture to fill the knowledge gap of field-based quantification of N₂O production and consumption in response to land-use/management change.

Moreover, quantifying the relationships of gross N₂O production and consumption with controlling factors will advance our predictive understanding of the soil N₂O flux dynamics (Sihi et al., 2020; Yang & Silver, 2016a). The ¹⁵N₂O pool dilution (¹⁵N₂O PD) technique enables the simultaneous measurement of gross N₂O fluxes without extensive soil disturbance (e.g., Wen et al., 2016; Yang et al., 2011). Previous studies that applied this method denoted the terms “gross N₂O production” and “gross N₂O consumption” (Yang et al., 2011; Yang & Silver, 2016a, 2016b). Later, however, Wen et al. (2016) had compared the gas-flow soil core method (Butterbach-Bahl et al., 2002) with the ¹⁵N₂O PD technique, and their values differed. This suggests that while ¹⁵N₂O PD method quantifies gross rates of N₂O emitted and reduced within interconnected soil pores, it may have excluded anaerobic microsites (e.g., soil micro spots saturated with water, isolated pores filled with or enclosed by water, and water-entrapped N₂O) which are not in direct exchange with the soil air (Figure S2.1). Thus, Wen et al. (2016) proposed to use the terms “gross N₂O emission and uptake” when employing the ¹⁵N₂O PD technique, as we used in our present study. So far, gross N₂O emission and uptake have only been investigated in a few land-use systems: temperate forest (Wen et al., 2017), managed grassland (Yang et al., 2011), cropland and salt marsh landscape (Yang & Silver, 2016a, 2016b).

Denitrification and nitrification are the main sources of N₂O in the soil, while denitrification is the only known soil-borne sink of N₂O (i.e., N₂O reduction to N₂, catalyzed by N₂O reductase that is encoded by the *nos* gene cluster) (Chapuis-Lardy et al., 2007; Juhanson et al., 2017). Previous studies on gross N₂O emission and uptake reported that soil mineral N and available C are the main controls in a forest (Wen et al., 2017) and a fertilized corn cropland (Yang & Silver, 2016b). Soil moisture and temperature regulate gross N₂O fluxes through their effects on gas

diffusion and their redox influence on microbial N and C cycling processes (e.g., Butterbach-Bahl et al., 2013; Davidson et al., 2000; Müller & Sherlock, 2004). Moreover, soil texture, management practices associated with crop types or trees (i.e., agroforestry) and climate influence those small-scale regulating factors by altering available N and C levels, soil moisture, and microbial community composition (Beule & Karlovsky, 2021; Lang et al., 2019; Mitchell et al., 2020; Strickland et al., 2015). At our present study sites, agroforestry tree rows reduce wind speed and result in low evapotranspiration (Kanzler et al., 2019; Markwitz et al., 2020), which may maintain higher soil moisture compared to cropland monoculture. At the same study sites, agroforestry tree rows are unfertilized (Beule et al., 2020; Schmidt et al., 2021), and thus have a low soil mineral N but large N response efficiency due to the trees' high biomass production (Schmidt et al., 2021). As opposed to the commonly fertilized crop rows of agroforestry and monocultures, the high litter inputs in the agroforestry tree rows may lead to a lower mineral N-to-available C ratio, which favors N₂O reduction to N₂ (Weier et al., 1993). Also, Beule et al. (2020) found that tree rows promote the population size of denitrifying microorganisms relative to monoculture, suggesting a greater potential for complete denitrification (with N₂ as the end product) under the trees as compared to cropland monoculture. At present, there is lacking quantitative assessment of the relationships among gross N₂O fluxes, substrate levels, soil moisture and temperature conditions, and denitrification gene abundance in response to management change (i.e., monoculture to agroforestry); such field-based quantitative relationships may improve biogeochemical models at a large scale.

Our objectives were to: (1) quantify gross N₂O emission and gross N₂O uptake in cropland agroforestry and monoculture systems, and (2) assess the relationship of gross N₂O fluxes with soil controlling factors, including a suite of denitrification gene abundance (*nirK*, *nirS*, *nosZ* clades), during two growing seasons at three sites on different soils in Germany. We hypothesized that (1) cropland agroforestry will have lower gross N₂O emission and higher gross N₂O uptake than monocultures, and (2) this pattern of gross N₂O fluxes will reflect the changes in substrate levels, soil moisture and temperature conditions as well as in denitrifier population size. Our findings provide support on GHG regulation function for policy implementation of agroforestry.

2.3. Materials and Methods

2.3.1. Study sites and experimental design

Our study was conducted at three sites in Germany, of which two sites had paired cropland agroforestry and monoculture on a loam Calcaric Phaeozem soil (at Dornburg, Thuringia) and a clay Vertic Cambisol soil (at Wendhausen, Lower Saxony) and one site was a cropland monoculture on a sandy Arenosol soil (at Vechta, Lower Saxony) (Figure 2.1a; soil characteristics in Table S2.1). Hereafter, we refer to these study sites by their soil types, based on FAO World Reference Base soil classification. The cropland agroforestry systems at the two sites were established by converting cropland monoculture into poplar-based alley cropping systems. At each site, the crops of the adjacent cropland agroforestry and monoculture were managed identically (i.e., the same crops, fertilization period and rates, and cultivation and harvesting methods; Table 2.1), and the monoculture served as the reference land use prior to agroforestry conversion. The two cropland agroforestry systems were established in 2007 at the site with a Phaeozem soil and in 2008 at the site with a Cambisol soil. Each agroforestry system consisted of 12-m wide poplar (poplar clone max 1; *Populus nigra* × *P. maximowiczii*) rows planted by hand from cuttings and 48-m wide crop rows in a north-south orientation, commonly done to minimize differences in light availability (Pardon et al., 2018; Swieter et al., 2019). The aboveground tree biomass of the agroforestry systems in the Phaeozem and Cambisol soils was harvested for biofuel at the beginning of 2015 and 2014 (Table 2.1), respectively. The regrown poplar trees at these two agroforestry sites were 4 to 5 years old during our study period (from March 2018 to September 2019). The crop rotations at the three study sites included summer barley (*Hordeum vulgare*), winter oilseed rape (*Brassica napus*), winter wheat (*Triticum aestivum*), rye (*Secale cereale*), corn (*Zea mays*), and potato (*Solanum tuberosum*) (Table 2.1). Fertilization was generally applied in spring to cropland monocultures and agroforestry crop rows. The agroforestry tree rows were not fertilized, as commonly practiced in temperate agroforestry systems (Tsonkova et al., 2012; Schmidt et al., 2021).

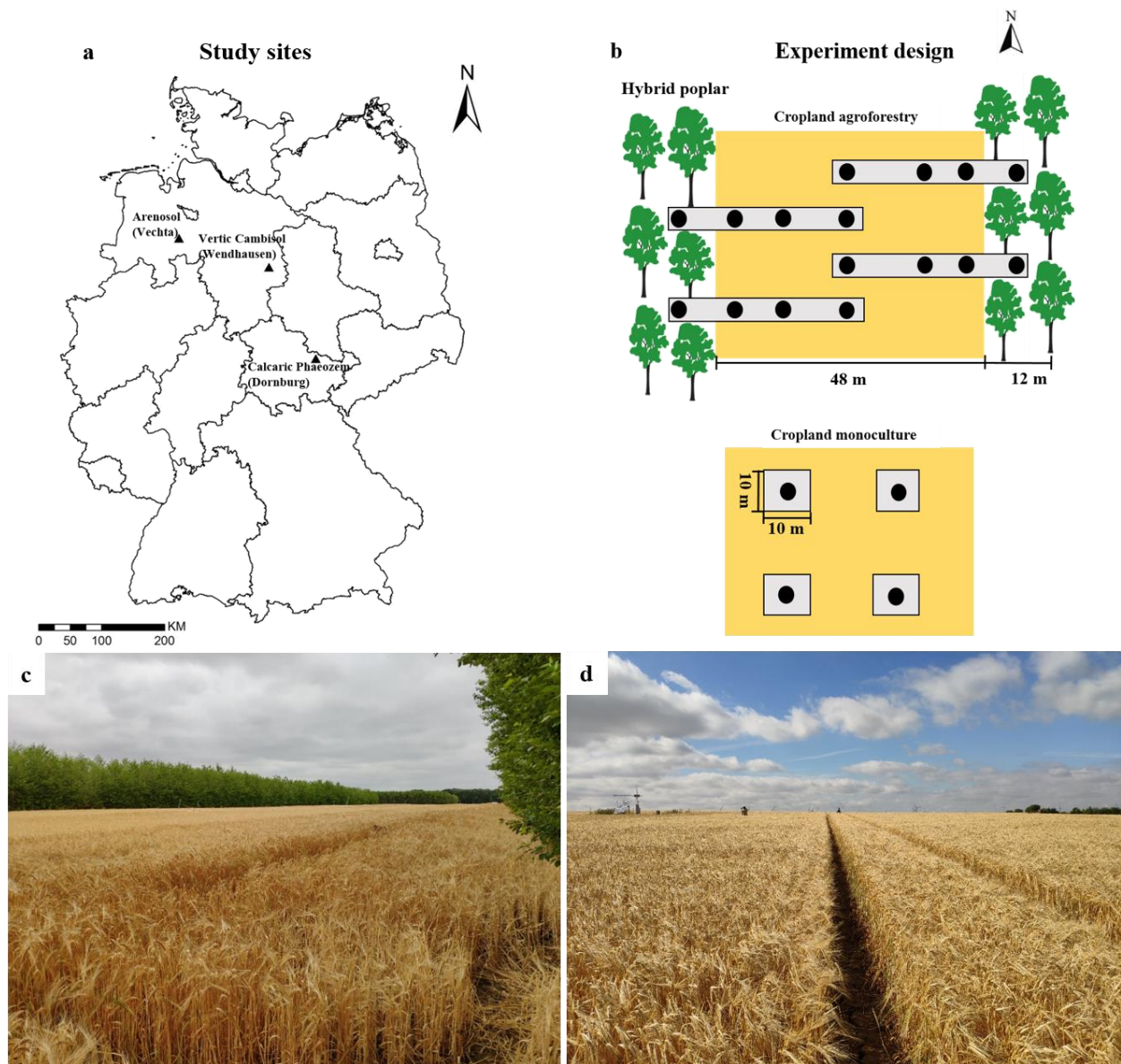


Figure 2.1 (a) Locations of the three study sites in Germany. (b) The layout of the experimental design: ● indicate sampling locations (in the cropland agroforestry, each replicate plot (□) was sampled at the tree row, 1-m, 7-m, and 24-m distances from the tree row; in the cropland monoculture, measurements were taken in the center of each replicate plot). (c) Cropland agroforestry and (d) monoculture at Dornburg in the Phaeozem soil (picture credit: G. Shao).

Table 2.1*Site Characteristics and Management Practices at Three Sites of Cropland Agroforestry and Cropland Monocultures in Germany*

Study site	Dornburg	Wendhausen	Vechta
Soil type	Calcaric Phaeozem	Vertic Cambisol	Arenosol
Location	51°00'40" N, 11°38'46" E	52°20'00" N, 10°37'55" E	52°45'29" N, 8°32'5" E
Mean annual air temperature			
Long-term (2010-2019)	10.7 ± 0.3 °C ^a	10.7 ± 0.3 °C ^b	10.1 ± 0.1 °C ^c
Study period (2018-2019)	11.5 ± 0.1 °C ^a	11.5 ± 0.1 °C ^b	10.9 ± 0.1 °C ^c
Mean annual precipitation			
Long-term (2010-2019)	567 ± 32 mm ^a	587 ± 41 mm ^b	643 ± 35 mm ^c
Study period (2018-2019)	450 ± 35 mm ^a	479 ± 99 mm ^b	577 ± 157 mm ^c
Elevation (m above sea level)	289	82	38
Year of agroforestry establishment	2007	2008	none
Harvest of the aboveground tree biomass in the agroforestry	January 2015	January 2014	none

Crops rotation in 2016-2017-2018-2019	Summer barley-winter oilseed rape-winter wheat-summer barley	Winter oilseed rape- winter wheat-winter wheat-corn	Corn-potato-rye-corn
Sowing and harvest of the crops	October 2017, July 2018 March 2019, July 2019	October 2017, July 2018 April 2019, October 2019	October 2017, July 2018 April 2019, September 2019
Fertilization rates in 2018 & 2019 (kg N-P-K ha ⁻¹ yr ⁻¹)	213 - 0 - 0 (2018) 36 - 22 - 31 (2019)	166 - 0 - 116 (2018) 101 - 0 - 0 (2019)	188 - 26 - 108 (2018) 153 - 54 - 62 (2019)

Note. ^a climate station at Jena (station ID: 2444), ^b Braunschweig (station ID: 662), and ^c Diepolz (station ID: 963) of the German Meteorological Service.

Four replicate plots were established at each of the cropland agroforestry and monoculture systems in the Phaeozem and Cambisol soils, and eight replicate plots were established in the cropland monoculture in the Arenosol soil. Each replicate plot in the cropland agroforestry represented a transect spanning from the center of the tree row into the center of the crop row to capture a spatial gradient induced by the tree rows. Each of these transects had four sampling locations: at the center of tree row and from the tree row at 1 m, 7 m, and 24 m within the crop row (Figure 2.1b). In the field, we observed that the fertilizer broadcaster drove at 12 m from the tree row; the fertilizers were broadcasted for the entire 12 m length at each side, and the broadcaster turned around for the remaining 24 m crop row to be fertilized. At mid-way (24 m) of the agroforestry crop row, the fertilizers were broadcasted with about 1 m overlapped, such that at the middle of this crop row the amount of fertilizers were possibly more than the rest of the length of the crop row. In the cropland monocultures, measurements were carried out at the center of each replicate plot (Figure 2.1b). Thus, on each monthly sampling, there were 20 measurements in the Phaeozem and Cambisol soils (4 replicate plots in the agroforestry \times 4 sampling locations + 4 replicate plots in the monoculture), and eight measurements in the Arenosol soil (8 replicate plots in the monoculture).

2.3.2. Measurement of gross N₂O emission and uptake

Gross N₂O emission and gross N₂O uptake were measured monthly from March 2018 to September 2019 in the field, using the ¹⁵N₂O pool dilution technique as described by Wen et al. (2016, 2017) and adapted from Yang et al. (2011). At each of the four sampling locations per replicate plot of the agroforestry or at each replicate plot in the monoculture systems, four intact 250-cm³ soil cores of the top 5-cm depth were collected and placed in an air-tight chamber (glass desiccator of 6.6 L volume), equipped with a Luer-lock stopcock on the lid (Figure S2.2), for immediate incubation in the field. We injected 7 ml of ¹⁵N₂O label gas into the chamber headspace, which was composed of 100 ppm_v of 98% single labeled ¹⁵N-N₂O, 275 ppb_v sulfur hexafluoride (SF₆, as a tracer for possible physical loss of gases from the chamber headspace) and balanced with synthetic air (Westfalen AG, Münster, Germany). This label gas resulted in initial headspace concentrations of approximately 125 ppb_v N₂O with 13.2% ¹⁵N initial enrichment and 344 ppt_v SF₆. Based on conservative calculations, the diffusion of labeled ¹⁵N₂O through the 5 cm long soil cores shows that the labeled ¹⁵N₂O diffuses into the soil and back to

the headspace within 0.5 h (Wen et al., 2016). Thus, our sampling of the chamber headspace at 0.5 h and thereafter hourly during a 3-hour in-situ incubation was sufficient to allow a homogeneous mixture of $^{15}\text{N}_2\text{O}$ with soil-derived N_2O . At 0.5 h, 1 h, 2 h, and 3 h in-situ incubation, gas samples of 100 ml and 23 ml were taken from the chamber headspace and injected respectively into a pre-evacuated 100-ml glass bottle and 12-ml glass vial (Exetainer; Labco Limited, Lampeter, UK) with rubber septa (Figure S2.2). To maintain the headspace at atmospheric pressure and oxygen concentration, the sampled air volume at each time was replaced by a 123 ml gas mixture of 80% helium and 20% oxygen (v/v) so as not to change the ^{15}N - N_2O isotope composition in the headspace (Wen et al., 2016, 2017). The dilution caused by this replacement was accounted for in the calculations. The 100-ml gas samples were analyzed for isotopic composition using an isotope ratio mass spectrometer (Finnigan Delta^{plus} XP, Thermo Electron Corporation, Bremen, Germany). The 23-ml gas samples were analyzed for N_2O and SF_6 concentrations, using a gas chromatograph (SRI 8610C, SRI Instruments Europe GmbH, Bad Honnef, Germany) with an electron capture detector (and a make-up gas of 5% CO_2 -95% N_2 , 5.0 purity grade), as well as for CO_2 concentrations using the same gas chromatograph but with a methanizer and flame ionization detector. During each in-situ incubation, air temperature and pressure were measured as well as ambient air samples were taken (23 ml for determination of ambient N_2O concentration and 100 ml for analysis of natural abundance $^{15}\text{N}_2\text{O}$ signatures) to be used for the gross N_2O flux calculations. Atmospheric N_2O concentration was 345.9 ± 0.5 ppb_v and ^{15}N natural abundance was 0.3691 ± 0.0001 atom% across the three sites over the 1.5-year measurement period. Details on the principles and calculations of gross N_2O emission and uptake were given in our earlier works (Wen et al., 2016, 2017). Net soil N_2O and CO_2 fluxes were calculated from the linear increase of their concentrations during the incubation period and adjusted with the measured air temperature and pressure (e.g., Matson et al., 2017).

Gross N_2O , net N_2O , and soil CO_2 fluxes were expressed on the dry mass of intact soil cores, determined from the concurrently measured gravimetric moisture content (see Section 2.3). Annual soil gross N_2O fluxes from each sampling location at each replicate plot were calculated by trapezoidal interpolation between fluxes and sampling day intervals from March 2018 to February 2019 (e.g., Koehler et al., 2009; Matson et al., 2017; Veldkamp et al., 2013). The annual fluxes were converted from mass-basis to area-basis for the top 5-cm depth, using the

measured soil bulk density (see Section 2.3), which was averaged for each site (1.0 g cm^{-3} for the Phaeozem and Cambisol soils, and 1.3 g cm^{-3} for the Arenosol soil).

For the agroforestry system as a whole, gross N_2O fluxes at each replicate plot were weighted by the areal coverages of the tree row and the crop row sampling locations. The weighting factors were calculated by considering half of the widths of the tree row (6 m) and the crop row (24 m), totaling to 30 m, since these alternating tree and crop rows indicated that half of their widths represented each side of the rows (Figure 1b). Considering the 1-m width overlap of the fertilizer broadcaster at 24 m (see above), we calculated the overall values for agroforestry in two ways. First, only considering the weighting factors of the tree row (0.2, for 6 m/30 m), 1 m (0.13, for 4 m/30 m), and 7 m (0.67, for 20 m/30 m). Second, we included the 24 m using a weighting factor of 0.07 (for 2 m/30 m) and adjusting the weighting factor of the 7 m to 0.6 (for 18 m/30 m). This weighting factor of 24 m was derived by a 1-m increment adjustment between the 7 m and 24 m, and we found that the statistical results did not change regardless of the adjusted weighting factors between these two sampling locations.

2.3.3. Soil controlling factors

Following the measurement of the gross N_2O fluxes, soil controlling factors (temperature, WFPS, NO_3^- , ammonium [NH_4^+] and denitrification genes *nirK*, *nirS*, *nosZ* clade I and II, see section 2.3.4) were all determined from the soil cores on each sampling day. Additionally, microbial biomass C and N were measured at a quarterly interval from the soil cores following gross N_2O flux measurements. The gravimetric moisture content (oven-drying soil sample at $105 \text{ }^\circ\text{C}$ for 1 day) was expressed in WFPS using the average bulk density (determined from one of the four soil cores used for the monthly measurements of gross N_2O fluxes) for each soil type (or site) and the mineral soil particle density of 2.65 g cm^{-3} . The remaining three soil cores were pooled, mixed thoroughly in the field and a subsample was immediately put into a pre-weighed extraction bottle containing 150 ml $0.5 \text{ M K}_2\text{SO}_4$ for the determination of extractable mineral N. Additionally, a subsample of approximately 20 g soil was directly transferred to a sterile 15-ml polypropylene Falcon tube and frozen at $-20 \text{ }^\circ\text{C}$ in the field for DNA extraction and quantification of denitrification genes (see section 2.4). Upon arrival at the laboratory, extraction bottles were shaken for 1 h, filtered and the extracts were frozen immediately until further analysis. Microbial biomass C and N were determined using the chloroform fumigation-

extraction method (Brookes et al., 1985) by fumigating about 20 g fresh soil for 5 days, followed by extraction with 100 ml 0.5 M K_2SO_4 . The dry mass of the extracted fresh soils as well as the fumigated soils was calculated using the concurrently measured gravimetric moisture content. Microbial biomass C and N were calculated as the difference in the extractable C and total extractable N between the paired fumigated and un-fumigated soils divided by k_C and k_N factors of 0.45 and 0.68, respectively (Shen et al., 1984). Extractable organic C concentration was measured using ultraviolet-enhanced persulfate oxidation using a Total Organic Carbon Analyzer (TOC-Vwp, Shimadzu Europa GmbH, Duisburg, Germany). The extractable mineral N (NH_4^+ , NO_3^-) and total extractable N concentrations were analyzed using continuous flow injection colorimetry (SEAL Analytical AA3, SEAL Analytical GmbH, Norderstedt, Germany), where NH_4^+ was determined by salicylate and dichloroisocyanuric acid reaction, NO_3^- by cadmium reduction method with NH_4Cl buffer and total extractable N by ultraviolet-persulfate digestion followed by hydrazine sulfate reduction.

General soil characteristics in the top 30 cm (pH, total N, organic C, effective cation exchange capacity, base saturation, and clay content) were determined using standard methods as described in our previous work (Schmidt et al., 2021; Table S2.1).

2.3.4. Quantification of denitrification genes in soil

Denitrification genes were quantified in the Phaeozem and Cambisol soils from the soil samples frozen right at the field following gross N_2O flux measurement. Frozen soils were freeze-dried for 72 h and subsequently homogenized using a swing mill (MM400, Retsch, Haan, Germany) at 25 Hz for 1 minute. Soil DNA was extracted from 50 mg finely ground freeze-dried soil, using a modified protocol of Brandfass and Karlovsky (2008), as described previously (Beule et al., 2019a). Briefly, the soil was suspended in 1 ml cetyltrimethylammonium bromide buffer with proteinase K. The mixture was incubated at 42 °C and subsequently at 65°C for 10 minutes each, and 800 μ l phenol was added. The mixture was shaken, centrifuged and the supernatant was extracted twice with chloroform/isoamylalcohol. DNA from the obtained supernatant was precipitated using polyethylene glycol/NaCl, pelleted using centrifugation, washed twice with 80% (w/v) EtOH and dried using a vacuum centrifuge. The dried pellets were re-suspended in 50 μ l TE buffer (10 mM Tris/HCl, 1 mM EDTA, pH 8.0). Extraction success was verified on agarose

gels. Soil DNA extracts were tested for PCR inhibitors as described previously (Guerra et al., 2020) and diluted in 1:50 double-distilled H₂O to overcome inhibitory effects on PCR.

Nitrite (NO₂⁻) reductase (*nirK* and *nirS*) and N₂O reductase genes (*nosZ* clade I and II) were quantified using real-time PCR (qPCR), as described previously (Beule et al., 2019a). Briefly, denitrification genes were amplified from diluted soil DNA extracts in a CFX 384 Thermocycler (Biorad, Rüdigenheim, Germany) using 4 µl reaction volume. The reaction volume contained Standard *Taq* Reaction Buffer (New England Biolabs, Beverly, Massachusetts, USA; 10 mM Tris-HCl, 50 mM KCl, 1.5 mM MgCl₂, pH 8.3 at 25°C) adjusted to different final concentrations of MgCl₂ (Table S2.2), 100 µM of each deoxyribonucleoside triphosphate, 0.5 or 1.0 µM of each primer (Table S2.2), 1 µg/µl bovine serum albumin, 0.03 u/µl Hot Start *Taq* DNA Polymerase (New England Biolabs, Beverly, Massachusetts, USA), 0.1 × SYBR Green I solution (Invitrogen, Karlsruhe, Germany) and 1 µl template DNA or in double-distilled H₂O for negative controls. Primer choice and thermocycling conditions are listed in Table S2.3.

2.3.5. Statistical analysis

First, we tested each parameter for normal distribution using Shapiro-Wilk's test and for equality of variance using Levene's test. Parameters with non-normal distribution or unequal variances were either logarithmically (i.e., soil respiration, total mineral N [sum of NO₃⁻ and NH₄⁺], *nirK*, *nirS*, *nosZ* clade I, and II) or cube-root transformed (i.e., gross N₂O emission, gross N₂O uptake, and microbial biomass N). Linear mixed effect (LME) models were used to assess the differences between agroforestry and monocultures at each site with management system as fixed effect or the differences among cropland monocultures with soil type as fixed effect; sampling day and replicate plot were considered as random effects (Crawley, 2007). These LME models were extended to include either (1) a variance function (varIdent) that allow variance heteroscedasticity of the fixed effect, and/or (2) a first-order temporal autoregressive function that assumes decreasing auto-correlation between sampling days with increasing time difference (Zuur et al., 2009) if this improved the relative goodness of the model fit based on the Akaike information criterion. To evaluate the differences in gross rates of N₂O fluxes between the agroforestry as a whole and the monoculture, the agroforestry was weighted by the areal coverage of the agroforestry sampling locations and LME was conducted as above.

To assess the temporal relationships between concurrently measured soil gross N₂O fluxes and soil variables, we carried out a stepwise analysis: first within each management system at each site, and then across management systems and sites when the relationships were similar. We used the average of the four (for Phaeozem and Cambisol soils) or eight plots (Arenosol soil) on each monthly measurement and conducted Pearson correlation as well as regression analyses over the entire measurement period. The 95% confidence interval of the regression parameters is provided for an estimate of dispersion. Across sites, the total number of observations (n) was 167; the Phaeozem soil had $n = 75$ (i.e., 15 monthly measurements \times 4 sampling locations in the agroforestry + 15 monthly measurements in monoculture), the Cambisol soil had $n = 80$ (i.e., 16 monthly measurements \times 4 sampling locations in the agroforestry + 16 monthly measurements in monoculture), and the Arenosol soil had $n = 12$ (12 monthly measurements in monoculture). For the denitrification genes, these were measured in the Phaeozem and Cambisol soils, and hence $n = 155$. The combined effects of soil variables (which are not auto-correlated based on Pearson correlation tests) on gross N₂O fluxes were assessed using a stepwise multiple regression with forward variable selection. We conducted this multiple regression analysis separately for agroforestry and monoculture systems, with the purpose that such regression relationships may be useful in adapting predictive models for similar temperate land-use management. All statistical tests were considered significant at $P \leq 0.05$. We conducted all statistical analyses using R version 3.6.3 (R Core Team, 2019).

2.4. Results

2.4.1. Gross N₂O fluxes

Peaks of gross N₂O emissions in crop rows of agroforestry and monoculture (Figure 2.2a-c) corresponded to the periods of fertilization in spring when WFPS was high (Figure S2.3a-c) and soil temperature was increasing (Figure S2.3d-f). Gross N₂O emissions from the agroforestry were lower in the tree row than in the crop row in both Phaeozem and Cambisol soils ($P \leq 0.002$; Table 2.2). Despite slight decreases in gross N₂O emissions in agroforestry as a whole (area-weighted by the tree and crop rows), these did not differ from the monocultures ($P \geq 0.15$; Table 2.2). Among the cropland monocultures, the clay Cambisol soils had larger gross N₂O emissions than the sandy Arenosol soil ($P = 0.006$; Table 2.2).

On the other hand, no clear seasonal pattern of gross N₂O uptake was observed at our sites (Figure 2.2d-f). Gross N₂O uptake was higher in the tree row than in the center of the crop row in the Phaeozem soil ($P = 0.012$; Table 2.2), and the entire agroforestry showed higher N₂O uptake than the monoculture ($P = 0.046$; Table 2.2). This pattern was not statistically significant in the Cambisol soil ($P = 0.31$; Table 2.2).

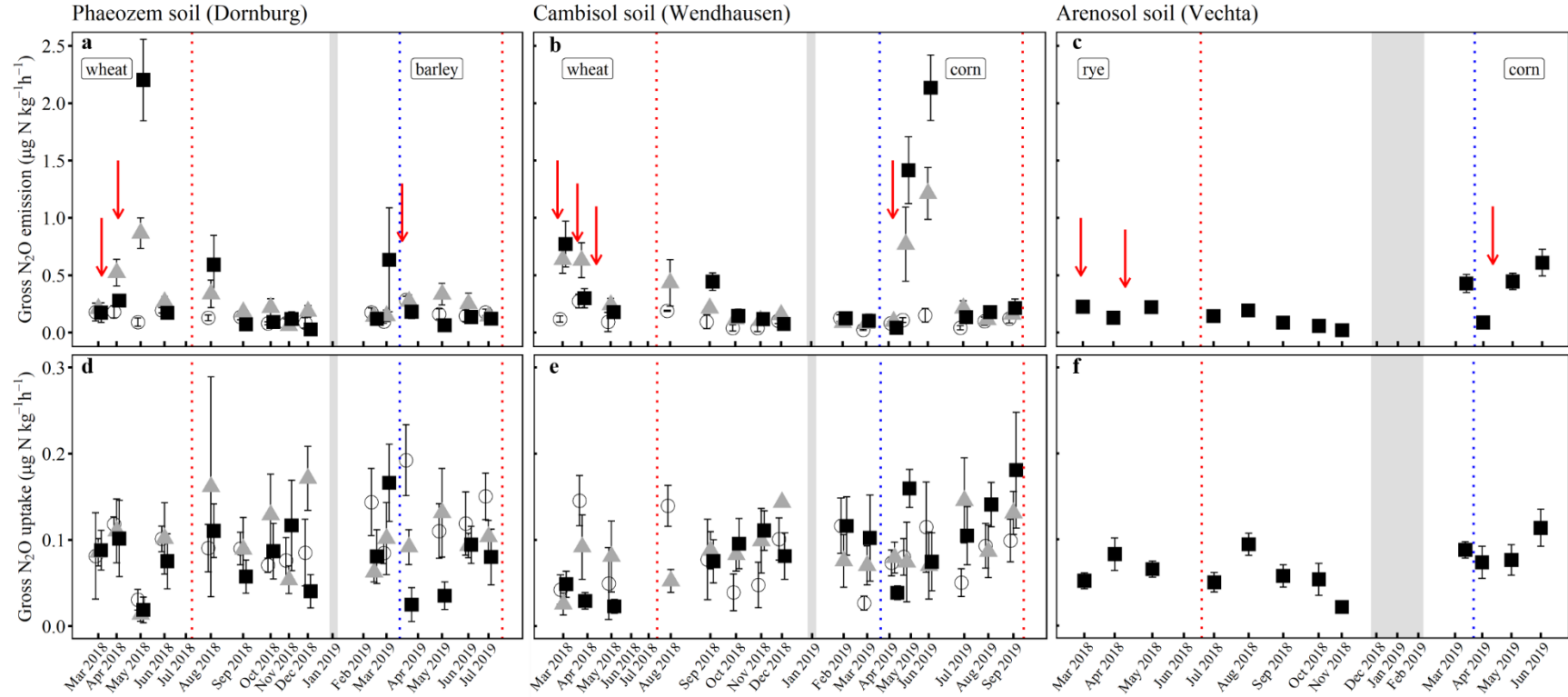


Figure 2.2 Mean (\pm SE, $n = 4$ plots for the Phaeozem and Cambisol soils, $n = 8$ plots for the Arenosol soil) gross rates of soil N₂O emission (upper panels, a, b, c) and uptake (lower panels, d, e, f), measured monthly in the top 5-cm depth using ¹⁵N₂O pool dilution technique at three sites of cropland agroforestry and cropland monocultures in Germany. Agroforestry tree row (○) and crop row (area-weighted average of the 1-m, 7-m, and 24-m sampling locations, ▲); monoculture (■). The site with an Arenosol soil was a cropland monoculture during the measurement period. June and July 2018 were extremely dry months, during which intact soil cores cannot be collected. Red dotted lines indicate harvest and blue dotted lines indicate sowing; gray shadings indicate frozen soil during winter when intact soil cores cannot be collected; red arrows indicate fertilizer applications in the agroforestry crop row (tree rows are commonly not fertilized) and the monocultures (fertilization rates are in Table 2.1).

Table 2.2

Mean (\pm SE, $n = 4$ Plots for the Phaeozem and Cambisol Soils, $n = 8$ Plots for the Arenosol Soil) and Annual Gross Rates of Soil N₂O Emission and Uptake across Monthly Measurements from March 2018 to September 2019 in the Top 5-cm Depth, Measured using ¹⁵N₂O Pool Dilution Technique, at Three Sites of Cropland Agroforestry and Cropland Monocultures in Germany

Soil type (Site)	Management system	Gross N ₂ O emission ($\mu\text{g N kg}^{-1} \text{ h}^{-1}$)	Gross N ₂ O uptake ($\mu\text{g N kg}^{-1} \text{ h}^{-1}$)	Annual gross N ₂ O emission ($\text{kg N ha}^{-1} \text{ yr}^{-1}$)	Annual gross N ₂ O uptake ($\text{kg N ha}^{-1} \text{ yr}^{-1}$)
Phaeozem (Dornburg; 2018 – Wheat; 2019 – Barley)	Tree row	0.15 ± 0.02^b	0.10 ± 0.02^a	0.54 ± 0.05	0.38 ± 0.04
	1 m crop row	0.21 ± 0.06^b	0.09 ± 0.02^{ab}	0.98 ± 0.27	0.37 ± 0.06
	7 m crop row	0.27 ± 0.07^{ab}	0.11 ± 0.03^{ab}	1.17 ± 0.15	0.48 ± 0.10
	24 m crop row	0.46 ± 0.12^a	0.07 ± 0.02^b	2.22 ± 0.39	0.27 ± 0.03
	Agroforestry	0.24 ± 0.05^A	0.10 ± 0.02^A	1.02 ± 0.08	0.44 ± 0.06
			(0.25 ± 0.05^A)	(0.10 ± 0.02^A)	(1.09 ± 0.07)
	Monoculture	0.33 ± 0.16^{abA}	0.08 ± 0.02^{abB}	1.59 ± 0.26	0.31 ± 0.02
Cambisol (Wendhausen; 2018 – Wheat;	Tree row	0.11 ± 0.01^b	0.08 ± 0.01^a	0.53 ± 0.07	0.38 ± 0.05
	1 m crop row	0.31 ± 0.05^a	0.09 ± 0.00^a	1.42 ± 0.46	0.38 ± 0.03

2019 – Corn)	7 m crop row	0.33 ± 0.03 ^a	0.09 ± 0.01 ^a	0.99 ± 0.04	0.38 ± 0.03
	24 m crop row	0.40 ± 0.06 ^a	0.11 ± 0.01 ^a	1.34 ± 0.09	0.42 ± 0.05
	Agroforestry	0.27 ± 0.08 ^A	0.08 ± 0.01 ^A	0.96 ± 0.06	0.38 ± 0.02
		(0.28 ± 0.08 ^A)	(0.09 ± 0.01 ^A)	(0.98 ± 0.05)	(0.39 ± 0.02)
Monoculture	0.42 ± 0.16 ^{aA}	0.09 ± 0.01 ^{aA}	1.04 ± 0.15	0.30 ± 0.03	
Arenosol (Vechta)	Monoculture	0.21 ± 0.08	0.07 ± 0.02	0.63 ± 0.08	0.30 ± 0.02

Note. For each site, means with different lowercase letters indicate significant differences between the monoculture and sampling locations within the agroforestry (linear mixed effect models with Fisher’s least significant difference test at $P \leq 0.05$). The different uppercase letters indicate significant differences between the monoculture and agroforestry as a whole, weighted by the areal coverage of the tree row and crop row sampling locations (linear mixed effect models with Fisher’s least significant difference test at $P \leq 0.05$). For agroforestry, the first values are area-weighted by the tree row, and at 1 m and 7 m distances from the tree row; the second values in parenthesis include the 24 m distance in area-weighting (see section 2.3.2). The site with the Arenosol soil was a cropland monoculture during the measurement period. Annual fluxes from March 2018 to February 2019 were not tested statistically for differences between agroforestry and monoculture since these values are trapezoidal extrapolations. Annual fluxes on mass-basis were converted into area-basis using the averaged soil bulk density in the top 5 cm measured at each site.

2.4.2. Soil variables

In the loam Phaeozem and clay Cambisol soils, WFPS was highest in the tree rows, followed by the crop rows and lowest in the monocultures ($P \leq 0.003$; Table 2.3). At these sites, WFPS ranged from 21 to 67 % during spring, from 22 to 45 % during summer, and from 23 to 65 % during fall (Figure S2.3a-b). The monoculture in the sandy Arenosol soil had the lowest WFPS ($P < 0.001$; Table 2.3), ranging from 19 to 46 % during spring, 18 to 23 % during summer, and 26 to 30 % during fall (Figure S2.3c). Soil temperature neither differed between management systems nor among sites, ranged from 7.1 to 25.2 °C during spring, from 15.7 to 29.2 °C during summer, and from -0.5 to 18.6 °C during fall (Figure S2.3d-f). In the Phaeozem and Cambisol soils, soil respiration showed a similar seasonal pattern as the WFPS and temperature (Figure S2.3g-i). Soil respiration was larger in the tree rows than in the crop rows and monocultures ($P \leq 0.014$; Table 2.3) whereas mineral N showed the converse pattern ($P \leq 0.011$; Table 2.3). Ratios of mineral N-to-soil CO₂-C in the Phaeozem and Cambisol soils, respectively, were: 4 ± 0 and 8 ± 1 in the agroforestry tree rows, 38 ± 1 and 112 ± 20 in the crop rows, and 101 ± 19 and 147 ± 28 in the monoculture. In the Phaeozem and Cambisol soils, microbial biomass C and N decreased with increasing distance from the tree row into the crop row ($P \leq 0.048$; Table 2.3) whereas the monocultures showed intermediate values ($P \geq 0.68$). The monoculture in Arenosol soil had the lowest microbial biomass C and N ($P < 0.001$; Table 2.3).

Table 2.3

Mean (\pm SE, $n = 4$ Plots for the Phaeozem and Cambisol Soils, $n = 8$ Plots for the Arenosol Soil) Water Content, Soil Respiration, Mineral N, Microbial Biomass N and C across Monthly Measurements from March 2018 to September 2019 in the Top 5-cm Depth at Three Sites of Cropland Agroforestry and Cropland Monocultures in Germany

Soil type (site)	Management system	Water-filled pore space (%)	Soil respiration (mg CO ₂ -C kg ⁻¹ h ⁻¹)	Total mineral N (mg kg ⁻¹)	Microbial biomass N (mg kg ⁻¹)	Microbial biomass C (mg kg ⁻¹)
Phaeozem (Dornburg)	Agroforestry					
	Tree row	47 ± 4 ^a	1.3 ± 0.2 ^a	4 ± 1 ^d	91 ± 9 ^a	573 ± 39 ^a
	1 m crop row	42 ± 3 ^a	0.9 ± 0.1 ^{bc}	12 ± 3 ^c	66 ± 8 ^{bc}	492 ± 49 ^{ab}
	7 m crop row	42 ± 2 ^a	1.1 ± 0.2 ^{ab}	24 ± 8 ^{bc}	69 ± 7 ^{ab}	474 ± 36 ^b
	24 m crop row	42 ± 2 ^a	1.0 ± 0.2 ^{ab}	63 ± 22 ^a	54 ± 16 ^c	377 ± 37 ^c
	Monoculture	34 ± 2 ^b	0.6 ± 0.1 ^c	38 ± 14 ^{ab}	81 ± 6 ^{ab}	565 ± 29 ^a
Cambisol (Wendhausen)	Agroforestry					
	Tree row	47 ± 3 ^a	0.7 ± 0.1 ^a	4 ± 1 ^b	108 ± 8 ^a	570 ± 110 ^a
	1 m crop row	41 ± 2 ^b	0.5 ± 0.1 ^b	30 ± 7 ^a	106 ± 29 ^{ab}	448 ± 51 ^{ab}

	7 m crop row	40 ± 2^b	0.5 ± 0.1^b	42 ± 12^a	64 ± 16^b	372 ± 53^b
	24 m crop row	41 ± 2^b	0.5 ± 0.1^b	39 ± 11^a	74 ± 14^{ab}	352 ± 74^b
	Monoculture	35 ± 2^c	0.4 ± 0.1^b	42 ± 12^a	75 ± 23^{ab}	311 ± 53^b
Arenosol (Vechta)	Monoculture	30 ± 3	0.7 ± 0.2	29 ± 14	33 ± 7	217 ± 22

Note. For each site, means with different lowercase letters indicate significant differences between the monoculture and sampling locations within the agroforestry (linear mixed effect models with Fisher's least significant difference test at $P \leq 0.05$).

2.4.3. Denitrification gene abundance

Among the denitrification genes, *nirK* (encoding for NO_2^- reductase) was the most abundant. The abundance of *nirK* gene decreased with increasing distance from the tree row into the crop row of the agroforestry systems and was lowest in the monoculture systems ($P \leq 0.013$; Table 2.4). The abundance of *nirS* gene (encoding for NO_2^- reductase) followed a similar spatial pattern as *nirK* among sampling locations ($P \leq 0.004$; Table 2.4). The abundance of *nosZ* clade I gene (encoding for N_2O reductase) was comparable between the agroforestry and monoculture in the Phaeozem soil (Table 2.4). In the Cambisol soil, *nosZ* clade I gene abundance was higher in the tree row than in the crop row of the agroforestry ($P < 0.001$; Table 2.4) but comparable to the cropland monoculture ($P = 0.07$; Table 2.4). The abundance of *nosZ* clade II gene (encoding for N_2O reductase) did not differ among sampling locations in the Phaeozem and Cambisol soils ($P \geq 0.13$; Table 2.4).

Table 2.4

Mean (\pm SE, $n = 4$ Plots for the Phaeozem and Cambisol Soils, $n = 8$ Plots for the Arenosol Soil) Denitrification Gene Abundances (*NirK*, *NirS*, *NosZ* Clade I, *NosZ* Clade II) across Monthly Measurements from March 2018 to September 2019 in the Top 5-cm Depth at Three Sites of Cropland Agroforestry and Cropland Monocultures in Germany

Soil type (site)	Management system	<i>nirK</i>	<i>nirS</i>	<i>nosZ</i> clade I	<i>nosZ</i> clade II
		(1 \times 10 ⁸ gene copy number g ⁻¹ dry soil)			
Phaeozem (Dornburg)	Agroforestry				
	Tree row	15.8 \pm 2.4 ^a	0.9 \pm 0.1 ^a	1.3 \pm 0.2 ^a	2.4 \pm 0.4 ^a
	1 m crop row	10.8 \pm 1.2 ^b	1.6 \pm 0.5 ^a	0.9 \pm 0.1 ^a	2.7 \pm 0.3 ^a
	7 m crop row	11.1 \pm 1.4 ^b	0.7 \pm 0.1 ^{ab}	1.0 \pm 0.1 ^a	2.6 \pm 0.3 ^a
	24 m crop row	10.5 \pm 1.7 ^b	0.6 \pm 0.1 ^b	1.0 \pm 0.2 ^a	2.5 \pm 0.3 ^a
	Monoculture	9.4 \pm 1.2 ^b	0.6 \pm 0.1 ^{ab}	1.2 \pm 0.2 ^a	2.1 \pm 0.2 ^a
Cambisol (Wendhausen)	Agroforestry				
	Tree row	10.9 \pm 1.9 ^a	1.1 \pm 0.2 ^a	2.3 \pm 0.4 ^a	1.5 \pm 0.3 ^a
	1 m crop row	4.7 \pm 0.7 ^b	0.7 \pm 0.1 ^b	1.3 \pm 0.2 ^{bc}	1.1 \pm 0.2 ^a
	7 m crop row	4.3 \pm 1.0 ^b	0.6 \pm 0.1 ^b	1.3 \pm 0.2 ^c	1.1 \pm 0.2 ^a

24 m crop row	4.2 ± 0.7^b	0.6 ± 0.1^b	1.2 ± 0.2^c	0.9 ± 0.2^a
Monoculture	3.9 ± 0.6^b	0.5 ± 0.1^b	1.7 ± 0.2^{ab}	0.9 ± 0.1^a

Note. For each site, means with different lowercase letters indicate significant differences between the monoculture and sampling locations within the agroforestry (linear mixed effect models with Fisher's least significant difference test at $P \leq 0.05$).

2.4.4. Temporal relationships between gross N₂O fluxes and soil factors

Gross N₂O emissions rather than gross N₂O uptake strongly determined net N₂O flux either across the three study sites (Figure 2.3a) or separately for each management system (Table 2.5). Across sites, gross N₂O emissions were influenced by total mineral N (Figure 2.3b) and soil respiration (Table S2.4). Although soil temperature showed a correlation with gross N₂O emissions, this was not solely by temperature but also by its auto-correlation with total mineral N and soil respiration (Table S2.4). Considering the variables that were not auto-correlated with each other (Table S2.4), the best predictive relationships for gross N₂O emissions from the agroforestry were total mineral N and soil respiration. Separating between the tree and crop rows of the agroforestry, total mineral N was the best predictor (or the limiting factor) for gross N₂O emissions from tree rows whereas both total mineral N and WFPS regulated the gross N₂O emissions from the crop rows (Table 2.5). For the monocultures, total mineral N, available C (which was lowest in monocultures; Table 2.3), and WFPS regulated the gross N₂O emissions (Table 2.5). We did not detect any significant correlations between gross N₂O emissions and the denitrification gene abundance.

On the other hand, there were no significant correlations between gross N₂O uptake and any of the measured soil variables either across sites or separately for agroforestry and monoculture systems. However, considering only the tree rows of the agroforestry, gross N₂O uptake was correlated with *nirK* gene abundance (Figure 2.3c), which was also linked with the *nosZ* clade II gene abundance (Pearson's $r = 0.62$, $P < 0.001$, $n = 31$). The *nosZ* clade II gene abundance was negatively correlated to mineral N-to-soil CO₂-C ratio, particularly when ratios were less than 10 (Figure 2.3d).

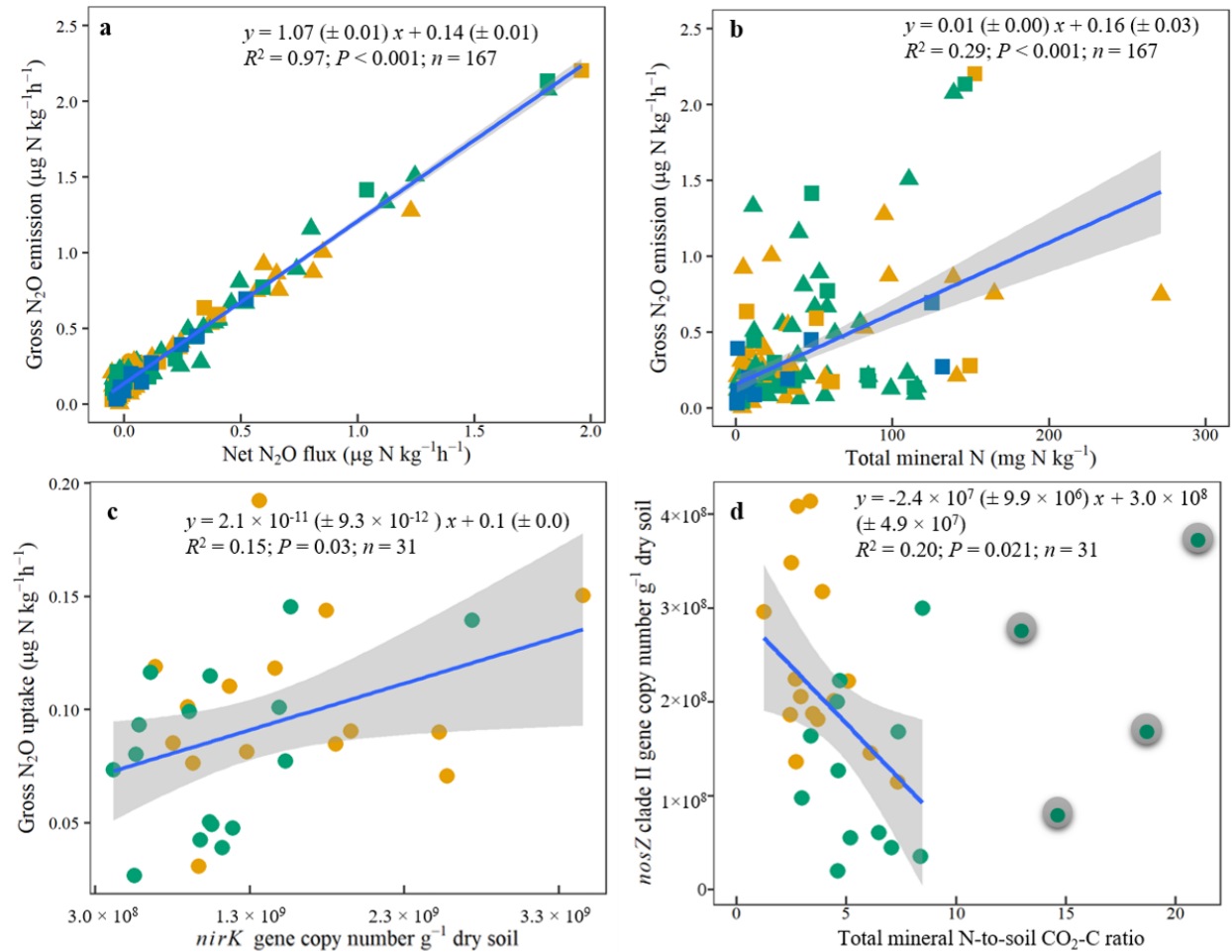


Figure 2.3 Cropland agroforestry and monocultures over 1.5 years of measurements: regression (parameter estimates \pm 95% confidence interval) of gross N₂O emission with net N₂O flux (a) and total mineral N (b) across three sites. Agroforestry tree rows over 1.5 years of measurements: regressions between gross N₂O uptake and *nirK* gene abundance (c), and between *nosZ* clade II gene abundance and mineral N-to-soil CO₂-C ratio (d, including only ratios <10). Each data point is a monthly mean of four (in Phaeozem and Cambisol soils) or eight replicate plots (in Arenosol soil). Tree row (●), crop row (1-m, 7-m, 24-m sampling locations, ▲), monoculture (■), Phaeozem soil (●), Cambisol soil (●), Arenosol soil (●).

Table 2.5

Multiple Regressions between Gross N₂O Emission and Soil Factors (which are not auto-correlated with each other) separately for Cropland Agroforestry and Monoculture, and the Relationships between Gross and Net N₂O Fluxes

Management systems	<i>n</i>	Regression equations	<i>P</i> value	<i>R</i> ²
Agroforestry	124	Gross N ₂ O emission = 0.004 × total mineral N + 0.132 × soil respiration + 0.072	< 0.001	0.32
Tree row	31	Gross N ₂ O emission = 0.017 × total mineral N + 0.056	0.002	0.28
Crop row	93	Gross N ₂ O emission = 0.004 × total mineral N + 0.009 × WFPS – 0.159	< 0.001	0.26
Monoculture	43	Gross N ₂ O emission = 0.006 × total mineral N + 0.019 × WFPS + 0.271 × soil respiration – 0.677	< 0.001	0.49
Between gross and net N ₂ O fluxes				
Agroforestry	124	Gross N ₂ O emission = 1.048 × net N ₂ O flux + 0.143	< 0.001	0.96
Tree row	31	Gross N ₂ O emission = 1.473 × net N ₂ O flux + 0.143	< 0.001	0.34
Crop row	93	Gross N ₂ O emission = 1.045 × net N ₂ O flux + 0.146	< 0.001	0.97
Monoculture	43	Gross N ₂ O emission = 1.103 × net N ₂ O flux + 0.125	< 0.001	0.99

2.5. Discussion

2.5.1. Gross N₂O emissions

To date, gross N₂O fluxes had not yet been systematically compared between cropland agroforestry and monoculture, and our study uniquely linked gross N₂O fluxes with denitrification gene abundance in addition to the commonly measured soil controlling factors. In the agroforestry tree rows, the high WFPS (Table 2.3), high abundance of denitrification genes (Table 2.4) and low mineral N-to-soil CO₂-C ratio would have favored enhanced gross N₂O emission (Yang & Silver, 2016a). The latter, i.e., low mineral N-to-soil CO₂-C ratio (of which heterotrophic respiration from available C can account for 70%–85%; Chen et al., 2019; van Straaten et al., 2011; Zhang et al., 2013), favors for N₂O-to-N₂ reduction during high WFPS conditions (Weier et al., 1993); this last step of the denitrification process is included in the quantification of gross N₂O emission by ¹⁵N₂O PD technique (Wen et al., 2016). Thus, the low gross N₂O emissions from the agroforestry tree rows (Table 2.2) indicated the overriding influence of its low mineral N levels (Table 2.3). Indeed, in the agroforestry tree rows, the only soil factor correlating with gross N₂O emissions was mineral N (Table 2.5), suggesting that this substrate as electron acceptor limited the production of N₂O rather than the electron donor (as reflected by the high soil CO₂ that partly includes heterotrophic respiration of available C as well as by the high microbial C in the tree row; Table 2.3). Similar findings were reported for beech and spruce stands in Germany, whereby NO₃⁻ levels predominantly regulate soil gross N₂O emissions (Wen et al., 2017). In contrast, the larger gross N₂O emissions from the crop rows were mirrored with their larger ratios of mineral N-to-soil CO₂-C while WFPS remained high (Table 2.3); this signified the secondary control of WFPS once N availability was increased by fertilization at the crop row (Table 2.5). At our study sites, the high WFPS in the agroforestry (Table 2.3) has been attributed to the reduction of wind speed by trees (Kanzler et al., 2019; Swieter et al., 2019) and thereby lowering evapotranspiration (Markwitz et al., 2020).

Across agroforestry tree and crop rows at two sites, the positive relationship of gross N₂O emissions with mineral N (Tables 2.5 and S2.4) reflected their similar patterns from the tree to the crop rows (Tables 2.2 and 2.3). The positive relationship of gross N₂O emissions with soil CO₂ largely depicted the parallel patterns of these variables between these two sites (Phaeozem > Cambisol; Tables 2.2 and 2.3). The effect of soil temperature was only indirect in that it was auto-correlated with mineral N and soil respiration (Table S2.4). For example,

soil temperature increased from spring, when fertilization occurred (Figure S2.3d and S2.3e), to summer and decreased towards fall, which also reflected the seasonal pattern of soil respiration (Figure S2.3g and S2.3h). Altogether, the benefit of agroforestry tree rows in controlling gross N₂O emission was largely on reduced electron acceptor (mineral N) relative to electron donor (as reflected partly by the soil CO₂ and microbial C), since WFPS and denitrification gene abundance were favorably large in the tree rows (Tables 2.3 and 2.4; see Section 2.5.2).

In cropland monocultures, the temporal variations of gross N₂O emissions were mirrored with seasonal changes in substrate availability and soil aeration (Table 2.5). The pulse N₂O emissions following one-time N fertilization to corn during spring (Figure 2.2b and 2.2c) with high WFPS and temperature (Figure S2.3b and S2.3c, S2.3e and S2.3f) may be attributed to low N uptake of corn seedlings at the start of the growing season; indeed, soil mineral N in spring was higher than in summer when N uptake was probably substantial as the corn grew. Yang and Silver (2016b) reported for corn cropland that plant uptake of N indirectly regulates gross N₂O emission. When our studied croplands had winter wheat and spring N fertilization was staggered (split in 2-3 applications; Figure 2.2a and 2.2b), the pulses of gross N₂O emissions were not as high as those when the crop was corn, possibly because winter wheat had an early growth start that stimulated N uptake in spring. When the crop was barley, spring N fertilization rate was the lowest (Table 2.1), and gross N₂O emissions in spring were not as high as those in the above crops (Figure 2.2a). These fertilization practices, as practiced by farmers for these crops, reflected the pattern of soil mineral N levels at these sites. Moreover, the influence of soil respiration on gross N₂O emissions from monocultures (Table 2.5) was exhibited through its similarity in seasonal patterns with soil temperature (Figure S2.3d-S2.3i), indicating soil CO₂-C increased from spring to summer and decreased towards fall. The regulation of WFPS on gross N₂O emissions from monocultures (Table 2.5) was related to the differences in soil textures of our study sites (Table S2.1) with the fine-textured soils (Phaeozem and Cambisol) exhibiting larger WFPS than the sandy Arenosol soil (Table 2.3 and Figure S2.3a-S2.3c). It should also be noted that 2018 had a lower precipitation than the 10-year average (Table 2.1), and the monoculture (without the wind reduction from trees as that in agroforestry; Markwitz et al., 2020) had the lowest WFPS (Table 2.3 and Figure S2.3a-S2.3c); this may have a dampening effect on gross N₂O emission as otherwise may occur in years with normal precipitation. Therefore, in addition to precipitation, management practices (fertilization, crops) and soil

texture, which influenced mineral N and WFPS at a local scale, were large-scale controllers of gross N₂O emissions from monocultures.

The whole (area-weighted for tree and crop rows) agroforestry had 6% (Cambisol soil) to 36% (Phaeozem soil) less annual gross N₂O emissions than the monocultures (Table 2.2) although the tree rows only occupied 20% of the agroforestry area. The predominant control of mineral N on gross N₂O emissions across agroforestry and monoculture systems (Table 2.5 and Figure 2.3b) reflected the clear benefit from unfertilized tree rows on reducing gross N₂O emissions, especially that gross N₂O emissions were the main determinant of net N₂O emissions from the soils (Table 2.5 and Figure 2.3a). This also suggests for optimal adjustments of the areal coverages between tree and crop rows to optimize benefits between provision (e.g. food, biomass, soil nutrients) and regulation functions (e.g. GHG, water quality).

2.5.2. Denitrification gene abundance

The increased microbial biomass in the agroforestry tree rows at our sites (Table 2.3) agreed with molecular studies that found promotion of microbial population size in the tree rows as compared to the crop rows or monoculture croplands in temperate regions (Banerjee et al., 2016; Beule et al., 2020). A much detailed molecular quantification of the microbial population at our study sites showed that the tree rows not only increase the bacterial and fungal population as well as denitrification gene abundance (Beule et al., 2020) but also alter the community composition of soil microorganisms (Beule and Karlovsky, 2021; Beule et al., 2021), implying changes in microbial community functions. However, denitrifier population size may only represent the genetic potential for denitrification rather than a reliable predictor of soil N₂O fluxes, which explained the contrasting spatial patterns of denitrification gene abundance and gross N₂O emission between agroforestry tree and crop rows or monoculture (Tables 2.2 and 2.4). Similar opposing findings of denitrification gene abundance and net N₂O fluxes were reported from field studies in temperate croplands (Dandie et al., 2008) and sclerophyll forest (Liu et al., 2013). Denitrification is a facultative physiological trait since all known denitrifying bacteria are capable of aerobic respiration (Chen and Strous, 2013). Denitrifier abundance may become a limiting factor for gross N₂O emissions when substrate levels and anaerobic conditions already prevail. Thus, it was not surprising that in the tree rows, N availability (Table 2.5) rather than denitrifier population size controlled gross N₂O emissions. This conflicts with the assumption that the functional gene abundance of

microorganisms can serve as a predictor of soil process rates. Although links between gene abundance and soil processes are frequently reported, a significant part of these studies is conducted under controlled laboratory conditions (e.g. Chen et al., 2020), ignoring the complexity of conditions occurring in the field. We, therefore, question to which extent results obtained from laboratory incubation studies can predict the actual processes occurring under field conditions. We argue that extensive field rather than laboratory studies are essential to understand the interactions between soil microbial communities and the processes they carry out.

2.5.3. Gross N₂O uptake

The increased gross N₂O uptake in the agroforestry tree rows in the Phaeozem soil (Table 2.2) was paralleled with low mineral N-to-soil CO₂-C ratio and high WFPS, which concurred with earlier findings (Wen et al., 2017; Yang & Silver, 2016a). At this site, the high WFPS and soil CO₂ (which partly indicated high heterotrophic respiration of available C; Chen et al., 2019; van Straaten et al., 2011; Zhang et al., 2013) in the tree row would favor for reduction of N₂O to N₂, resulting in higher gross N₂O uptake in the agroforestry relative to the monoculture (Table 2.2). The positive correlation of gross N₂O uptake with *nirK* gene abundance in agroforestry tree rows across two sites (Figure 2.3c) suggests that in a condition of low mineral N with high available C (e.g., high soil CO₂ and microbial C) and WFPS (Table 2.3) denitrifiers could not gain enough energy from only NO₂⁻-to-N₂O reduction, and thus completed the final step of denitrification, N₂O-to-N₂ reduction. The latter was further supported by the increasing *nosZ* clade II gene abundance with decreasing mineral N-to-soil CO₂-C ratio (Figure 2.3d), indicating that the ratio of mineral N-to-soil CO₂-C (Phaeozem < Cambisol soil) could be the underlying factor driving the difference in gross N₂O uptake in the tree rows between the two sites (Phaeozem > Cambisol soil) through its effect on the population size of *nosZ* clade II (Phaeozem > Cambisol soil). Annual gross N₂O uptake in the agroforestry system tended to increase by 27% (Cambisol soil) to 42% (Phaeozem soil) compared to the monocultures (Table 2.2). Collectively, the practical merit of trees in the agroforestry system, with regard to enhanced gross N₂O uptake, was mainly through an increase in C availability (as reflected partly by soil respiration and microbial C; Table 2.3) with an absence of fertilization.

2.5.4. Implications

Our sites of cropland agroforestry and monocultures have been shown to display nutrient saturation (Schmidt et al., 2021). As mineral N predominantly controlled gross N₂O emissions (which in turn influenced net soil N₂O emission) from both agroforestry and monocultures, our findings suggest that if fertilizer inputs are optimized without sacrificing crop yield or profit, combined with the impact of tree rows on increased N₂O uptake, agroforestry will be an efficient mitigation strategy to curb N₂O emission from croplands. From the aspect of economic performance, less investment in fertilizer inputs associated with environmental benefits (e.g., reduced N₂O emission) and diversified sources of income (crop yield, biofuel feedstock from tree biomass) would improve the profitability of agroforestry and facilitate its adoption by farmers. Overall, the GHG regulation function of the agroforestry system should be considered in the economic and ecological valuation to support its policy implementation (Kay et al., 2019).

2.6. Acknowledgments

This work was funded by the Bundesministerium für Bildung und Forschung (Bonares-SIGNAL project, 031A562A/031B0510A). Jie Luo was supported by China Scholarship Council. We thank Julia Morley, Helena Römer, Selena Algermissen, Antje Sophie Makowski, Andrea Bauer, Kerstin Langs, Dirk Böttger, and Martina Knaust for all the field and laboratory assistance.

Data Availability Statement

The data of this study are available from the BonaRes Data Centre repository (<https://doi.org/10.20387/bonares-x13m-z796>).

2.7. References

- Almaraz, M., Wong, M. Y., & Yang, W. H. (2020). Looking back to look ahead: a vision for soil denitrification research. *Ecology*, *101*(1):e02917. <https://doi.org/10.1002/ecy.2917>
- Amadi, C. C., Farrell, R. E., & van Rees, K. C. (2017). Greenhouse gas emissions along a shelterbelt-cropped field transect. *Agriculture, Ecosystems & Environment*, *241*, 110–120. <https://doi.org/10.1016/j.agee.2016.09.037>
- Amadi, C. C., van Rees, K. C., & Farrell, R. E. (2016). Soil–atmosphere exchange of carbon dioxide, methane and nitrous oxide in shelterbelts compared with adjacent cropped fields.

- Agriculture, Ecosystems & Environment*, 223, 123–134.
<https://doi.org/10.1016/j.agee.2016.02.026>
- Banerjee, S., Baah-Acheamfour, M., Carlyle, C. N., Bissett, A., Richardson, A. E., & Siddique, T., et al. (2016). Determinants of bacterial communities in Canadian agroforestry systems. *Environmental Microbiology*, 18(6), 1805–1816.
<https://doi.org/10.1111/1462-2920.12986>
- Beaudette, C., Bradley, R. L., Whalen, J. K., McVetty, P., Vessey, K., & Smith, D. L. (2010). Tree-based intercropping does not compromise canola (*Brassica napus* L.) seed oil yield and reduces soil nitrous oxide emissions. *Agriculture, Ecosystems & Environment*, 139(1-2), 33–39. <https://doi.org/10.1016/j.agee.2010.06.014>
- Beule, L., Arndt, M., & Karlovsky, P. (2021). Relative Abundances of Species or Sequence Variants Can Be Misleading: Soil Fungal Communities as an Example. *Microorganisms*, 9(3). <https://doi.org/10.3390/microorganisms9030589>
- Beule, L., Corre, M. D., Schmidt, M., Göbel, L., Veldkamp, E., & Karlovsky, P. (2019a). Conversion of monoculture cropland and open grassland to agroforestry alters the abundance of soil bacteria, fungi and soil-N-cycling genes. *PloS One*, 14(6), 1-19. <https://doi.org/10.1371/journal.pone.0218779>
- Beule, L., & Karlovsky, P. (2021). Tree rows in temperate agroforestry croplands alter the composition of soil bacterial communities. *PloS One*, 16(2), e0246919. <https://doi.org/10.1371/journal.pone.0246919>
- Beule, L., Lehtsaar, E., Corre, M. D., Schmidt, M., Veldkamp, E., & Karlovsky, P. (2020). Poplar Rows in Temperate Agroforestry Croplands Promote Bacteria, Fungi, and Denitrification Genes in Soils. *Frontiers in Microbiology*, 10, 1–5. <https://doi.org/10.3389/fmicb.2019.03108>
- Beule, L., Lehtsaar, E., Rathgeb, A., & Karlovsky, P. (2019b). Crop Diseases and Mycotoxin Accumulation in Temperate Agroforestry Systems. *Sustainability*, 11(10), 2925. <https://doi.org/10.3390/su11102925>
- Brandfass, C., & Karlovsky, P. (2008). Upscaled CTAB-based DNA extraction and real-time PCR assays for *Fusarium culmorum* and *F. graminearum* DNA in plant material with reduced sampling error. *International Journal of Molecular Sciences*, 9(11), 2306–2321. <https://doi.org/10.3390/ijms9112306>
- Brookes, P. C., Landman, A., Pruden, G., & Jenkinson, D. S. (1985). Chloroform fumigation and the release of soil nitrogen: A rapid direct extraction method to microbial biomass

- nitrogen in soil. *Soil Biology and Biochemistry*, 17(6), 837–842. [https://doi.org/10.1016/00380717\(85\)90144-0](https://doi.org/10.1016/00380717(85)90144-0)
- Butterbach-Bahl, K., Willibald, G., & Papen, H. (2002). Soil core method for direct simultaneous determination of N₂ and N₂O emissions from forest soils. *Plant and Soil*, 240(1), 105–116. <https://doi.org/10.1023/A:1015870518723>
- Butterbach-Bahl, K., Baggs, E. M., Dannenmann, M., Kiese, R., & Zechmeister-Boltenstern, S. (2013). Nitrous oxide emissions from soils: how well do we understand the processes and their controls? *Philosophical Transactions of the Royal Society of London. Series B, Biological Sciences*, 368(1621), 20130122. <https://doi.org/10.1098/rstb.2013.0122>
- Chapman, M., Walker, W. S., Cook-Patton, S. C., Ellis, P. W., Farina, M., Griscom, B. W., & Baccini, A. (2020). Large climate mitigation potential from adding trees to agricultural lands. *Global Change Biology*. (26), 4357–4365. <https://doi.org/10.1111/gcb.15121>
- Chapuis-Lardy, L., Wrage, N., Metay, A., Chotte, J.-L., & Bernoux, M. (2007). Soils, a sink for N₂O? A review. *Global Change Biology*, 13(1), 1–17. <https://doi.org/10.1111/j.1365-2486.2006.01280.x>
- Chen, F., Yan, G., Xing, Y., Zhang, J., Wang, Q., & Wang, H., et al. (2019). Effects of N addition and precipitation reduction on soil respiration and its components in a temperate forest. *Agricultural and Forest Meteorology*, 271, 336–345. <https://doi.org/10.1016/j.agrformet.2019.03.021>
- Chen, J., & Strous, M. (2013). Denitrification and aerobic respiration, hybrid electron transport chains and co-evolution. *Biochimica Et Biophysica Acta*, 1827(2), 136–144. <https://doi.org/10.1016/j.bbabi.2012.10.002>
- Chen, Y., Liu, F., Kang, L., Zhang, D., Kou, D., & Mao, C., et al. (2020). Large-scale evidence for microbial response and associated carbon release after permafrost thaw. *Global Change Biology*. (00), 1–12. <https://doi.org/10.1111/gcb.15487>
- Crawley, M.J. (2007). *The R Book*. John Wiley & Sons Ltd., Chichester, West Sussex.
- Dandie, C. E., Burton, D. L., Zebarth, B. J., Henderson, S. L., Trevors, J. T., & Goyer, C. (2008). Changes in bacterial denitrifier community abundance over time in an agricultural field and their relationship with denitrification activity. *Applied and Environmental Microbiology*, 74(19), 5997–6005. <https://doi.org/10.1128/AEM.00441-08>
- Davidson, E. A., Keller, M., Erickson, H. E., Verchot, L. V., & Veldkamp, E. (2000). Testing a Conceptual Model of Soil Emissions of Nitrous and Nitric Oxides. *BioScience*, 50(8), 667. [https://doi.org/10.1641/0006-3568\(2000\)050\[0667:TACMOS\]2.0.CO;2](https://doi.org/10.1641/0006-3568(2000)050[0667:TACMOS]2.0.CO;2)

- Foley, J. A., Ramankutty, N., Brauman, K. A., Cassidy, E. S., Gerber, J. S., & Johnston, M., et al. (2011). Solutions for a cultivated planet. *Nature*, 478(7369), 337–342. <https://doi.org/10.1038/nature10452>
- Guerra, V., Beule, L., Lehtsaar, E., Liao, H.-L., & Karlovsky, P. (2020). Improved Protocol for DNA Extraction from Subsoils Using Phosphate Lysis Buffer. *Microorganisms*, 8(4). <https://doi.org/10.3390/microorganisms8040532>
- IPCC. (2014). *Climate Change 2014: Synthesis Report. Contribution of Working Groups I, II and III to the Fifth Assessment Report of the Intergovernmental Panel on Climate Change* [Core Writing Team, R.K. Pachauri and L.A. Meyer (eds.)]. IPCC, Geneva, Switzerland, 151. <https://www.ipcc.ch/report/ar5/syr/>
- IPCC. (2019). *Climate Change and Land: an IPCC special report on climate change, desertification, land degradation, sustainable land management, food security, and greenhouse gas fluxes in terrestrial ecosystems*. IPCC, Geneva, Switzerland, 551–672. <https://www.ipcc.ch/srccl/chapter/chapter-6/>
- Juhanson, J., Hallin, S., Söderström, M., Stenberg, M., & Jones, C. M. (2017). Spatial and phyloecological analyses of *nosZ* genes underscore niche differentiation amongst terrestrial N₂O reducing communities. *BioScience*, 115, 82–91. <https://doi.org/10.1016/j.soilbio.2017.08.013>
- Kanzler, M., Böhm, C., Mirck, J., Schmitt, D., & Veste, M. (2019). Microclimate effects on evaporation and winter wheat (*Triticum aestivum* L.) yield within a temperate agroforestry system. *Agroforestry Systems*, 93(5), 1821–1841. <https://doi.org/10.1007/s10457-018-0289-4>
- Kay, S., Graves, A., Palma, J. H., Moreno, G., Rocas-Díaz, J. V., & Aviron, S., et al. (2019). Agroforestry is paying off – Economic evaluation of ecosystem services in European landscapes with and without agroforestry systems. *Ecosystem Services*, 36, 100896. <https://doi.org/10.1016/j.ecoser.2019.100896>
- Koehler, B., Corre, M. D., Veldkamp, E., Wullaert, H., & Wright, S. J. (2009). Immediate and long-term nitrogen oxide emissions from tropical forest soils exposed to elevated nitrogen input. *Global Change Biology*, 15(8), 2049–2066. <https://doi.org/10.1111/j.1365-2486.2008.01826.x>
- Lang, M., Li, P., Ti, C., Zhu, S., Yan, X., & Chang, S. X. (2019). Soil gross nitrogen transformations are related to land-uses in two agroforestry systems. *Ecological Engineering*, 127, 431–439. <https://doi.org/10.1016/j.ecoleng.2018.12.022>

- Langenberg, J., Feldmann, M., & Theuvsen, L. (2018). Agroforestry systems: using Monte-Carlo simulation for a risk analysis in comparison with arable farming systems. *German Journal of Agricultural Economics*, *67*, 95–112. <https://doi.org/10.22004/AG.ECON.309977>
- Liu, X., Chen, C. R., Wang, W. J., Hughes, J. M., Lewis, T., Hou, E. Q., & Shen, J. (2013). Soil environmental factors rather than denitrification gene abundance control N₂O fluxes in a wet sclerophyll forest with different burning frequency. *BioScience*, *57*, 292–300. <https://doi.org/10.1016/j.soilbio.2012.10.009>
- Ma, Z., Chen, H. Y. H., Bork, E. W., Carlyle, C. N., & Chang, S. X. (2020). Carbon accumulation in agroforestry systems is affected by tree species diversity, age and regional climate: A global meta-analysis. *Global Ecology and Biogeography*, *00*, 1–12. <https://doi.org/10.1111/geb.13145>
- Markwitz, C., Knohl, A., & Siebicke, L. (2020). Evapotranspiration over agroforestry sites in Germany. *Biogeosciences*, *17*(20), 5183–5208. <https://doi.org/10.5194/bg-17-5183-2020>
- Matson, A. L., Corre, M. D., Langs, K., & Veldkamp, E. (2017). Soil trace gas fluxes along orthogonal precipitation and soil fertility gradients in tropical lowland forests of Panama. *Biogeosciences*, *14*(14), 3509–3524. <https://doi.org/10.5194/bg-14-3509-2017>
- Mitchell, E., Scheer, C., Rowlings, D., Cotrufo, M. F., Conant, R. T., Friedl, J., & Grace, P. (2020). Trade-off between ‘new’ SOC stabilisation from above-ground inputs and priming of native C as determined by soil type and residue placement. *Biogeochemistry*, *149*(2), 221–236. <https://doi.org/10.1007/s10533-020-00675-6>
- Müller, C., Sherlock, R. R. (2004). Nitrous oxide emissions from temperate grassland ecosystems in the Northern and Southern Hemispheres. *Global Biogeochemical Cycles*, *18*(1), 1-11. <https://doi.org/10.1029/2003GB002175>
- Pardon, P., Reubens, B., Mertens, J., Verheyen, K., Frenne, P. de, & Smet, G. de, et al. (2018). Effects of temperate agroforestry on yield and quality of different arable intercrops. *Agricultural Systems*, *166*, 135–151. <https://doi.org/10.1016/j.agsy.2018.08.008>
- Pardon, P., Reubens, B., Reheul, D., Mertens, J., Frenne, P. de, & Coussement, T., et al. (2017). Trees increase soil organic carbon and nutrient availability in temperate agroforestry systems. *Agriculture, Ecosystems & Environment*, *247*, 98–111. <https://doi.org/10.1016/j.agee.2017.06.018>
- R Core Team. (2019). *R: A language and environment for statistical computing*. Vienna, Austria: R Foundation for Statistical Computing. <https://www.r-project.org/>

- Schmidt, M., Corre, M. D., Kim, B., Morley, J., Göbel, L., & Sharma, A. S. I., et al. (2021). Nutrient saturation of crop monocultures and agroforestry indicated by nutrient response efficiency. *Nutrient Cycling in Agroecosystems*, 119(1), 69–82. <https://doi.org/10.1007/s10705-020-10113-6>
- Shen, S. M., Pruden, G., & Jenkinson, D. S. (1984). PII: Mineralization and immobilization of nitrogen in fumigated soil and the measurement of microbial biomass nitrogen. *Soil Biology and Biochemistry*, 16, 437–444. [https://doi.org/10.1016/0038-0717\(84\)90049-X](https://doi.org/10.1016/0038-0717(84)90049-X)
- Sihi, D., Davidson, E. A., Savage, K. E., & Liang, D. (2020). Simultaneous numerical representation of soil microsite production and consumption of carbon dioxide, methane, and nitrous oxide using probability distribution functions. *Global Change Biology*, 26(1), 200–218. <https://doi.org/10.1111/gcb.14855>
- Smith, J., Pearce, B. D., & Wolfe, M. S. (2013). Reconciling productivity with protection of the environment: Is temperate agroforestry the answer? *Renewable Agriculture and Food Systems*, 28(1), 80–92. <https://doi.org/10.1017/S1742170511000585>
- Strickland, M. S., Leggett, Z. H., Sucre, E. B., & Bradford, M. A. (2015). Biofuel intercropping effects on soil carbon and microbial activity. *Ecological Applications*, 140–150. <https://doi.org/10.1890/14-0285.1>
- Swieter, A., Langhof, M., Lamerre, J., & Greef, J. M. (2019). Long-term yields of oilseed rape and winter wheat in a short rotation alley cropping agroforestry system. *Agroforestry Systems*, 93(5), 1853–1864. <https://doi.org/10.1007/s10457-018-0288-5>
- Throbäck, I. N., Enwall, K., Jarvis, A., & Hallin, S. (2004). Reassessing PCR primers targeting *nirS*, *nirK* and *nosZ* genes for community surveys of denitrifying bacteria with DGGE. *FEMS Microbiology Ecology*, 49(3), 401–417. <https://doi.org/10.1016/j.femsec.2004.04.011>
- Tian, H., Yang, J., Xu, R., Lu, C., Canadell, J. G., & Davidson, E. A., et al. (2018). Global soil nitrous oxide emissions since the preindustrial era estimated by an ensemble of terrestrial biosphere models: Magnitude, attribution, and uncertainty. *Global Change Biology*, 1–12. <https://doi.org/10.1111/gcb.14514>
- Tsonkova, P., Böhm, C., Quinkenstein, A., & Freese, D. (2012). Ecological benefits provided by alley cropping systems for production of woody biomass in the temperate region: a review. *Agroforestry Systems*, 85(1), 133–152. <https://doi.org/10.1007/s10457-012-9494-8>

- Van Straaten, O., Veldkamp, E., & Corre, M. D. (2011). Simulated drought reduces soil CO₂ efflux and production in a tropical forest in Sulawesi, Indonesia. *Ecosphere*, 2(10), art119. <https://doi.org/10.1890/ES11-00079.1>
- Veldkamp, E., Koehler, B., & Corre, M. D. (2013). Indications of nitrogen-limited methane uptake in tropical forest soils. *Biogeosciences*, 10(8), 5367–5379. <https://doi.org/10.5194/bg-10-5367-2013>
- Weier, K. L., Doran, J. W., Power, J. F., & Walters, D. T. (1993). Denitrification and the Dinitrogen/Nitrous Oxide Ratio as Affected by Soil Water, Available Carbon, and Nitrate. *Proceedings of the National Academy of Sciences*, 57(1), 66–72. <https://doi.org/10.2136/sssaj1993.03615995005700010013x>
- Wen, Y., Chen, Z., Dannenmann, M., Carminati, A., Willibald, G., & Kiese, R., et al. (2016). Disentangling gross N₂O production and consumption in soil. *Scientific Reports*, 6, 36517. <https://doi.org/10.1038/srep36517>
- Wen, Y., Corre, M. D., Schrell, W., & Veldkamp, E. (2017). Gross N₂O emission and gross N₂O uptake in soils under temperate spruce and beech forests. *Soil Biology and Biochemistry*, 112, 228–236. <https://doi.org/10.1016/j.soilbio.2017.05.011>
- Wolz, K. J., Lovell, S. T., Branham, B. E., Eddy, W. C., Keeley, K., & Revord, R. S., et al. (2018). Frontiers in alley cropping: Transformative solutions for temperate agriculture. *Global Change Biology*, 24(3), 883–894. <https://doi.org/10.1111/gcb.13986>
- Yang, W. H., & Silver, W. L. (2016a). Gross nitrous oxide production drives net nitrous oxide fluxes across a salt marsh landscape. *Global Change Biology*, 22(6), 2228–2237. <https://doi.org/10.1111/gcb.13203>
- Yang, W. H., & Silver, W. L. (2016b). Net soil–atmosphere fluxes mask patterns in gross production and consumption of nitrous oxide and methane in a managed ecosystem. *Biogeosciences*, 13(5), 1705–1715. <https://doi.org/10.5194/bg-13-1705-2016>
- Yang, W. H., Teh, Y. A., & Silver, W. L. (2011). A test of a field-based ¹⁵N-nitrous oxide pool dilution technique to measure gross N₂O production in soil. *Global Change Biology*, 17(12), 3577–3588. <https://doi.org/10.1111/j.1365-2486.2011.02481.x>
- Seasonal variations in soil respiration, heterotrophic respiration and autotrophic respiration of a wheat and maize rotation cropland in the North China Plain. *Agricultural and Forest Meteorology*, 180, 34–43. <https://doi.org/10.1016/j.agrformet.2013.04.028>
- Zuur, A. F., Ieno, E. N., Walker, N., Saveliev, A. A., & Smith, G. M. (2009). *Mixed effects models and extensions in ecology with R. Statistics for Biology and Health*: Springer, New York.

References from the Supporting Information

- Henry, S., Bru, D., Stres, B., Hallet, S., & Philippot, L. (2006). Quantitative detection of the *nosZ* gene, encoding nitrous oxide reductase, and comparison of the abundances of 16S rRNA, *narG*, *nirK*, and *nosZ* genes in soils. *Applied and Environmental Microbiology*, 72(8), 5181–5189. <https://doi.org/10.1128/AEM.00231-06>
- Henry, S., Baudoin, E., López-Gutiérrez, J. C., Martin-Laurent, F., Brauman, A., & Philippot, L. (2004). Quantification of denitrifying bacteria in soils by *nirK* gene targeted real-time PCR. *Journal of Microbiological Methods*, 59(3), 327–335. <https://doi.org/10.1016/j.mimet.2004.07.002>
- Jones, C. M., Graf, D. R. H., Bru, D., Philippot, L., & Hallin, S. (2013). The unaccounted yet abundant nitrous oxide-reducing microbial community: a potential nitrous oxide sink. *The ISME Journal*, 7(2), 417–426. <https://doi.org/10.1038/ismej.2012.125>
- Michotey, V., Méjean, V., & Bonin, P. (2000). Comparison of methods for quantification of cytochrome cd(1)-denitrifying bacteria in environmental marine samples. *Applied and Environmental Microbiology*, 66(4), 1564–1571. <https://doi.org/10.1128/AEM.66.4.1564-1571.2000>
- Wen, Y., Chen, Z., Dannenmann, M., Carminati, A., Willibald, G., & Kiese, R., et al. (2016). Disentangling gross N₂O production and consumption in soil. *Scientific Reports*, 6, 36517. <https://doi.org/10.1038/srep36517>

2.8. Appendix

Table S2.1. Soil biochemical and physical properties (0-30-cm depth) at the three sites of cropland agroforestry and cropland monocultures in Germany. At each site, mean (\pm SE, $n = 4$ plots for the Phaeozem and Cambisol soils, $n = 8$ plots for the Arenosol soil) followed by different lowercase letters indicate significant differences between management systems at each site (ANOVA with Tukey HSD or Kruskal-Wallis test with multiple comparison extension at $P \leq 0.05$).

Soil (Site)	type	Management system	pH (1:4 soil- H ₂ O ratio)	Total N (kg N m ⁻²)	Organic C (kg C m ⁻²)	C:N ratio	ECEC (mmol _c kg ⁻¹)	BS (%)	Clay Content (%)
Phaeozem (Dornburg)		Agroforestry							
		tree row	6.5 \pm 0.1 ^c	0.53 \pm 0.02 ^a	5.14 \pm 0.40 ^a	9.6 \pm 0.4 ^a	152 \pm 5 ^b	99 \pm 0 ^a	20 \pm 1 ^b
		crop row	6.7 \pm 0.0 ^b	0.49 \pm 0.01 ^a	4.27 \pm 0.02 ^a	8.7 \pm 0.2 ^{ab}	159 \pm 3 ^b	99 \pm 0 ^a	24 \pm 1 ^b
Cambisol (Wendhausen)		Monoculture	7.9 \pm 0.1 ^a	0.47 \pm 0.06 ^a	3.86 \pm 0.61 ^a	8.1 \pm 0.4 ^b	590 \pm 101 ^a	100 \pm 0 ^a	38 \pm 2 ^a
		Agroforestry							
		tree row	7.1 \pm 0.2 ^a	0.66 \pm 0.03 ^a	7.04 \pm 0.30 ^a	10.5 \pm 0.2 ^a	350 \pm 75 ^a	100 \pm 0 ^a	35 \pm 2 ^a
		crop row	7.3 \pm 0.2 ^a	0.66 \pm 0.02 ^a	6.47 \pm 0.22 ^{ab}	10.0 \pm 0.2 ^b	366 \pm 100 ^a	100 \pm 0 ^a	28 \pm 2 ^a
		Monoculture	7.3 \pm 0.1 ^a	0.60 \pm 0.01 ^a	5.79 \pm 0.07 ^b	9.7 \pm 0.0 ^b	298 \pm 10 ^a	100 \pm 0 ^a	44 \pm 3 ^a
Arenosol (Vechta)		Monoculture	6.1 \pm 0.1	0.45 \pm 0.03	6.07 \pm 0.41	13.3 \pm 0.2	43 \pm 4	95 \pm 1	7 \pm 1

Note. At each site, mean (\pm SE, $n = 4$ plots for the Phaeozem and Cambisol soils, $n = 8$ plots for the Arenosol soil) followed by different lowercase letters indicate significant differences between management systems at each site (ANOVA with Tukey HSD or Kruskal-Wallis test with multiple comparison extension at $P \leq 0.05$). ECEC – effective cation exchange capacity, BS – base saturation. Soil characteristics were measured in 2016 for the Phaeozem soil (Schmidt et al., 2021), 2019 for the Cambisol soil, and 2018 for the Arenosol soil.

Table S2.2. Final MgCl₂ and primer concentrations.

Target gene	Final MgCl ₂ concentration (mM)	Primer concentration (μ M)
<i>nirK</i>	2.5	0.5
<i>nirS</i>	2.0	0.5
<i>nosZ</i> clade I	1.5	0.5
<i>nosZ</i> clade II	2.0	1.0

Table S2.3. Thermocycling conditions and primer choice for the quantification of denitrification genes.

Target gene	Initial denaturation	35 cycles			Primer	Primer source
		Denaturation	Annealing	Extension		
<i>nirK</i>	95 °C, 120 s	94 °C, 20 s	58 °C, 30 s	68 °C, 30 s	<i>nirK876F</i> <i>nirK1040R</i>	(Henry et al., 2004)
<i>nirS</i>	95 °C, 120 s	94 °C, 20 s	53 °C, 30 s	68 °C, 30 s	cd3aF R3cd	(Michotey et al., 2000; Throbäck et al., 2004)
<i>nosZ</i> clade I	95 °C, 120 s	94 °C, 20 s	60 °C, 30 s	68 °C, 30 s	<i>nosZ2F</i> <i>nosZ2R</i>	(Henry et al., 2006)
<i>nosZ</i> clade II	95 °C, 120 s	94 °C, 20 s	58 °C, 30 s	68 °C, 45 s	<i>nosZ-II-F</i> <i>nosZ-II-R</i>	(Jones et al., 2013)

Note. The first three genes were analyzed using six touchdown cycles after the initial denaturation. Cycling conditions were identical to those in the table except that the annealing temperature was raised to 63 °C, 58 °C, and 65 °C for *nirK*, *nirS*, and *nosZ* clade I, respectively, with a decrease of the annealing temperature by 1 °C per cycle.

Table S2.4. Pearson correlations of monthly average gross N₂O emission with soil controlling factors across sites, and separately for agroforestry and monoculture systems.

Across agroforestry and monoculture at three sites over 1.5 years of measurements (<i>n</i> = 167)				
	Gross N ₂ O emission	Mineral N	Soil temperature	Soil respiration
Mineral N	0.54**			
Soil temperature	0.37**	0.33**		
Soil respiration	0.24**	0.04	0.63**	
WFPS	0.10	-0.05	-0.14	0.26**
Agroforestry at two sites over 1.5 years of measurements (<i>n</i> = 124)				
	Gross N ₂ O emission	Mineral N	Soil temperature	Soil respiration
Mineral N	0.52**			
Soil temperature	0.37**	0.31**		
Soil respiration	0.26**	0.06	0.63**	
WFPS	0.11	0	-0.12	0.26**
Monoculture at three sites over 1.5 years of measurements (<i>n</i> = 43)				
	Gross N ₂ O emission	Mineral N	Soil temperature	Soil respiration
Mineral N	0.60**			
Soil temperature	0.38*	0.38*		
Soil respiration	0.28	0.07	0.73**	
WFPS	0.21	-0.06	-0.23	-0.10

Note. * $P < 0.05$, ** $P < 0.01$.

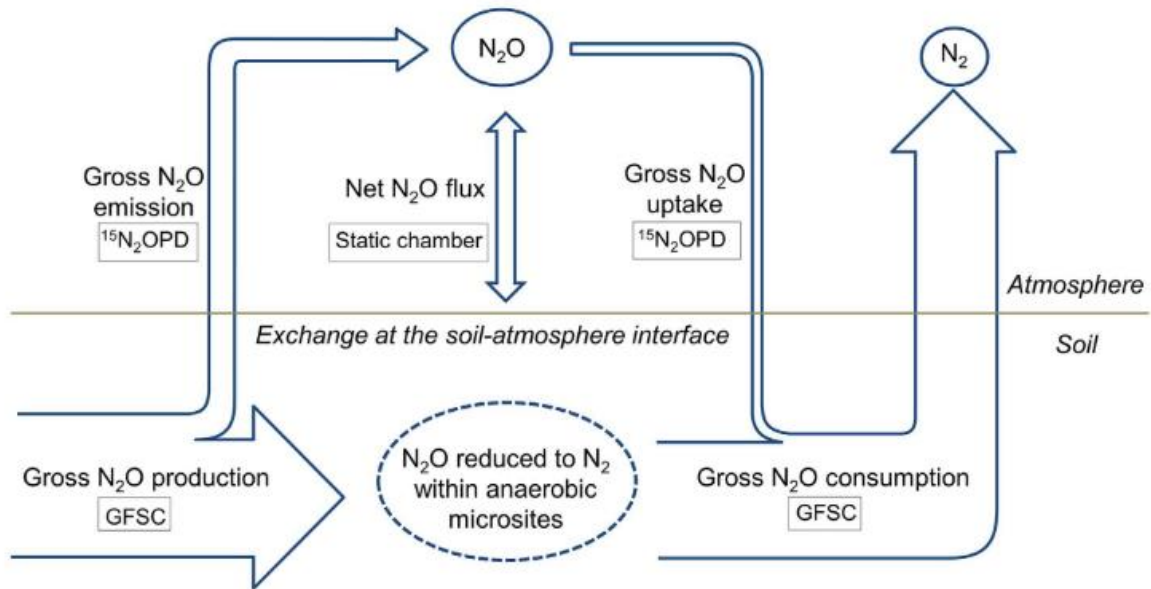


Figure S2.1. Conceptual diagram of gross N_2O fluxes, based on the comparison between $^{15}\text{N}_2\text{O}$ pool dilution ($^{15}\text{N}_2\text{O}$ PD) and gas-flow soil core (GFSC) methods as discussed in our previous study (Wen et al., 2016). Gross N_2O emission and gross N_2O uptake are the terms suggested to be used when measured with $^{15}\text{N}_2\text{O}$ PD technique, which largely includes gas exchange in interconnected air-filled pores in the soil. Gross N_2O production and gross N_2O consumption are the terms recommended to be used when measured with GFSC method, which encompasses the soil air-filled pores as well as anaerobic microsites (e.g., soil micro spots saturated with water, isolated pores filled with or enclosed by water, and water-entrapped N_2O).

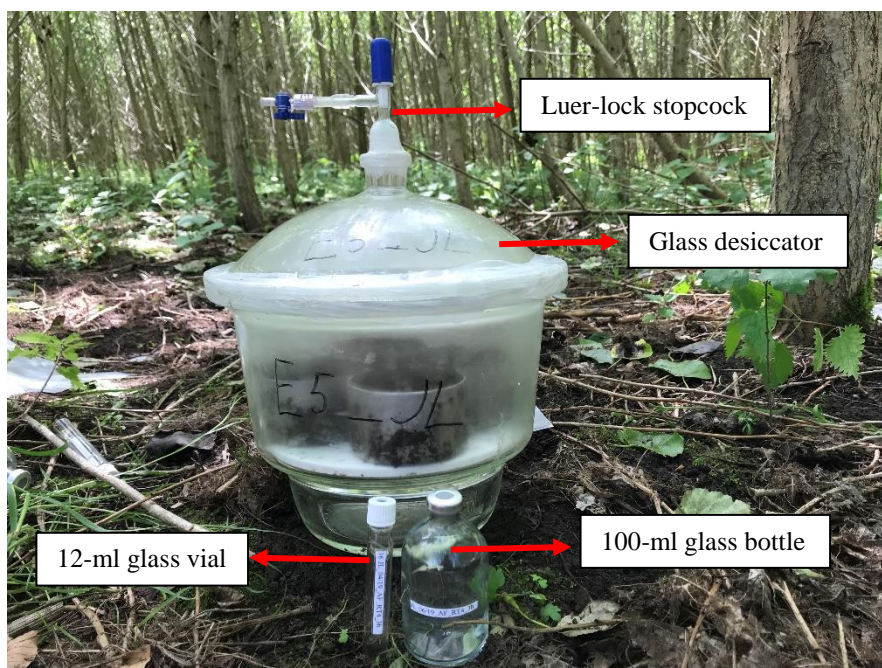


Figure S2.2. Four intact soil cores (250 cm^3 each) from the top 5 cm incubated in a glass desiccator (6.6 L), equipped with a Luer-lock stopcock on the lid; 100-ml glass bottle containing sample for $^{15}\text{N}_2\text{O}$ analysis; and 12-ml glass vial (Exetainer; Labco Limited, Lampeter, UK) for N_2O , SF_6 , and CO_2 concentrations determination

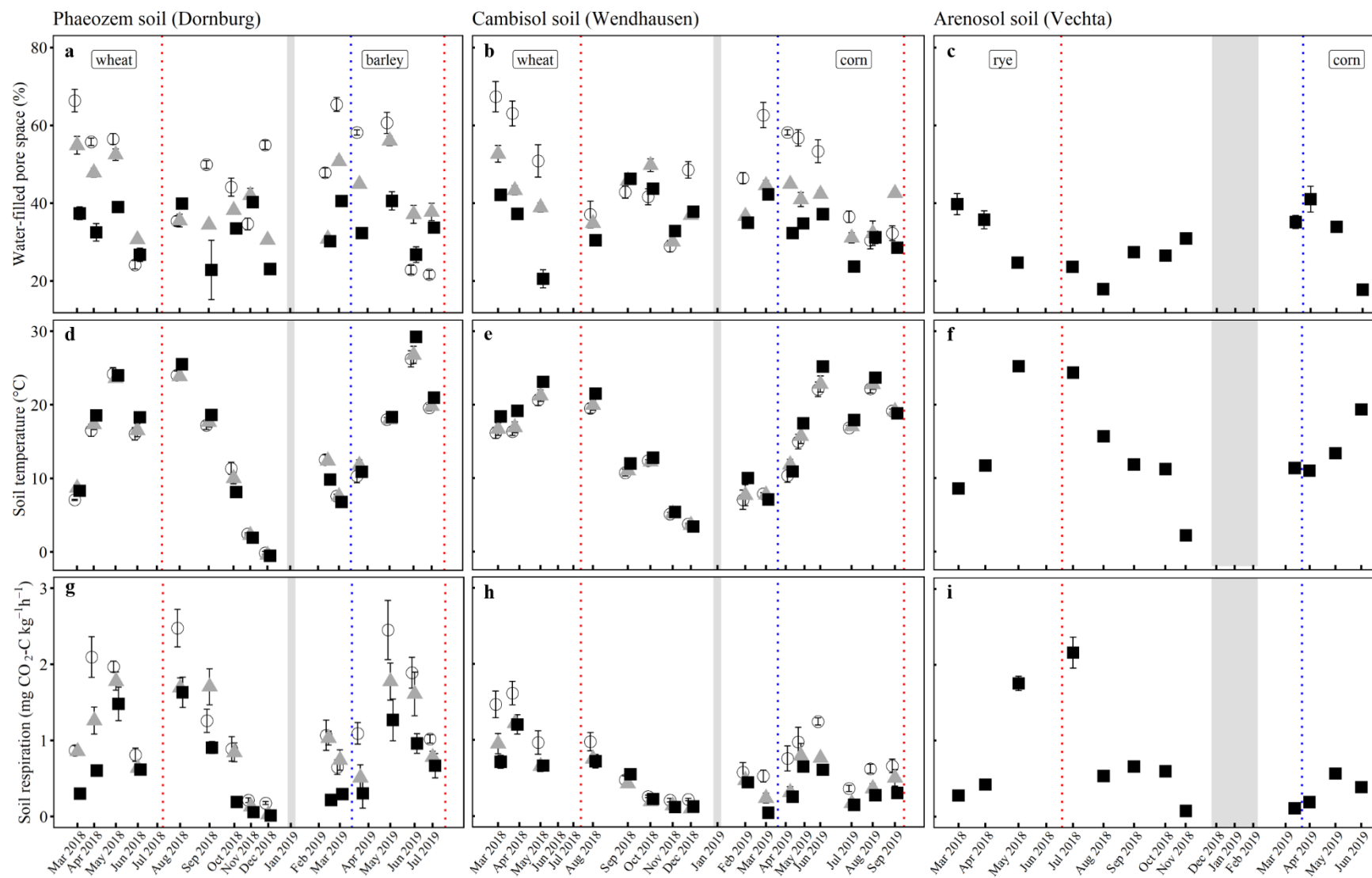


Figure S2.3. Mean (\pm SE, $n = 4$ plots for the Phaeozem and Cambisol soils, $n = 8$ plots for the Arenosol soil) soil water-filled pore space (a, b, c), soil temperature (d, e, f) and soil respiration (g, h, i), measured monthly in the top 5-cm depth at three sites of cropland agroforestry and cropland monocultures in Germany. Agroforestry tree row (\circ) and crop row (area-weighted average of the 1-m, 7-m, and 24-m sampling locations, \blacktriangle); monoculture (\blacksquare). The site with an Arenosol soil was a cropland monoculture during the measurement period. June and July 2018 were extremely dry months, during which no intact soil cores could be collected. Red dotted lines indicate harvest and blue dotted lines indicate sowing; gray shadings indicate frozen soil during winter when intact soil cores cannot be collected.

Chapter 3

Soil gross N₂O emission and uptake under two contrasting agroforestry systems (riparian tree buffer vs trees of alley cropping)

Jie Luo¹, Lukas Beule², Guodong Shao¹, Edzo Veldkamp¹, and Marife D. Corre¹

¹Soil Science of Tropical and Subtropical Ecosystems, Faculty of Forest Sciences and Forest Ecology, University of Goettingen, Goettingen, Büsgenweg 2 37077, Germany

²Julius Kühn Institute (JKI) – Federal Research Centre for Cultivated Plants, Institute for Ecological Chemistry, Plant Analysis and Stored Product Protection, Berlin, Germany

3.1. Abstract

The integration of riparian tree buffer and trees into cropland aims to reduce the threat to groundwater quality and the atmosphere due to the excess nitrogen (N) from intensive agricultural management. Presently, little information is known about how different types of agroforestry systems with contrasting soil characteristics affected gross nitrous oxide (N₂O) emission and uptake and how depths affected these fluxes. We used in situ measurements of gross N₂O fluxes using ¹⁵N₂O pool dilution at two depths (0 – 5 and 40 – 60 cm) in a riparian buffer and tree row of alley cropping in Germany. Our results showed that gross N₂O emissions and uptake in topsoil were higher ($P \leq 0.03$) in riparian tree buffer than tree row of alley cropping but were comparable ($P \geq 0.06$) in subsoil between the two agroforestry systems. However, gross N₂O fluxes did not differ ($P \geq 0.06$) between the two depths at each agroforestry system. Gross N₂O emissions were mainly driven by mineral N, biodegradable organic carbon, and aeration status rather than microbial population size either across topsoil of agroforestry systems or across depths in the riparian tree buffer. Gross N₂O uptake in topsoil was driven by available carbon and *nirK* gene abundance across agroforestry systems. Subsoil in both agroforestry systems showed a sink of N₂O due to low mineral N, indicating a great capacity of removal of leached NO₃⁻-N. Soil temperature was another important factor regulating the temporal pattern of gross N₂O uptake in subsoil in each agroforestry system. Overall, we illustrated the underlying mechanisms and controls of gross N₂O fluxes across different agroforestry systems and depths.

Keywords: Nitrous oxide, agroforestry systems, riparian buffer, ¹⁵N₂O pool dilution, gross N₂O emission, gross N₂O uptake

3.2. Introduction

The excess nitrogen (N) from intensive agricultural management is regarded as an escalating global threat because of its impact on groundwater quality and the atmosphere (Stark and Richards, 2008), strategies should thus be adopted to mitigate such problems. Agroforestry systems, incorporating trees into the arable land, are considered as sustainable management due to delivering a series of ecosystem services, e.g., water quality enhancement, and climate change mitigation (Chapman et al., 2020; Kim et al., 2016). Modern agroforestry systems can take different forms including alley cropping, riparian buffers, and silvopasture systems (Baah-Acheamfour et al., 2020). The alley-cropping system consists of alternating rows of trees and crops. The tree rows in the alley cropping are unfertilized as commonly practiced by farmers in temperate regions (Schmidt et al., 2021). These tree roots can serve as a ‘safety net’ through intercepting the leached nutrients such as nitrate (NO_3^-) from the fertilized crops, thereby enhancing water quality (Allen et al., 2004). In contrast to the alley-cropping system, riparian buffers are located between terrestrial and aquatic ecosystems and serve as a natural filter for pollutants from adjacent agricultural land, including NO_3^- transported in overland flow and subsurface pathways (Boleman and Jacobson, 2021; Baskerville et al., 2021). They can reduce overland flow velocity due to their low-gradient topography, leading to greater residence time and more efficient N removal (Fisher et al., 2014). Much interest in riparian buffers has been motivated by beneficial effects on water quality as effective NO_3^- sinks (Lutz et al., 2020; Hill, 2019) but this could also contribute to environmental problems through the emissions of nitrous oxide (N_2O) (Davis et al., 2019).

N_2O is a contributor to ozone-depleting and a potent greenhouse gas with 298 times global warming potential relative to carbon dioxide (CO_2) (Allen, 2015). It is mainly originated from microbial denitrification and nitrification. Challenges associated with simultaneously measuring N_2O and N_2 (i.e., the end product of denitrification), because of the high atmospheric background N_2 concentration (Groffman et al., 2006), hinder quantification of gross N_2O production and consumption in soils. To date, net N_2O flux as the result of gross N_2O production and consumption has been widely investigated by using the chamber method in natural and managed ecosystems. However, the separate two processes are rarely researched in the field as the commonly used methods, e.g., acetylene inhibition and ^{15}N tracing methods, are more focused on the laboratory due to their manipulation and limitations (Groffman et al., 2006; Butterbach-Bahl et al., 2013). The $^{15}\text{N}_2\text{O}$ pool dilution technique is currently the only choice to provide much-needed field measurements of gross N_2O emission

and gross N₂O uptake without extensive soil disturbance even though this technique may not capture all N₂ production in few conditions, like in anaerobic microsites (Wen et al., 2016; Yang et al., 2011). Given that happens, Wen et al. (2016) propose the term ‘gross N₂O emission’ and ‘gross N₂O uptake’. The ¹⁵N₂O pool dilution technique is rarely applied in terrestrial ecosystems (Wen et al., 2017; Yang and Silver, 2016a, 2016b; Yang et al., 2011). In response to a recent call for the adoption of new and improved methods for denitrification (Almaraz et al., 2020), applying ¹⁵N₂O pool dilution into two contrasting agroforestry systems, i.e., riparian buffer, and tree row of alley cropping, and at different depths, is to facilitate our understanding of field rates of gross N₂O fluxes and associated controls and how these fluxes vary across the soil profile.

Understanding mechanisms of gross N₂O emission and uptake are to advance the predictions of changes in net N₂O fluxes caused by future climate change and thus optimize the agroforestry management to achieve the goal of climate change mitigation. Factors regulating gross N₂O emission and uptake in soils, such as available N (NO₃⁻ and ammonium [NH₄⁺]), C availability, soil moisture content have been documented in a forest stand (Wen et al., 2017), a salt marsh landscape (Yang and Silver, 2016a) and a fertilized corn cropland (Yang and Silver, 2016b). Theoretically, the fluctuating water level of an aquatic ecosystem builds alternating aerobic and anaerobic conditions in riparian tree buffers, alternately triggering nitrification and denitrification (Bissett et al., 2013), consequently increasing rates of gross N₂O fluxes through the two tightly coupled processes. Because of the typically moist conditions, riparian buffers favor more C sequestration than upland forests as increased C sequestration commonly occurs in wetter conditions (Gundersen et al., 2010), thereby facilitating N₂O to N₂. Meanwhile, soil microbial communities and denitrification gene abundance are strongly associated with soil physicochemical conditions, including soil organic C (SOC), moisture, and available N (Ding et al., 2021; Ma et al., 2020a), indicating a greater denitrification potential in the riparian buffers than upland alley cropping. Thus, due to contrasting inherent properties (e.g., water tables, soil C levels, and NO₃⁻ concentrations) between the two agroforestry systems, we expect that there would be distinct differences in gross N₂O emission and uptake.

In addition, N₂O produced and consumed in soils has been mainly focused on the top few centimeters of the soil profile but they also occur at deeper depths during upward diffusion (Shcherbak and Robertson, 2019). However, much less is known about the quantification of

gross N₂O emission and uptake at depths, especially in the actual field. Subsoil denitrification has been suggested as an important mechanism for the removal of excess NO₃⁻ before leaching to groundwater (Jahangir et al., 2012). It is likely co-limited by NO₃⁻ concentration, C availability, and water-filled pore space (WFPS), which typically change with depth (Yang and Silver, 2016a). Similarly, due to changes in soil properties, soil denitrifying bacterial community significantly differs among soil depths (Han et al., 2020). McCarty and Bremner (1992) have found that N₂O emissions in subsoil are not restricted by denitrifying organisms but by readily available C while van Groenigen et al. (2005) have reported that N₂O emissions in subsoil are mainly affected by soil moisture rather than C or N availability. Little information about how soil depths affect gross N₂O fluxes in two contrasting agroforestry systems.

Therefore, we selected two agroforestry systems with distinct inherent properties to investigate gross N₂O emission and uptake by using ¹⁵N₂O pool dilution and the abundances of denitrifying genes and total bacterial, fungal abundances by using a DNA-based analysis. This can help us investigate the relationships between biogeochemical process rates and their associated functional genes and environmental factors. The objectives of this study were to: (1) compare tree row of alley cropping system with riparian tree buffer on their influence on gross N₂O emission and uptake, (2) compare two soil depths (0 – 5 cm vs. 40 – 60 cm) in both agroforestry systems for gross N₂O emission and uptake to elucidate the factors controlling their differences. We hypothesized that riparian tree buffer will have higher gross N₂O emission and uptake than tree row of alley cropping and topsoil (0 – 5 cm) will have higher gross N₂O emission and uptake than subsoil (40 – 60 cm).

3.3. Materials and methods

3.3.1. Site description and soil sampling

Top- and subsoil were collected in the tree rows of two different types of agroforestry systems: i) a riparian tree buffer and ii) a cropland alley cropping. The riparian tree buffer (Figure S3.1a) was established in 2012 on a poorly-drained Gleysol soil with a high groundwater level near Rosdorf, Germany (51°30'26" N, 9°52'58" E, 163 m above mean sea level). The cropland alley cropping (Fig S3.1b) was established in 2007 on a well-drained Phaeozem soil near Dornburg, Germany (51°00'40" N, 11°38'46" E, 289 m above sea level). The two sites had a comparable mean annual temperature and precipitation with 9.8 ± 0.3 and 10.7 ± 0.3 °C and 595 ± 34 and 567 ± 32 mm for the riparian tree buffer and alley cropping,

respectively (2010 – 2019; German Meteorological Service). Soils at both sites developed on loess deposits and field examination of the upper 50-cm depth revealed that soil texture at both sites was dominated by silt. Therefore, soil drainage (low drainage at the riparian tree buffer; high drainage at the alley cropping) was the main difference between the two sites.

The tree rows of both agroforestry systems consisted of hybrid poplar clones (cv. Max 1; *Populus nigra* × *P. maximowiczii*) and were not fertilized as commonly practiced in temperate agroforestry systems (Schmidt et al., 2021). The first harvest of the trees of the alley cropping was performed eight years after planting (spring 2015), while the trees in the riparian tree buffer were not harvested since planting in 2012. Therefore, the poplar trees at our sites were 4 and 7 years old during our study year (2019). We hereafter refer to the two sites by their type of agroforestry system, i.e. riparian tree buffer and tree row of alley cropping.

Within the tree rows of each agroforestry system, four sampling locations (replicate plots) with a minimum distance of 15 m from each other were selected. At each replicate plot, topsoil samples (0 to 5 cm depth) were collected by sampling four intact soil cores (5 cm height, 8 cm diameter). For subsoil samples, an intact soil core (20 cm height, 8 cm diameter) from 40 to 60 cm depth was collected. The intact soil cores were used for field measurements of gross N₂O emission and gross N₂O uptake as well as net N₂O and CO₂ fluxes in early spring (April), spring (June), summer (August), and autumn (October) 2019.

3.3.2. Measurement of gross N₂O emission and uptake

We measured gross N₂O emission and uptake using the ¹⁵N₂O pool dilution technique as described by Wen et al. (2016; 2017). This technique assumes a homogeneous mixture of injected ¹⁵N₂O with soil-borne N₂O in the soil air-filled pores (Wen et al., 2016), indicating that the soil pores must be interconnected to the soil surface for homogenous mixing to occur (Wen et al., 2016). Soil cores from the top-and subsoil of each replicate plot were separately placed in an air-tight chamber (glass desiccator of 6.6 L volume) equipped with a Luer-lock stopcock on the lid (Figure S3.1c). We injected 7 ml of ¹⁵N₂O label gas (Westfalen AG, Münster, Germany) into the chamber headspace. The label gas contained 100 ppm_v 98% single labeled ¹⁵N-N₂O, 275 ppb_v sulfur hexafluoride (SF₆, as a tracer for possible physical loss of gases from the chamber headspace), and synthetic air. The injection increased headspace concentrations by approximately 125 ppb_v N₂O with 13.2% ¹⁵N initial enrichment and 292 ppt_v SF₆. Gas samples of 100 and 23 ml were collected from the chamber headspace

after 0.5, 1, 2, and 3 hours of *in-situ* incubation and injected into pre-evacuated 100-ml glass bottles and 12-ml glass vials (Exetainer; Labco Limited, Lampeter, UK) with rubber septa, respectively. The 100-ml gas samples were analyzed for $^{15}\text{N-N}_2\text{O}$ using an isotope ratio mass spectrometer (Finnigan Delta^{plus} XP, Thermo Electron Corporation, Bremen, Germany). The 23-ml gas samples were analyzed for N_2O and SF_6 concentrations using a gas chromatograph (SRI 8610C, SRI Instruments Europe GmbH, Bad Honnef, Germany) equipped with an electron capture detector with make-up gas of 5% CO_2 -95% N_2 (v/v; 5.0 purity grade). CO_2 concentrations were determined from the same gas sample on the same gas chromatograph using a methanizer coupled to a flame ionization detector. Gas fluxes were calculated from the linear increase of their concentrations over the incubation period and adjusted for air temperature and atmospheric pressure (e.g. Matson et al., 2017). The headspace was kept at atmospheric pressure and oxygen concentration by injecting 123 ml of a gas mixture containing 80% helium and 20% oxygen (v/v) into the headspace following gas sampling. This does not change the $^{15}\text{N-N}_2\text{O}$ isotope composition within the headspace (Wen et al., 2016; 2017). We accounted for this dilution in all gas flux calculations. Following the incubation, ambient air samples for gross N_2O flux calculations were collected (23 ml for the determination of ambient N_2O concentration and 100 ml for analysis of the natural abundance of $^{15}\text{N}_2\text{O}$ signatures). Atmospheric N_2O concentration was 347.5 ± 0.7 ppbv and ^{15}N natural abundance was 0.3695 ± 0.0001 atom% across sites and sampling dates. Details on the principles and calculations of gross N_2O emission and uptake are given in our previous works (Wen et al., 2016; 2017). Gross N_2O and net N_2O and CO_2 fluxes were expressed on the basis of dry soil mass.

3.3.3. Soil characteristics

General soil characteristics (pH, soil organic C, total N, base saturation, and effective cation exchange capacity) in top- and subsoil at both sites were determined at the beginning of our study as described previously by (Schmidt et al., 2021) (Table 3.1). Following measurement of gross and net N_2O fluxes, soil cores from top- and subsoil of each replicate plot were thoroughly mixed per depth, to obtain one composite sample per replicate plot and soil depth. Each composite sample was divided into subsamples for the analysis of soil controlling factors (temperature, WFPS, NO_3^- -N, NH_4^+ -N, biodegradable organic C [BDOC], microbial biomass N [MBN], and DNA-based quantification of soil bacteria, fungi, and denitrification genes). WFPS was calculated from the gravimetric moisture content (oven drying at 105 °C for 24 h) and the soil bulk density, determined by the soil core method (Blake and Hartge

1986) using a mineral soil particle density of 2.65 g cm^{-3} . In the field, fresh soil was placed into a pre-weighed extraction bottle containing 150 ml 0.5 M K_2SO_4 for the determination of extractable mineral N. Upon arrival at the laboratory, these bottles were shaken for 1 h, filtered through pre-washed (with 0.5 M K_2SO_4) filter papers, and the extracts were stored at -20°C until further analysis. MBN was determined by fumigating 20 g fresh soil for 5 days using the chloroform fumigation-extraction method (Brookes et al. 1985). Following fumigation, total extractable N was extracted from the samples using 100 ml 0.5 M K_2SO_4 as described above. The dry mass of the extracted fresh soils and the fumigated soils were calculated using the gravimetric moisture content. MBN was calculated as the difference in total extractable N between the paired fumigated and un-fumigated samples divided by a correction factor (k_N) of 0.68 (Shen et al. 1984). Extractable mineral N (NH_4^+ , NO_3^-) and total extractable N were analyzed using continuous flow injection colorimetry (SEAL Analytical AA3, SEAL Analytical GmbH, Norderstedt, Germany), where NH_4^+ was determined by salicylate and dichloroisocyanuric acid reaction, NO_3^- by cadmium reduction method with NH_4Cl buffer, and total extractable N by ultraviolet-persulfate digestion followed by hydrazine sulfate reduction. BDOC was measured under batch incubation using a modified protocol of McDowell et al. (2006). Approximately 150 g of fresh soil was extracted by shaking in 750 ml deionized water for 1 h (Jones and Willett, 2006). The extract was centrifuged at $3,871 \times g$ for 20 min and passed through a $2 \mu\text{m}$ filter. From each filtrate, six times 50 ml were transferred to 100-ml flasks covered with perforated parafilm to allow air exchange and incubated at room temperature in the dark. At 0, 1, 3, 7, 14, and 28 days after the start of the incubation, the filtrate of one of the six flasks was passed through a $0.2 \mu\text{m}$ cellulose acetate filter and stored at -20°C until analysis. Dissolved organic carbon (DOC) concentrations were determined using ultraviolet-enhanced persulfate oxidation using a Total Organic Carbon Analyzer (TOC-Vwp, Shimadzu Europa GmbH, Duisburg, Germany). BDOC was determined as the difference between the maximum and minimum DOC concentration during the incubation period. For DNA extraction, approximately 20 g of fresh soil were transferred to a sterile 15-ml polypropylene Falcon tube and frozen at -20°C while in the field.

Table 3.1. Soil characteristics (means \pm 1 SE; n = 4 plots) in two agroforestry systems

Agroforestry type	Depth (cm)	SOC (g kg ⁻¹)	Total N (g kg ⁻¹)	pH	ECEC (mmol _c kg ⁻¹)	BS (%)	Bulk density [†] (g cm ⁻³)
Riparian tree buffer	0-5	102 \pm 10	9.4 \pm 0.8	6.9 \pm 0.1	458 \pm 39	100 \pm 0	0.7 \pm 0.0
	40-60	14 \pm 2	1.1 \pm 0.1	7.4 \pm 0.2	577 \pm 21	100 \pm 0	1.0 \pm 0.1
Tree row of alley cropping	0-30	17 \pm 1	1.8 \pm 0.1	6.6 \pm 0.1	152 \pm 5	99 \pm 0	1.0 \pm 0.0
	30-60	11 \pm 1	1.2 \pm 0.1	6.7 \pm 0.1	164 \pm 10	100 \pm 0	1.3 \pm 0.0

Notes: Soil characteristics were measured in 2019 for riparian tree buffer and 2016 for the tree row in alley cropping (Schmidt et al., 2021). SOC, soil organic C; ECEC, effective cation exchange capacity; BS, base saturation. [†] Bulk density of tree row in alley cropping was from 0 – 5 and 40 – 60 cm.

3.3.4. Quantification of bacteria, fungi, and denitrification genes in soil

Soil samples were stored at -20 °C upon arrival at the laboratory and subsequently freeze-dried. Freeze-dried samples were homogenized as described earlier (Beule et al., 2019a) and DNA was extracted from 200 mg finely ground soil using a phosphate lysis buffer protocol optimized for subsoils (Guerra et al., 2020). Briefly, soil material was suspended in 1 M phosphate buffer containing 0.5% (w/v) sodium dodecyl sulfate, the mixture was centrifuged, and the supernatant was extracted using phenol and chloroform-isoamyl alcohol. DNA was precipitated using polyethylene glycol-NaCl and the extracts were checked on 0.8% (w/v) agarose gels stained with ethidium bromide. To overcome PCR inhibition, the extracts were tested for PCR inhibitors using a DNA amplification inhibition test (Guerra et al., 2020) and diluted accordingly prior to PCR. The abundance of soil bacteria, fungi, and denitrification genes (*nirK*, *nirS*, *nosZ* clade I, and *nosZ* clade II) were analyzed using real-time PCR as described previously (Beule et al., 2020). Briefly, soil DNA extracts were amplified in 4- μ l reaction volumes in 384-well microplates in a CFX384 Thermocycler (Bio-Rad, Rüdigenheim, Germany). The choice of primers, the composition of the reaction volumes, and the thermocycling conditions are identical to those used by Beule et al. (2020).

3.3.5. Statistical analyses

At each site, the distance between the replicate plots (15 m) was tested for spatial independence using the first data set of soil gross and net N₂O fluxes. Based on von Neumann's ratio test for randomness (Bartels, 1982), these fluxes were not auto-correlated. Thus, our replicate plots were considered biological replicates in our statistical analysis. Each parameter was tested for normal distribution and equality of variances using Shapiro-Wilk and Levene's test, respectively. Seasonal patterns of all parameters at each depth per site were explored using one-way ANOVA followed by Tukey HSD test (parameters that met equality of variances and normal distribution) or Kruskal-Wallis test with multiple comparison extension (parameters that did not meet equality of variances and/or normal distribution). Differences between the two types of agroforestry systems (riparian tree buffer = 1, tree row in alley cropping = 2 reading as ordinal categorical variables) at each soil depth or between depths (0 – 5 cm depth = 1, 40 – 60 cm depth = 2) at each site were tested using linear mixed effect (LME) models. In the models, the agroforestry type/soil depth was set as a fixed effect and sampling day and replicate plot as random effects (Crawley, 2007). Parameters that did not meet normal distribution were either square-root (gross N₂O emission, WFPS, total mineral N [sum of NH₄⁺ and NO₃⁻], soil respiration, BDOC) or log-transformed (net N₂O flux, MBN, bacteria, fungi, and denitrification gene abundance) to meet the assumptions of LME. These LME models were developed to include a variance function (varIdent) to account for heteroscedasticity of the fixed effect and/or a first-order temporal autoregressive function that accounted for decreasing correlation of the measurements with increasing time (Zuur et al., 2009) if this improved the relative goodness of the model fit based on the Akaike information criterion.

We performed a structural equation model (SEM) to identify how gross N₂O emissions were affected by the types of agroforestry system and soil depth using the 'lavaan' R package. Before SEM analysis, we used the data set from the LME model (i.e. transformed data) to conduct a principal component analysis (PCA) to group parameters that were auto-correlated into three groups: (1) substrate availability (BDOC, soil respiration, NH₄⁺, NO₃⁻), (2) microbial community (MBN, bacteria, and fungi), and (3) functional gene abundance (*nirK*, *nirS*, *nosZ* clade I and II). The first component (PC1) explained 68% to 94% of the total variance for each group (Figure S3.2) and PC1 scores corresponding to each replicate plot per sampling day and depth were considered as a new variable in SEM analysis (Barnes et al., 2017). The lower the PC1 score, the greater the values of the grouped parameters, thus, to

make it intuitive, we used inverse PC1 scores so that the greater PC1 scores directly indicate greater values of the parameters (Figure S3.3). The quality of the SEM model was assessed using chi-square goodness of fit ($P > 0.05$), standardized root mean square error of approximation (value < 0.08), and comparative fit index (value > 0.9) (Kline, 2014). Spearman's rank correlation test was used to explore temporal correlations i) at each depth within each agroforestry system ($n = 16$, i.e., 4 replicate plots \times 4 measurements \times 1 depth), ii) across depths within each agroforestry system ($n = 32$, i.e., 4 replicate plots \times 4 measurements \times 2 depths), and iii) at each depth across both agroforestry systems ($n = 32$, i.e., 4 replicate plots \times 4 measurements \times 2 sites). All statistical tests were considered significant at $P \leq 0.05$. We conducted all statistical analyses under R version 3.6.3 (R Core Team, 2019).

3.4. Results

3.4.1. Soil N₂O flux dynamics

Gross fluxes of N₂O in topsoil of both types of agroforestry systems were comparable among seasons ($P \geq 0.08$; Figure 3.1a, c). In contrast, a seasonal pattern emerged in subsoil where gross N₂O emissions and uptake were highest in spring ($P \leq 0.04$; Figure 3.1a, c). In the riparian tree buffer, net N₂O emissions at both depths were highest in early spring ($P \leq 0.03$; Figure 3.1e) while the season did not affect net emissions in the tree row of alley cropping. Across seasons, gross N₂O emissions and uptake were higher in the riparian tree buffer than in the tree row of alley cropping in topsoil ($P \leq 0.03$) but comparable in subsoil ($P \geq 0.06$; Figure 3.1b, d). Soil depth did not affect gross and net fluxes of N₂O at each agroforestry system across seasons ($P \geq 0.06$; Figure 3.1b, d, f), however, gross N₂O emissions in topsoil of the riparian tree buffer were 114% higher as compared to subsoil. Although the two agroforestry systems showed similar net N₂O fluxes ($P = 0.09$; Figure 3.1f), only topsoil in the riparian tree buffer was identified as a net source for N₂O (Figure 3.1f).

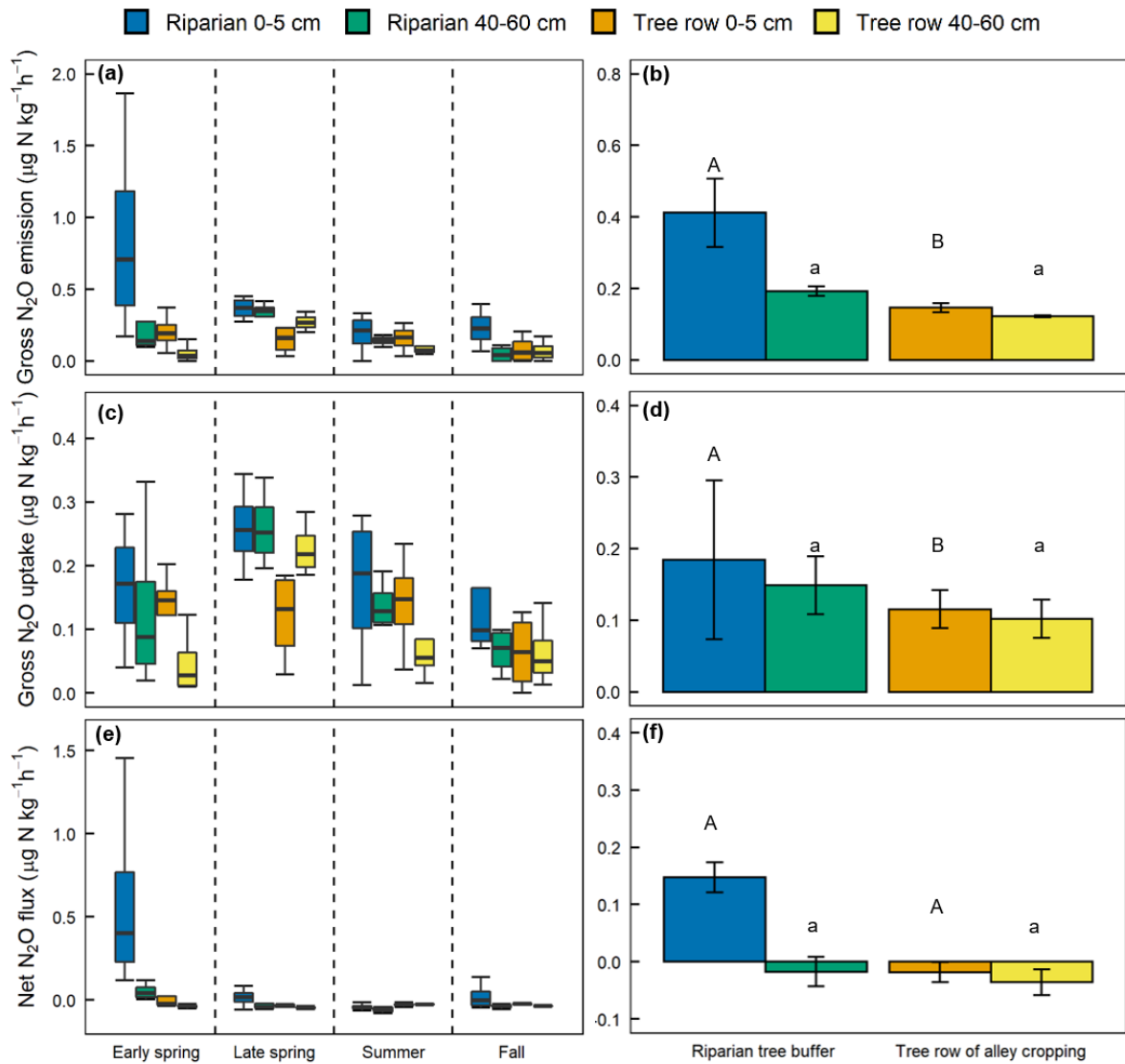


Figure 3.1. Soil gross N₂O emission (a, b), gross N₂O uptake (c, d), and net N₂O flux (e, f) at depths of 0 – 5 cm (topsoil) and 40 – 60 cm (subsoil) in riparian tree buffer and tree row of alley cropping. Means ± 1 SE for bars in b, d, f (n = 4 plots) followed by different capital letters indicate significant differences between agroforestry systems for the topsoil and different small letters for the subsoil (linear mixed effect model at $P \leq 0.05$).

3.4.2. Soil controlling factors

WFPS exhibited a strong seasonal dependence as it decreased from early spring to summer and increased in fall (Figure 3.2a). At each soil depth, the average WFPS was greater in the riparian tree buffer than in the tree row of alley cropping ($P \leq 0.05$; Figure 3.2b). While the WFPS was comparable across depths in the riparian tree buffer ($P = 0.99$), it was greater in topsoil than subsoil in the tree row of alley cropping ($P = 0.05$; Figure 3.2b). Soil temperature did not differ between the two types of agroforestry systems nor depths ($P \geq 0.09$).

Total mineral N in the riparian tree buffer at both depths was dominated by NO_3^- -N and was highest in early spring ($P \leq 0.008$; Figure 3.2c). In contrast, the total mineral N in the tree row of alley cropping was dominated by NH_4^+ -N. In topsoil of this system, mineral N was highest in spring ($P = 0.004$; Figure 3.2c), whereas no seasonal variation was observed in subsoil ($P = 0.19$; Figure 3.2c). At both sites, total mineral N declined from topsoil to subsoil ($P < 0.001$). In topsoil, the riparian tree buffer had higher mineral N content as compared to the tree row of alley cropping ($P < 0.001$); in subsoil, however, mineral N content was comparable between the two systems ($P = 0.21$; Figure 3.2d). Seasonal patterns of soil respiration and BDOC were similar to that of total mineral N (*cf.* Figure 3.2c, e, g). Average soil respiration and BDOC in the riparian tree buffer were greater than in the tree row of alley cropping ($P \leq 0.02$; Figure 3.2f, h). Topsoil sampled in the tree row of alley cropping had higher soil respiration as compared to subsoil ($P < 0.001$; Figure 3.2f). BDOC in the riparian tree buffer was greater in topsoil than subsoil ($P = 0.01$; Figure 3.2h)

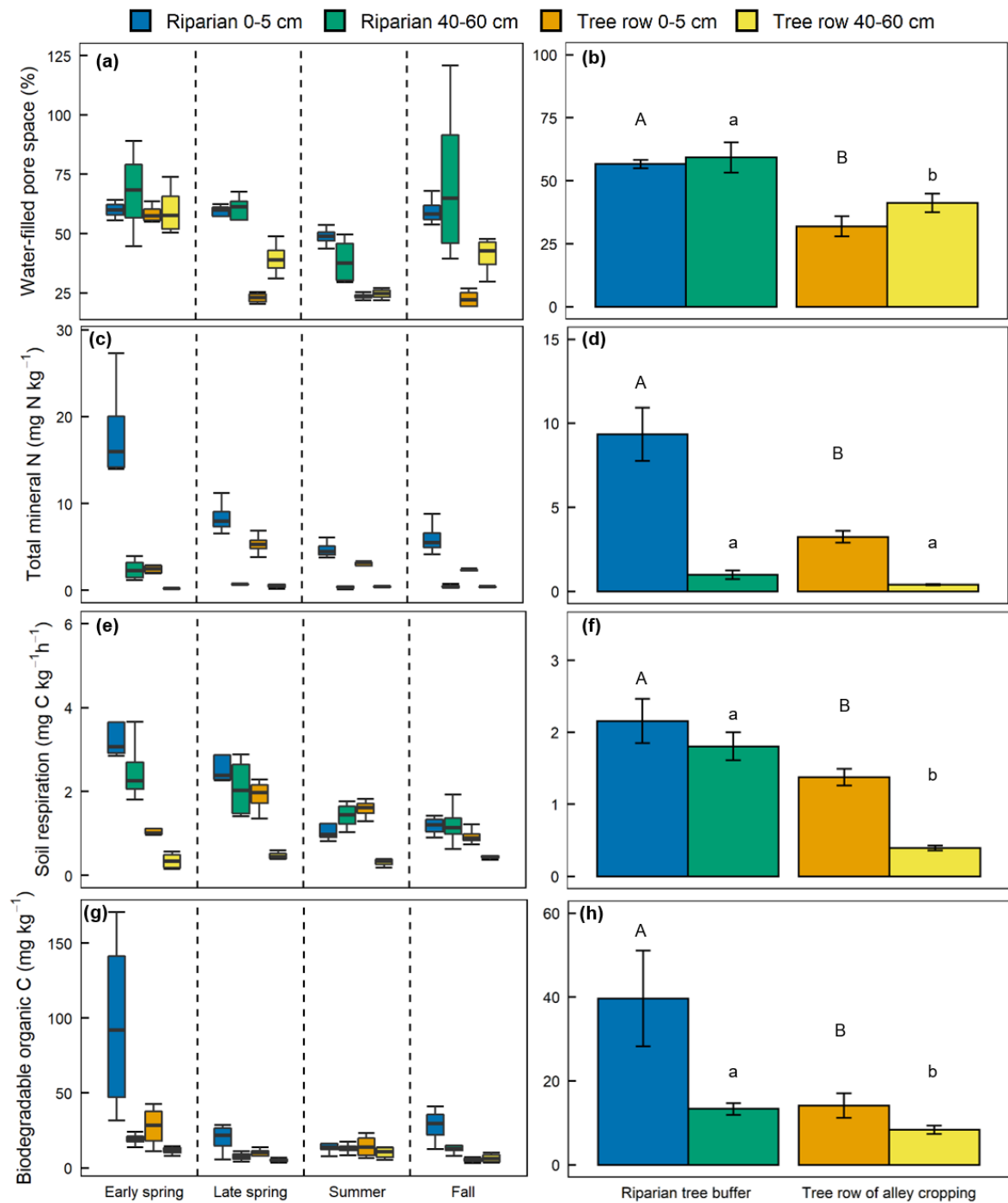


Figure 3.2. Soil water-filled pore space (a, b), total mineral N (c, d), soil respiration (e, f), and biodegradable organic C (g, h) at depths of 0 – 5 cm (topsoil) and 40 – 60 cm (subsoil) in riparian tree buffer and tree row of alley cropping. Means \pm 1 SE for bars in b, d, f, h ($n = 4$ plots) followed by different capital letters indicate significant differences between agroforestry systems for the topsoil and different small letters for the subsoil (linear mixed effect model at $P \leq 0.05$).

3.4.3. Microbial community and denitrification gene abundance

Besides high MBN in subsoil of the tree row of alley cropping in early spring, MBN, bacteria, and fungi lacked seasonal dynamics (Figure 3.3a, c, e). MBN and bacterial abundance were greater in the topsoil of the riparian tree buffer than the tree row of alley cropping ($P < 0.001$; Figure 3.3b, d). Conversely, the tree row of alley cropping showed greater MBN and bacterial population size in subsoil than the riparian tree buffer ($P \leq 0.04$; Figure 3.3b, d). Fungal population size in topsoil did not differ between the two agroforestry systems but was greater in subsoil of the tree row of alley cropping than the riparian tree buffer ($P < 0.001$; Figure 3.3f). All three measures of the microbial community size (MBN, bacterial 16S rRNA, and fungal 18S rRNA gene abundance) declined from topsoil to subsoil ($P < 0.001$; Figure 3.3b, d, f).

The abundance of microorganisms harboring denitrification genes (*nirK*, *nirS*, *nosZ* clade I and II) declined from topsoil to subsoil at both agroforestry systems ($P < 0.001$). No seasonal pattern of denitrification gene abundance was observed except that the abundance of *nosZ* clade I and II genes was greatest in summer ($P \leq 0.04$; Figure 3.4a,c,e,g). In topsoil, average copy numbers of *nirK*, *nirS*, and *nosZ* clade I genes were greater in the riparian tree buffer than in the tree row of alley cropping ($P \leq 0.01$) (Figure 3.4b,d,g). In subsoil, the riparian tree buffer harbored more microorganisms that carry *nirS* genes as compared to the tree row of alley cropping ($P = 0.01$) (Figure 3.4d). Conversely, *nirK* and *nosZ* clade II genes were more frequently recovered in subsoil samples of the tree row of alley cropping than the riparian tree buffer ($P < 0.001$) (Figure 3.4b,h).

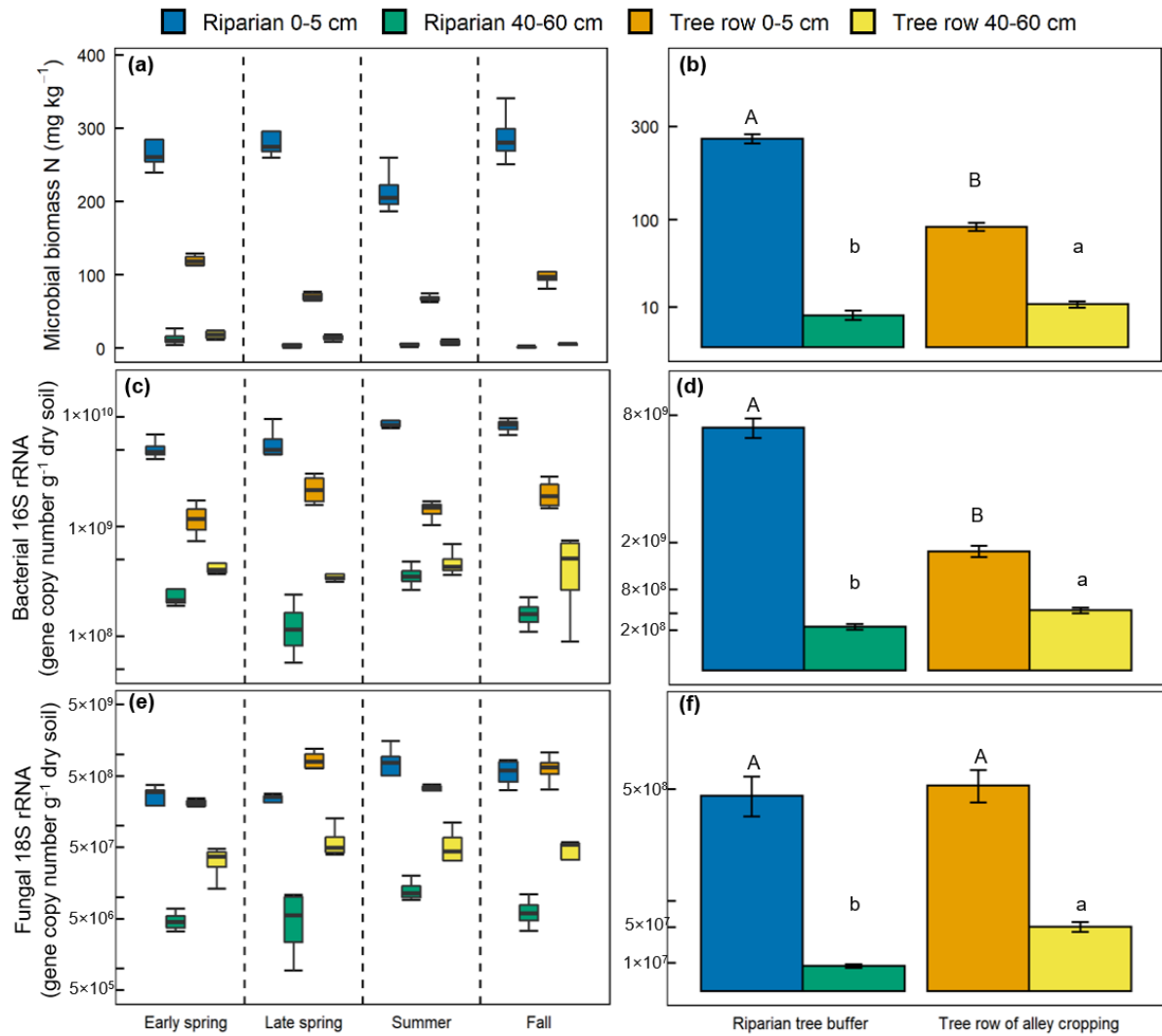


Figure 3.3. Soil microbial biomass N (a, b), bacterial 16S rRNA (c, d), and fungal 18S rRNA gene abundance (e, f) at depths of 0 – 5 cm (topsoil) and 40 – 60 cm (subsoil) in riparian tree buffer and tree row of alley cropping. Means \pm 1 SE for bars in b, d, f ($n = 4$ plots) followed by different capital letters indicate significant differences between agroforestry systems for the topsoil and different small letters for the subsoil (linear mixed effect model at $P \leq 0.05$).

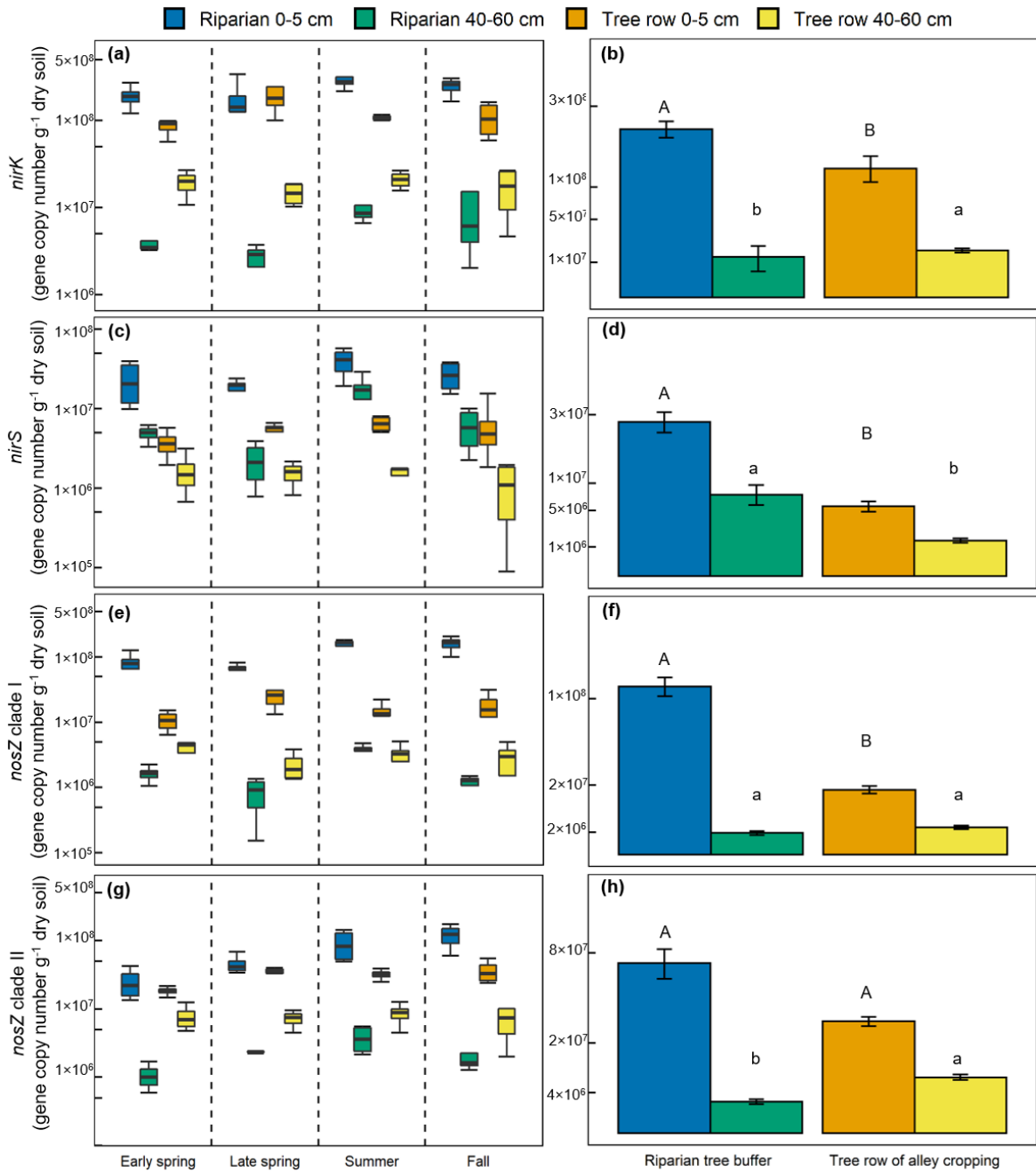
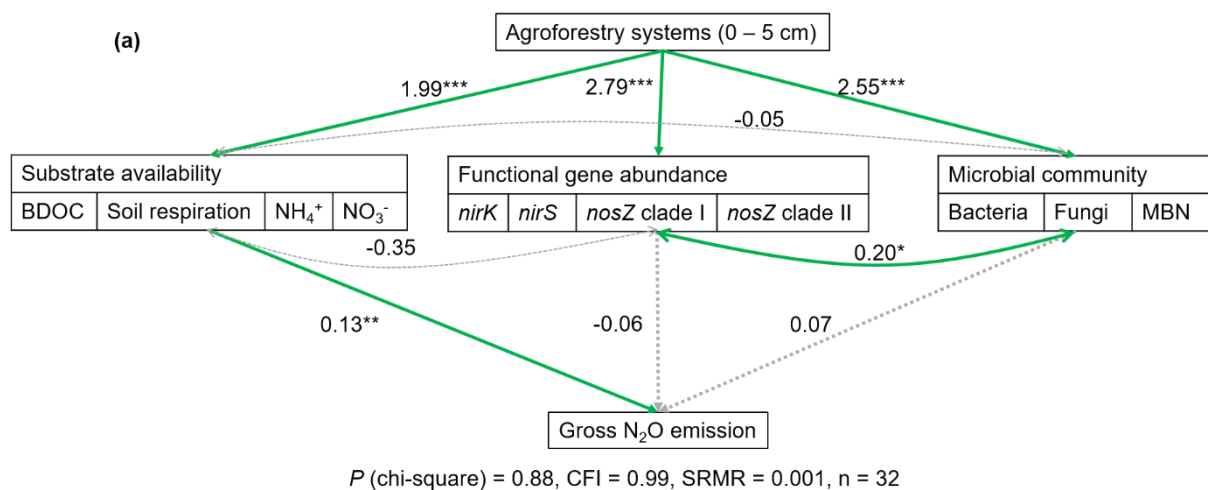


Figure 3.4. Soil denitrification gene abundance of *nirK* (a, b), *nirS* (c, d), *nosZ* clade I (e, f), and *nosZ* clade II (g, h) at depths of 0 – 5 cm (topsoil) and 40 – 60 cm (subsoil) in riparian tree buffer and tree row of alley cropping. Means \pm 1 SE for bars in b, d, f, h ($n = 4$ plots) followed by different capital letters indicate significant differences between agroforestry systems for the topsoil and different small letters for the subsoil (linear mixed effect model at $P \leq 0.05$).

3.4.4. Factors controlling gross N₂O fluxes

The SEM revealed that variations in gross N₂O emissions in the topsoil of both agroforestry systems (Figure 3.5a) and across soil depths in the riparian tree buffer (Figure 3.5b) were mainly due to substrate availability rather than functional gene abundance or microbial community size. Gross N₂O emissions were highly correlated with gross N₂O uptake (Figure S3.4a). In topsoil, we found positive relationships between gross N₂O emissions and total mineral N and BDOC across the agroforestry systems (Figure S3.4b, c). Gross N₂O emissions showed a positive correlation with the ratio of *nosZ* clade I-to-*nosZ* clade II gene copies (Figure S3.4d) due to its auto-correlation with total mineral N ($\rho = 0.62$, $n = 32$, $P < 0.001$) and BDOC ($\rho = 0.76$, $n = 32$, $P < 0.001$). Similarly, gross N₂O emissions in subsoil were positively linked to total mineral N across the two agroforestry systems ($\rho = 0.45$, $n = 32$, $P = 0.45$). The gross uptake of N₂O in topsoil increased with increasing soil respiration (Figure 3.6a) and *nirK* gene abundance (Figure 3.6b) but decreased as the ratio of BDOC to total mineral N increased (Figure 3.6c). Interestingly, gross N₂O uptake showed a positive relationship with total mineral N across the two agroforestry systems (Figure 3.6d).

In the riparian tree buffer, we only found a positive relationship between gross N₂O uptake and soil temperature in subsoil ($\rho = 0.52$, $n = 16$, $P = 0.04$). In the tree row of alley cropping, we did not detect any correlations of gross N₂O fluxes with the measured soil variables per depth or across depths.



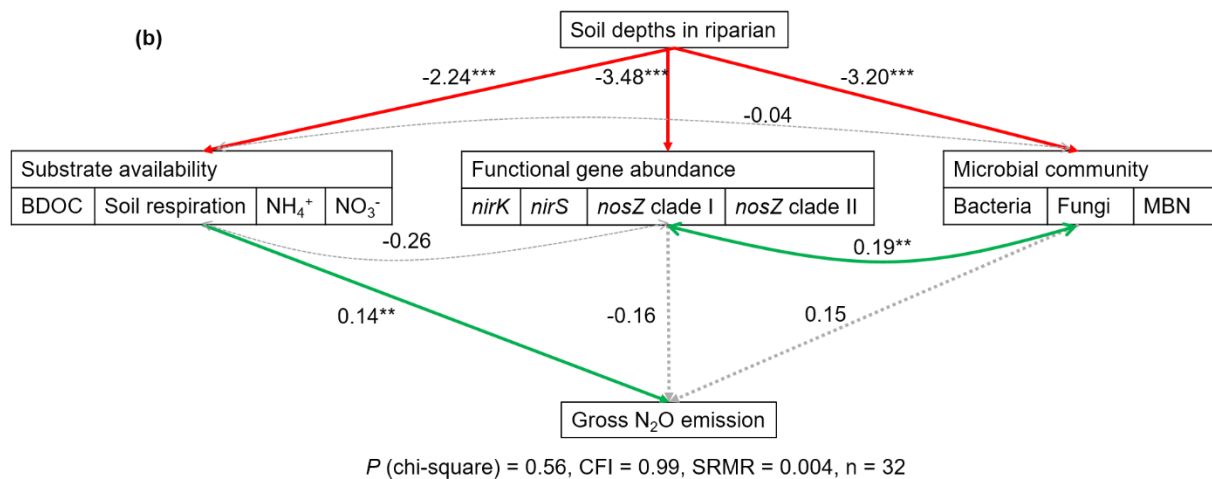


Figure 3.5. Structural equation modeling of the causal links of controlling factors on gross N₂O emission from 0 – 5 cm depth (topsoil) across agroforestry systems and seasons (a) and 0 – 5 cm and 40 – 60 cm depth (subsoil) in riparian tree buffer (b). Substrate availability included soil biodegradable organic C (BDOC), soil respiration, NH₄⁺, and NO₃⁻ concentrations from the first component (PC1) of the principal component analysis (PCA). Functional gene abundance included *nirK*, *nirS*, *nosZ* clade I, and *nosZ* clade II from PC1 of PCA. The microbial community included bacterial 16S and fungal 18S rRNA gene abundance, and microbial biomass N (MBN) from PC1 of PCA. Values next to the lines are standardized path coefficients (at * P < 0.05, ** P < 0.01, *** P < 0.001); green and red lines represent positive and negative pathways, respectively. Grey dashed lines represent non-significant pathways. Single-headed and double-headed arrows refer to unidirectional and bidirectional relationships, respectively. The quality of models was assessed by chi-square (P > 0.05), standardized root mean square error of approximation (SRMR, value < 0.08), and comparative fit index (CFI, value > 0.9). Agroforestry system and soil depth were read as ordinal categorical data: riparian tree buffer and 0 – 5 cm = 1; tree row in alley cropping and 40 – 60 cm = 2.

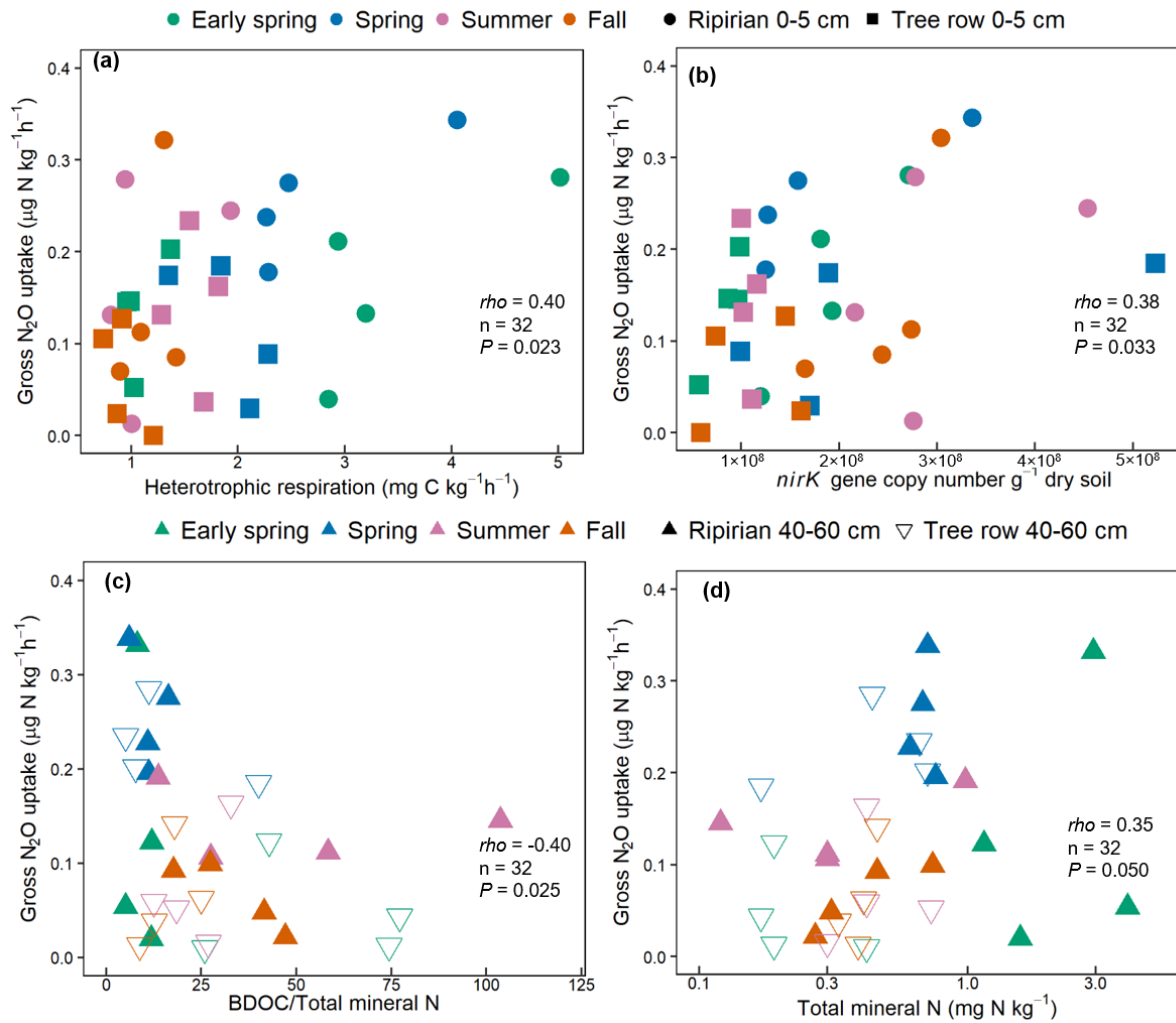


Figure 3.6. Spearman's rank correlations between gross N₂O uptake, soil respiration (a) and *nirK* gene abundance (b) in 0 – 5 cm, and between gross N₂O uptake, biodegradable organic C (BDOC)-to-total mineral N ratio (c), and total mineral N (d) in 40 – 60 cm.

3.5. Discussion

3.5.1. Gross N₂O fluxes in different agroforestry systems

Gross N₂O emissions and uptake in topsoil were greater in the poorly-drained (high WFPS; Figure 3.2a) soil of the riparian tree buffer than in the well-drained (low WFPS; Figure 3.2a) alley cropping system (Figure 3.1b), which agrees with our first hypothesis. The enhanced gross N₂O emissions in the riparian buffer are consistent with the findings of Wen et al. (2017) who also applied the ¹⁵N₂O pool dilution technique and reported that high WFPS results in anaerobic soil conditions and favors the production of N₂O. Additionally, the high total mineral N (electron acceptor; Figure 3.2d), BDOC (electron donor; Figure 3.2h), and denitrifier population size (Figures 3.3a,b,d, and 3.4) at the riparian tree buffer likely further promoted gross N₂O emissions at favorable WFPS. Our SEM (Figure 3.5a), however, indicated that gross N₂O emissions were mainly determined by substrate availability rather than denitrifiers, suggesting that the population size of denitrifiers did not limit denitrification. The observed positive correlation of gross N₂O emissions with total mineral N (Figure S3.4b) and BDOC (Figure S3.4c) also confirm the findings of previous studies performed in a forest stand (Wen et al., 2017) and a fertilized cropland (Yang and Silver, 2016b). The effect of *nosZ* clade I-to-*nosZ* clade II ratio on gross N₂O emissions (Figure S3.4d) was attributed to its auto-correlation with mineral N and BDOC, indicating a niche differentiation of *nosZ* clade I- and clade II-carrying microorganisms depending on available substrates. The greater ratio of *nosZ* clade I-to-*nosZ* clade II (1 – 5) in the riparian tree buffer than in the tree row of alley cropping (< 1; Figure S3.4d) was accompanied by a 10-fold increase of NO₃⁻-N in the riparian buffer as compared to the alley-cropping system, suggesting that *nosZ* clade II denitrifiers favor NO₃⁻ limiting conditions. This observation agrees with the work of Semedo et al. (2020), who proposed that the presence of NO₃⁻-N could restrict the expression of *nosZ* clade II genes and, thus, the reduction of N₂O to N₂. Although gene expression of denitrification genes was not assessed in our study, we argue that in the long term, the ratio of *nosZ* clade I- to clade II-carrying microorganisms will adjust to environmental conditions such as NO₃⁻-N concentrations.

The higher gross N₂O uptake in the riparian tree buffer than in the tree row of alley cropping could be driven by higher gross N₂O emissions because of their positive relationship (Figure S3.4a). Thus, the factors that favored gross N₂O emissions should have favored gross N₂O uptake. The high mineral N and BDOC, as well as favorable soil moisture in the riparian,

resulted in high gross N₂O emissions. Meanwhile, the generated N₂O was partly reduced to N₂ because the topsoil of riparian showed a source of N₂O (Figure 3.1f). Gross N₂O uptake was positively correlated with *nirK* gene abundance and soil respiration (as an indicator of C availability) (Figure 3.6a, b), suggesting that higher C availability would provide more resources for the population of denitrification genes (e.g., *nirK*) (Song et al., 2011), thereby more N₂O reduction to N₂. This could be explained by the co-occurrence of *nirK* and *nosZ* clades (Bowen et al., 2018; Graf et al., 2014). It suggested that higher *nosZ* clade I gene abundance was the one to drive more N₂O reduction to N₂ in the riparian because *nosZ* clade II gene abundance was similar between both agroforestry systems.

In subsoil, both agroforestry systems showed similar gross N₂O emissions and uptake (Figure 3.1b, d) but were characterized as a net sink for N₂O (Figure 3.1f). The strong correlation of gross N₂O uptake and emissions (Figure S3.4a) suggests that almost all of the N₂O produced in subsoil was further reduced to N₂ (Wen et al., 2016). As N₂O reduction is highly dependent on soil water content and C availability (Chapuis-Lardy et al., 2007), we expected that gross N₂O uptake would have been higher in the riparian tree buffer as compared to the tree row of alley cropping due to their differences in WFPS and C availability (i.e. soil respiration and BDOC) in subsoil. Gross N₂O uptake in subsoil, however, did not differ between agroforestry systems, which disagrees with our first hypothesis. We propose that the lower denitrification gene abundance (*nirK* and *nosZ* clade II) in the riparian tree buffer as compared to the tree row of alley cropping may have offset the advantage from abiotic factors (i.e., WFPS and C availability) and represented a microbial bottleneck for N₂O uptake in subsoil. The negative relationship between gross N₂O uptake and soil BDOC-to-total mineral N ratio (Figure 3.6c) in subsoil illustrated that the more electron donor relative to electron acceptor would not facilitate N₂O reduction to N₂. It is possibly because the total mineral N (< 5 mg kg⁻¹) was extremely low in both agroforestry systems, reflecting an N limitation rather than a C limitation for gross N₂O uptake in subsoil, as further delineated by the positive correlation of gross N₂O uptake and total mineral N (Figure 3.6d). The depletion of NO₃⁻-N is likely due to the effective uptake of NO₃⁻-N through the hybrid poplar trees as their deep-rooting system allows the uptake of nutrients from the subsoil (Truax et al., 2017). Therefore, similar total mineral N concentrations likely accounted for similar gross N₂O uptake in subsoil in the two agroforestry systems. Collectively, gross N₂O emissions were mainly driven by substrate availability across the two contrasting agroforestry systems but microbial attributes, to some extent, that solely functioned as mediators in regulating N₂O reduction to N₂.

3.5.2. Gross N₂O fluxes at depths

Contrary to our second hypothesis, soil depth did not influence gross N₂O emissions and uptake in both agroforestry systems (Figure 3.1b). In the riparian tree buffer, however, we found a 112% increase in gross N₂O emissions in topsoil relative to subsoil. It is possibly because of the large spatial variation of gross N₂O emissions in topsoil that masked the difference between depths. In particular, gross and net N₂O emissions in topsoil were largest in the early spring than in other seasons (Figure 3.1a, e). This is in parallel by similar spatial heterogeneity of the availability of mineral N and BDOC (Figure 3.2c, g) supported by our SEM results (Figure 3.5b). Similar to previous findings (Liu et al., 2015), soil depths had a significant effect on microbial population size (Figures 3.3 and 3.4), however, we did not find any relationships between gross N₂O emissions and functional gene abundance. It is possible because microbial population size remained much more stable in response to seasonal change relative to environmental factors. For example, soil mineral N was highest in the early spring when the poplar leaves just started to sprout and the plant N uptake was low, and then it decreased to summer when the leaves were flushing and plant N uptake was high, suggesting that plant N uptake indirectly regulated gross N₂O emissions. Thus, the early spring could act as a hot moment for net N₂O emissions owing to warm temperature, high WFPS, C and N availability, and low plant N uptake. In contrast, in the well-drained tree row of alley cropping, a similar net N₂O uptake was exhibited between topsoil and subsoil where both depths displayed very low mineral N (< 4 mg N kg⁻¹). This net uptake may be driven by low gross N₂O emissions that were paralleled by low mineral N availability. We expect that gross N₂O emissions in topsoil should have been stimulated by higher substrate availabilities and microbial population size. However, we did not find such results. It is possible because the lower WFPS in topsoil (Figure 3.2b) may have offset the advantage from substrate and microorganisms. Thus, the very low mineral N and WFPS were the predominant factors driving low and similar gross N₂O emissions between depths in the alley cropping.

In both agroforestry systems, gross N₂O uptake in topsoil was not influenced by seasonal change but affected in subsoil where the temporal variation of gross N₂O uptake was mirrored with similar seasonal changes in soil temperature, indicating that gross N₂O uptake in subsoil was more sensitive to the environmental change than topsoil. Additionally, the higher gross N₂O uptake was associated with higher temperature in spring, suggesting a positive feedback of climate change on N₂O reduction to N₂ in subsoil. This is possible

because an increase in soil temperature positively affects microbiological activity and gas diffusion while it negatively affects the solubility of N_2O (Heincke and Kaupenjohann, 1999). Overall, gross N_2O fluxes were mainly driven by environmental factors rather than microbial attributes at depths in each agroforestry system.

3.5.3. Coupling between gross N_2O fluxes and microbial population size

Finding the relationships between gross N_2O fluxes, microbial community, denitrification gene abundance, and environmental factors help to understand whether the controls of gross N_2O emissions and uptake in contrasting agroforestry systems are a physiological response in which increased rates because of supportable environmental conditions, or a population response in which increased rates because of an increase in denitrifiers. At present study, the microbial community size and denitrifying gene abundances were more temporally static than environmental factors (i.e., WFPS, C, and N availability), despite differences in these parameters on average between the two agroforestry systems or depths (Figures 3.2, 3.3, and 3.4). No direct or indirect paths coupling between gross N_2O emissions and microbial population size detected (Figure 3.5) suggested that DNA-based gene abundances are not a complete indicator for gross N_2O emissions between the two contrasting systems or the two soil depths, corroborating with the previous findings in an agricultural watershed in Minnesota (Tomasek et al., 2017). Therefore, tying biogeochemical process rates to gene abundances cannot be used blindly as a proxy for process rates since DNA-based measurements of gene abundances indicate the size of microbial community and denitrifying population in a soil sample instead of whether genes are actively transcribed (Tomasek et al., 2017; Rocca et al., 2015).

3.5.4. Implication

Our findings point to substrate availability rather than microbial population size as the main driver of gross N_2O fluxes between the two agroforestry systems or depths. In subsoil, the observed net N_2O uptake indicated a greater capability of NO_3^- -N reduction to N_2 due to the N limitation when NO_3^- -N leached to the subsoil. Nonetheless, there were still some missing depths between topsoil (0 – 5 cm) and subsoil (40 – 60 cm), hindering our understanding of how depths affect gross N_2O fluxes during N_2O upward diffusion. The measurement frequency of gross N_2O fluxes at depths should be increased to capture hot moments and

spots especially in the riparian tree buffer and further better constrain the contribution of subsoils to ecosystem N loss although this area is relatively small.

3.6. Acknowledgments

This work was funded by the Bundesministerium für Bildung und Forschung (Bonares-SIGNAL project, 031A562A/031B0510A). Jie Luo was supported by China Scholarship Council. We thank Antje Sophie Makowski, Andrea Bauer, Kerstin Langs, Dirk Böttger, and Martina Knaust for all the field and laboratory assistance.

3.7. References

- Allen, M. R. 2015. Climate change 2014. Synthesis report. [IPCC, WMO], [Geneva].
- Allen, S. C., S. Jose, P. Nair, B. J. Brecke, P. Nkedi-Kizza, and C. L. Ramsey. 2004. Safety-net role of tree roots: evidence from a pecan (*Carya illinoensis* K. Koch)–cotton (*Gossypium hirsutum* L.) alley cropping system in the southern United States. *Forest Ecology and Management* **192**:395–407.
- Almaraz, M., M. Y. Wong, and W. H. Yang. 2020. Looking back to look ahead: a vision for soil denitrification research. *Ecology* **101**:e02917.
- Baah-Acheamfour, M., C. N. Carlyle, E. W. Bork, and S. X. Chang. 2020. Forest and perennial herbland cover reduce microbial respiration but increase root respiration in agroforestry systems. *Agricultural and Forest Meteorology* **280**:107790.
- Barnes, A. D., K. Allen, H. Kreft, M. D. Corre, M. Jochum, E. Veldkamp, Y. Clough, R. Daniel, K. Darras, L. H. Denmead, N. Farikhah Haneda, D. Hertel, A. Knohl, M. M. Kotowska, S. Kurniawan, A. Meijide, K. Rembold, W. Edho Prabowo, D. Schneider, T. Tschardtke, and U. Brose. 2017. Direct and cascading impacts of tropical land-use change on multi-trophic biodiversity. *Nature ecology & evolution* **1**:1511–1519.
- Bartels, R. 1982. The Rank Version of von Neumann's Ratio Test for Randomness. *Journal of the American Statistical Association* **77**:40–46.
- Baskerville, M., N. Reddy, E. Ofori, N. V. Thevathasan, and M. Oelbermann. 2021. Vegetation type does not affect nitrous oxide emissions from riparian Zones in Agricultural Landscapes. *Environmental Management* **67**:371–383.
- Beule, L., M. D. Corre, M. Schmidt, L. Göbel, E. Veldkamp, and P. Karlovsky. 2019. Conversion of monoculture cropland and open grassland to agroforestry alters the abundance of soil bacteria, fungi and soil-N-cycling genes. *PloS one* **14**:1-19.

- Beule, L., E. Lehtsaar, M. D. Corre, M. Schmidt, E. Veldkamp, and P. Karlovsky. 2020. Poplar rows in temperate agroforestry croplands promote bacteria, fungi, and denitrification genes in soils. *Frontiers in Microbiology* **10**:1–5.
- Bissett, A., M. V. Brown, S. D. Siciliano, and P. H. Thrall. 2013. Microbial community responses to anthropogenically induced environmental change: towards a systems approach. *Ecology Letters* **16 Suppl 1**:128–139.
- Boleman, P., and M. Jacobson. 2021. Nitrogen credit trading as an incentive for riparian buffer establishment on Pennsylvania farmland. *Agroforestry Systems*.
- Butterbach-Bahl, K., E. M. Baggs, M. Dannenmann, R. Kiese, and S. Zechmeister-Boltenstern. 2013. Nitrous oxide emissions from soils: how well do we understand the processes and their controls? *Philosophical transactions of the Royal Society of London. Series B, Biological sciences* **368**:20130122.
- Chapman, M., W. S. Walker, S. C. Cook-Patton, P. W. Ellis, M. Farina, B. W. Griscom, and A. Baccini. 2020. Large climate mitigation potential from adding trees to agricultural lands. *Global Change Biology*:4357–4365.
- Crawley, M.J., 2007. *The R Book*. John Wiley & Sons Ltd., Chichester, West Sussex.
- Davis, M. P., T. A. Groh, D. B. Jaynes, T. B. Parkin, and T. M. Isenhardt. 2019. Nitrous oxide emissions from saturated riparian buffers: are we trading a water quality problem for an air quality problem? *Journal of Environment Quality* **48**:261.
- Ding, L., J. Zhou, Q. Li, J. Tang, and X. Chen. 2021. Effects of land-use type and flooding on the soil microbial community and functional genes in reservoir riparian zones. *Microbial Ecology*. doi:10.1007/s00248-021-01746-3.
- Fisher, K., P. A. Jacinthe, P. Vidon, X. Liu, and M. E. Baker. 2014. Nitrous oxide emission from cropland and adjacent riparian buffers in contrasting hydrogeomorphic settings. *Journal of environmental quality* **43**:338–348.
- Groffman, P. M., M. A. Altabet, J. K. Böhlke, K. Butterbach-Bahl, M. B. David, M. K. Firestone, A. E. Giblin, T. M. Kana, L. P. Nielsen, and M. A. Voytek. 2006. Methods for measuring denitrification: diverse approaches to a difficult problem. *Ecological Applications* **16**:2091–2122.
- Guerra, V., L. Beule, E. Lehtsaar, H.-L. Liao, and P. Karlovsky. 2020. Improved protocol for DNA extraction from subsoils using phosphate lysis buffer. *Microorganisms* **8**.
- Gundersen, P., A. Laurén, L. Finér, E. Ring, H. Koivusalo, M. Saetersdal, J.-O. Weslien, B. D. Sigurdsson, L. Högbom, J. Laine, and K. Hansen. 2010. Environmental services provided from riparian forests in the Nordic countries. *AMBIO* **39**:555–566.

- Han, X., C. Huang, S. Khan, Y. Zhang, Y. Chen, and J. Guo. 2020. nirS-type denitrifying bacterial communities in relation to soil physicochemical conditions and soil depths of two montane riparian meadows in North China. *Environmental Science and Pollution Research* **27**:28899–28911.
- Hill, A. R. 2019. Groundwater nitrate removal in riparian buffer zones: a review of research progress in the past 20 years. *Biogeochemistry* **143**:347–369.
- Jahangir, M., M. I. Khalil, P. Johnston, L. M. Cardenas, D. J. Hatch, M. Butler, M. Barrett, V. O’flaherty, and K. G. Richards. 2012. Denitrification potential in subsoils: A mechanism to reduce nitrate leaching to groundwater. *Agriculture, Ecosystems & Environment* **147**:13–23.
- JONES, D., and V. WILLETT. 2006. Experimental evaluation of methods to quantify dissolved organic nitrogen (DON) and dissolved organic carbon (DOC) in soil. *Soil Biology and Biochemistry* **38**:991–999.
- Kim, D.-G., M. U. Kirschbaum, and T. L. Beedy. 2016. Carbon sequestration and net emissions of CH₄ and N₂O under agroforestry: Synthesizing available data and suggestions for future studies. *Agriculture, Ecosystems & Environment* **226**:65–78.
- Kline, R. B. 2014. Convergence of Structural Equation Modeling and Multilevel Modeling. Pages 562–589 in W. P. Vogt and M. Williams, editors. *The SAGE handbook of innovation in social research methods*. SAGE Publications, Los Angeles.
- Lutz, S. R., N. Trauth, A. Musolff, B. M. van Breukelen, K. Knöller, and J. H. Fleckenstein. 2020. How important is denitrification in riparian zones? Combining end-member mixing and isotope modeling to quantify nitrate removal from riparian groundwater. *Water Resources Research* **56**.
- Ma, L., Z. Xiong, L. Yao, G. Liu, Q. Zhang, and W. Liu. 2020. Soil properties alter plant and microbial communities to modulate denitrification rates in subtropical riparian wetlands. *Land Degradation & Development* **31**:1792–1802.
- Matson, A. L., M. D. Corre, K. Langs, and E. Veldkamp. 2017. Soil trace gas fluxes along orthogonal precipitation and soil fertility gradients in tropical lowland forests of Panama. *Biogeosciences* **14**:3509–3524.
- McCarty, G. W., and J. M. Bremner. 1992. Availability of organic carbon for denitrification of nitrate in subsoils. *Biology and Fertility of Soils* **14**:219–222.
- McDowell, W. H., A. Zsolnay, J. A. Aitkenhead-Peterson, E. G. Gregorich, D. L. Jones, D. Jödemann, K. Kalbitz, B. Marschner, and D. Schwesig. 2006. A comparison of methods

- to determine the biodegradable dissolved organic carbon from different terrestrial sources. *Soil Biology and Biochemistry* **38**:1933–1942.
- R Core Team. 2019. R: A language and environment for statistical computing, Vienna, Austria: R Foundation for Statistical Computing. Retrieved from <https://www.r-project.org/>.
- Schmidt, M., M. D. Corre, B. Kim, J. Morley, L. Göbel, A. S. I. Sharma, S. Setriuc, and E. Veldkamp. 2021. Nutrient saturation of crop monocultures and agroforestry indicated by nutrient response efficiency. *Nutrient Cycling in Agroecosystems* **119**:69–82.
- Shcherbak, I., and G. P. Robertson. 2019. Nitrous oxide (N₂O) emissions from subsurface soils of agricultural ecosystems. *Ecosystems* **22**:1650–1663.
- Stark, C. H., and K. G. Richards. 2008. The continuing challenge of agricultural nitrogen loss to the environment in the context of global change and advancing research.
- van Groenigen, J. W., P. J. Georgiuis, C. van Kessel, E. W. Hummelink, G. L. Velthof, and K. B. Zwart. 2005. Subsoil ¹⁵N-N₂O Concentrations in a sandy soil profile after application of ¹⁵N-fertilizer. *Nutrient Cycling in Agroecosystems* **72**:13–25.
- Wen, Y., Z. Chen, M. Dannenmann, A. Carminati, G. Willibald, R. Kiese, B. Wolf, E. Veldkamp, K. Butterbach-Bahl, and M. D. Corre. 2016. Disentangling gross N₂O production and consumption in soil. *Scientific reports* **6**:36517.
- Wen, Y., M. D. Corre, W. Schrell, and E. Veldkamp. 2017. Gross N₂O emission and gross N₂O uptake in soils under temperate spruce and beech forests. *Soil Biology and Biochemistry* **112**:228–236.
- Yang, W. H., and W. L. Silver. 2016a. Gross nitrous oxide production drives net nitrous oxide fluxes across a salt marsh landscape. *Global change biology* **22**:2228–2237.
- Yang, W. H., and W. L. Silver. 2016b. Net soil–atmosphere fluxes mask patterns in gross production and consumption of nitrous oxide and methane in a managed ecosystem. *Biogeosciences* **13**:1705–1715.
- Yang, W. H., Y. A. Teh, and W. L. Silver. 2011. A test of a field-based ¹⁵N-nitrous oxide pool dilution technique to measure gross N₂O production in soil. *Global Change Biology* **17**:3577–3588.
- Zuur, A. F., E. N. Ieno, N. Walker, A. A. Saveliev, and G. M. Smith. 2009. Mixed effects models and extensions in ecology with R. Springer, New York.

3.8. Appendix

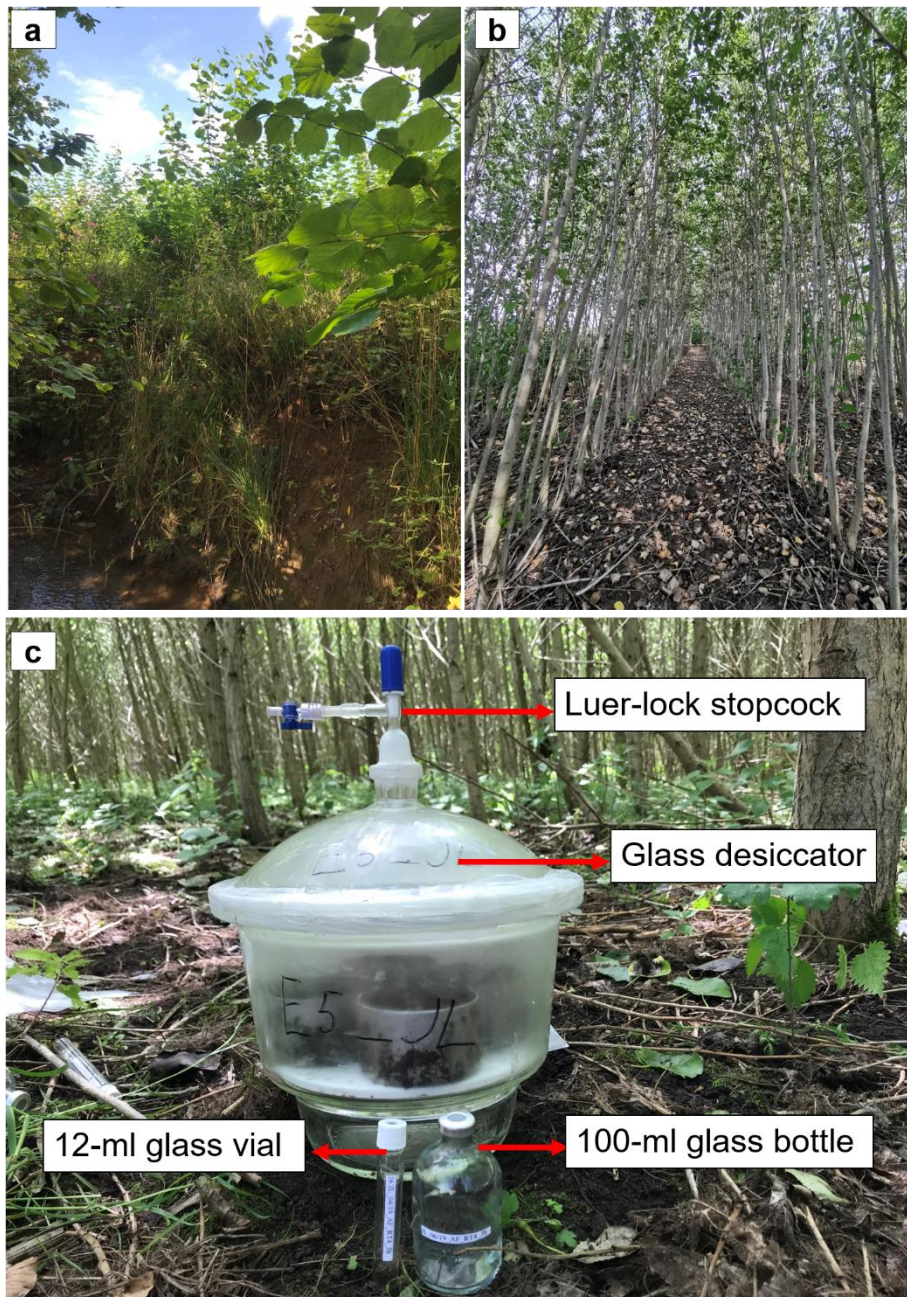


Figure S3.1. Riparian tree buffer (a) and tree row of alley cropping (b). Four intact soil cores (250 cm³ each) from the top 5 cm incubated in a glass desiccator (6.6 L), equipped with a Luer-lock stopcock on the lid; 100-ml glass bottle containing gas sample for ¹⁵N₂O analysis; and 12-ml glass vial (Exetainer; Labco Limited, Lampeter, UK) for N₂O, SF₆, and CO₂ concentration determinations

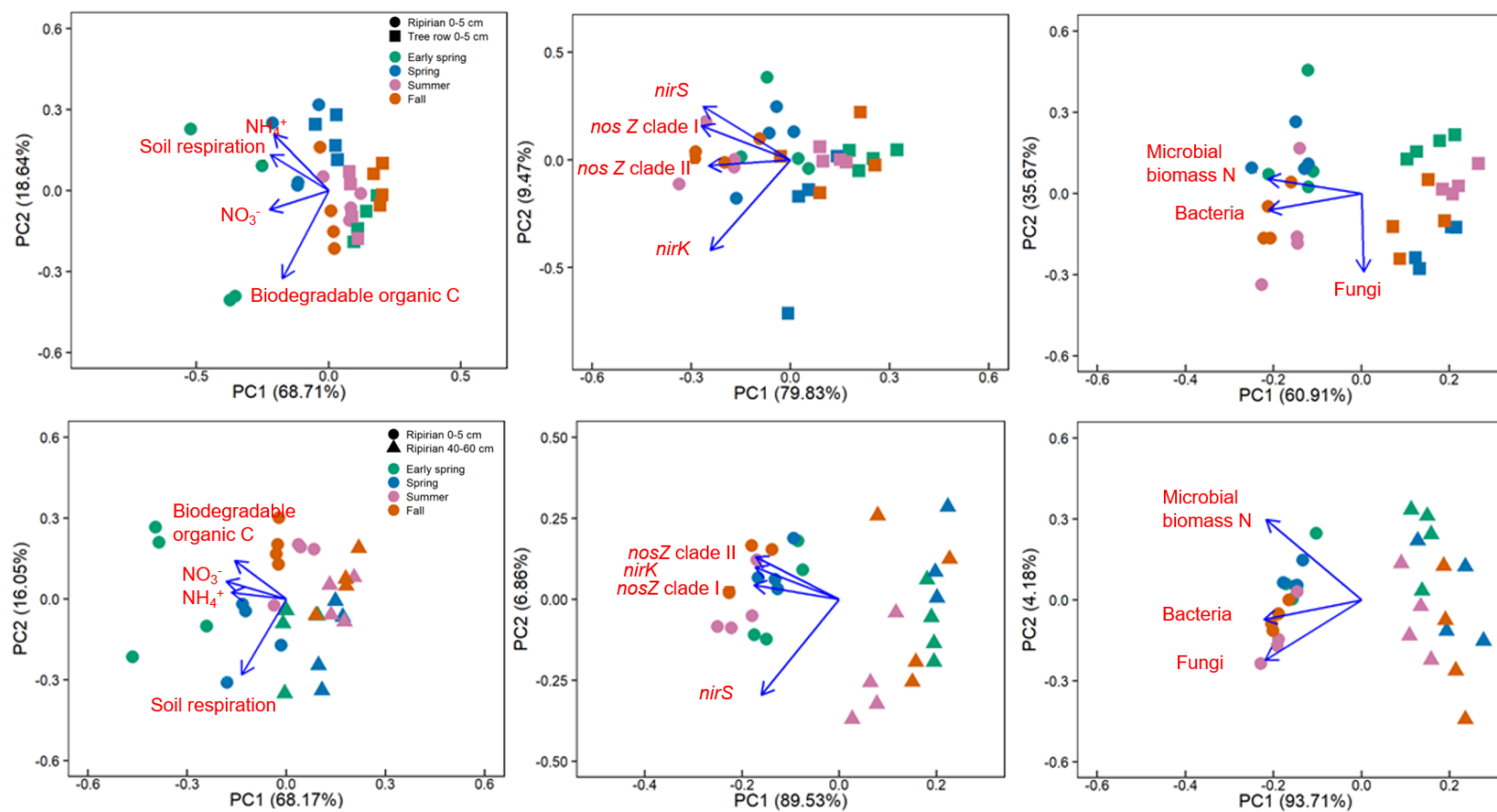
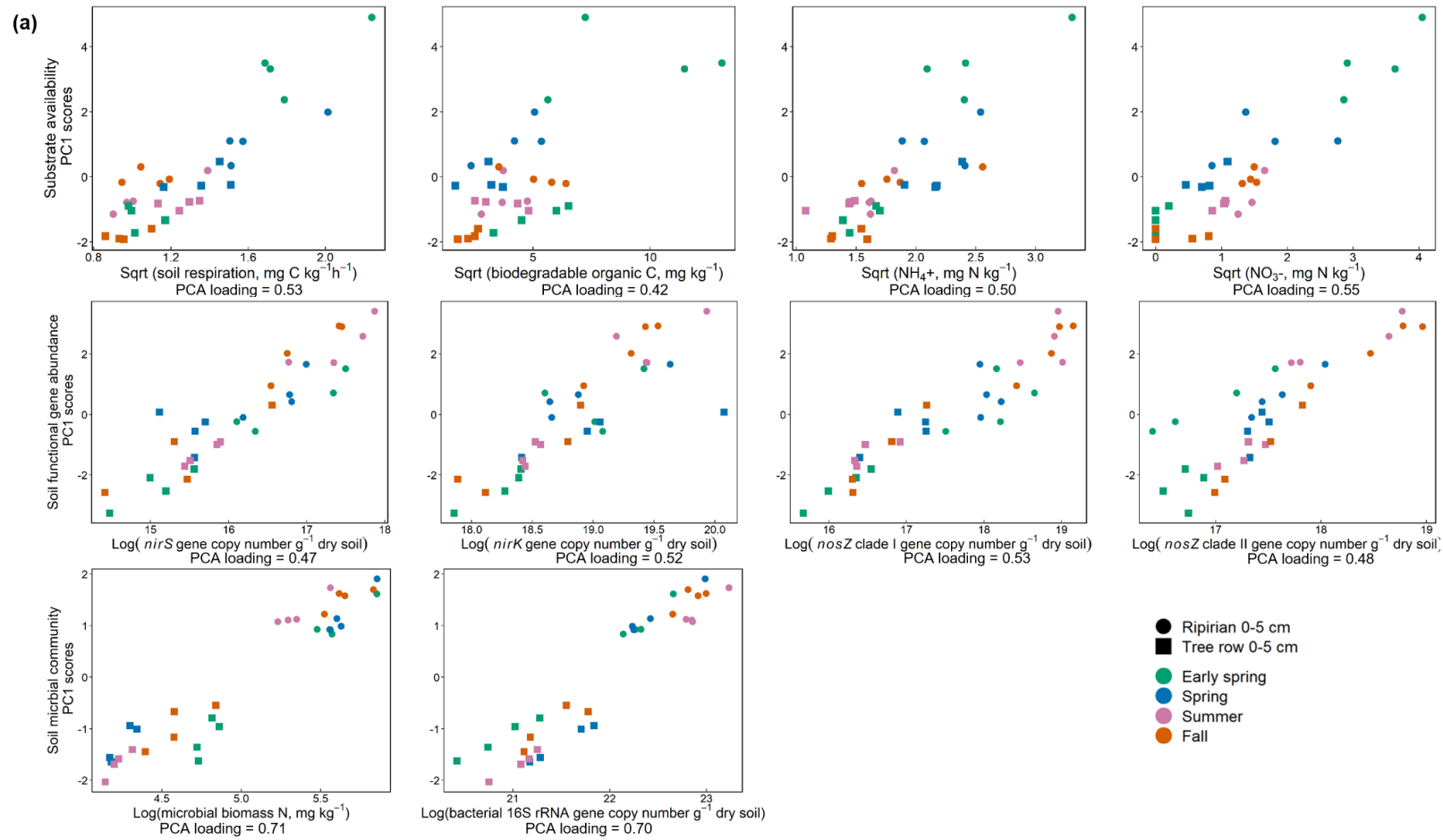


Figure S3.2. Principle component analysis (PCA) of the composited parameters for each of the grouping factors (i.e. substrate availability, functional gene abundance, and microbial community) that were used in the structural equation modeling separately for 0 – 5 cm across both agroforestry systems (top panel) and riparian tree buffer across both depths (0 – 5 and 40 – 60 cm; bottom panel).



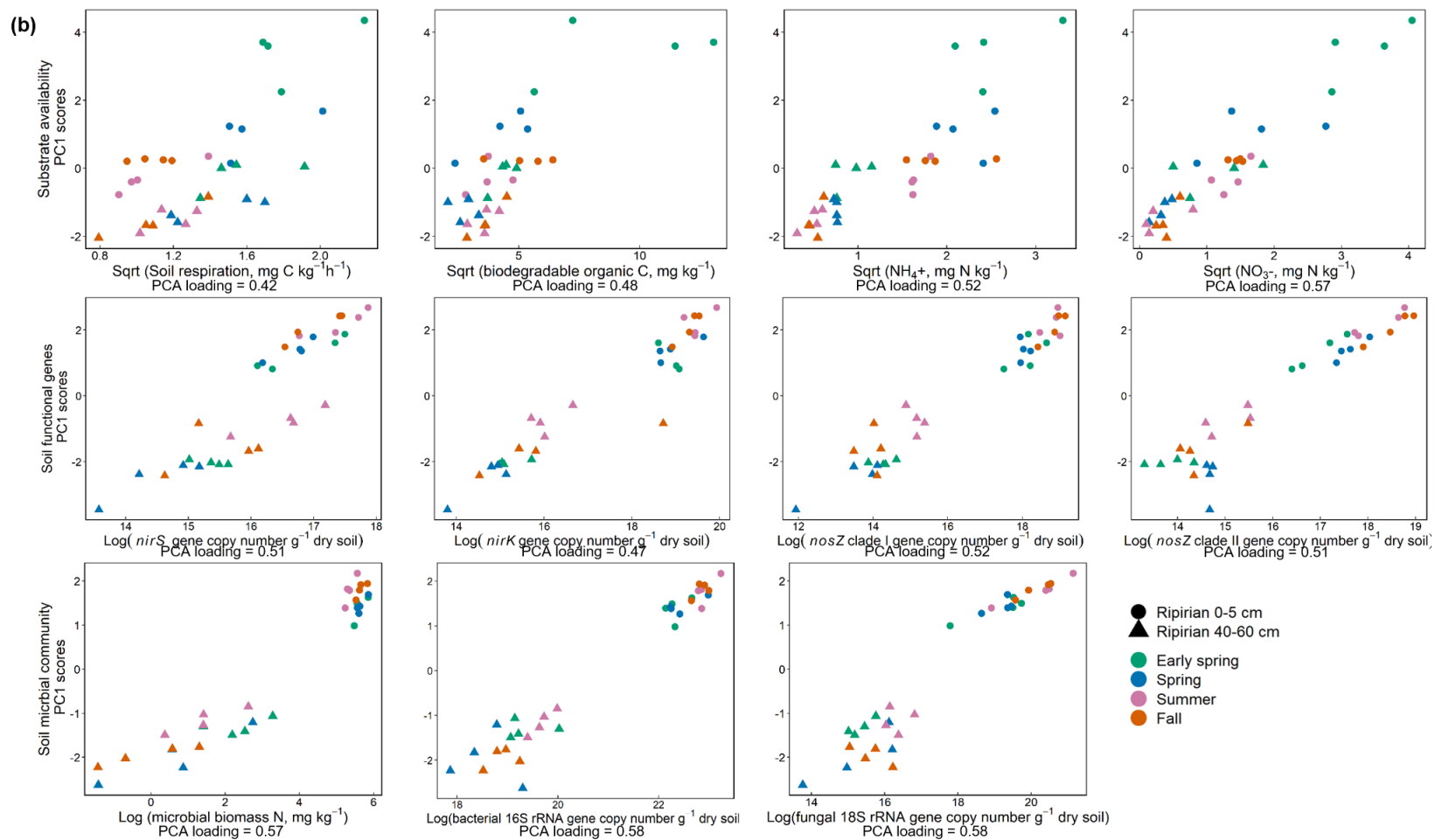


Figure S3.3. Relationships between the PC1 scores and values of each parameter (with PCA loading >0.40) for 0 – 5 cm depth across both agroforestry systems (a), and for the riparian tree buffer across both depths (0 – 5 and 40 – 60 cm; b).

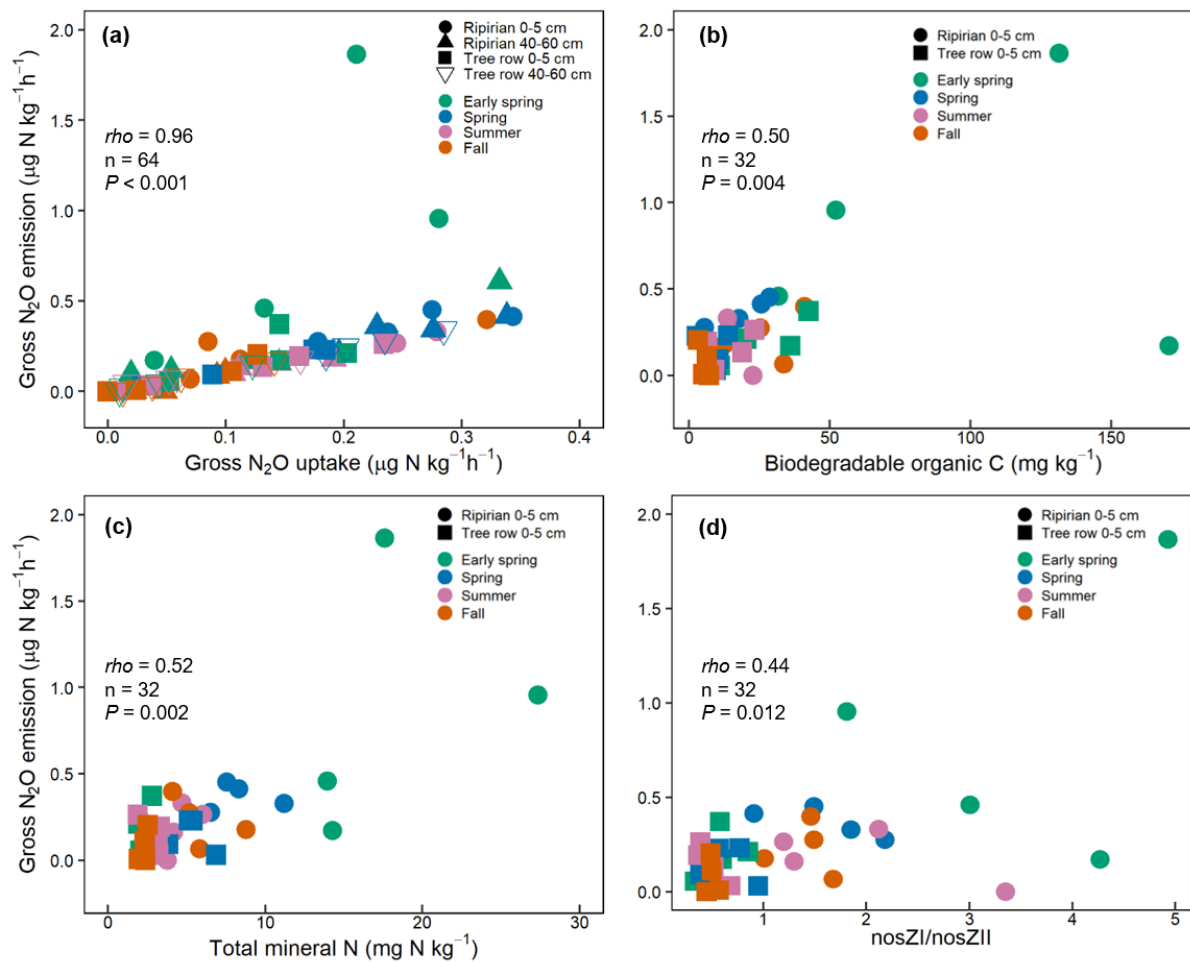


Figure S3.4. Spearman's rank correlation of gross N₂O emission with gross N₂O uptake across the two agroforestry systems, seasons and depths (a); Spearman's rank correlation of gross N₂O emission with biodegradable organic C (b), total mineral N (c) and the ratio of *nosZ* clade I (*nosZI*) to *nosZ* clade II (*nosZII*) (d) in 0 – 5 cm across the two agroforestry systems and seasons.

Chapter 4

Synthesis

4.1. Key findings of this thesis

4.1.1. Gross N₂O fluxes in temperate cropland agroforestry and monoculture

Regarding our hypothesis, we expected that cropland agroforestry would decrease gross N₂O emissions and increase gross N₂O uptake because of the existence of the unfertilized trees, and consequently achieving the goal of N₂O mitigation. However, we did not find a significant difference between cropland agroforestry and monoculture. Nonetheless, our study revealed that annual gross N₂O emissions in the top-5 cm soil decreased by 6% to 36% in the agroforestry (0.98–1.02 kg N₂O-N ha⁻¹ yr⁻¹) compared to monoculture (1.04–1.59 kg N₂O-N ha⁻¹ yr⁻¹) although tree rows only accounted for 20% in the agroforestry. The agroforestry tree row increased soil gross N₂O uptake in the top-5 cm soil by 27% to 42% (0.38–0.44 kg N₂O-N ha⁻¹ yr⁻¹) compared to monoculture (0.30–0.31 kg N₂O-N ha⁻¹ yr⁻¹). It was the first study to measure annual gross N₂O fluxes using the ¹⁵N₂O pool dilution (¹⁵N₂OPD) in agricultural soils. Thus, no comparison was conducted with other studies. The study filled in the knowledge gap of field rates of N₂O production and consumption in response to land-use/management change. Among the controlling factors of these two co-occurring processes (Chapter 2), mineral N availability was most important for regulating gross N₂O emissions and uptake. Combined with N saturation in soils at our agroforestry sites as shown by our previous work (Schmidt et al., 2021), reducing or optimizing fertilizer input and adjustments of areal coverages between tree and crop rows will augment the benefits of agroforestry in mitigating N₂O emissions. Thus, our study can be as part of the evidence in support of policy to include these ecological services in the economic valuation of agroforestry.

4.1.2. Gross N₂O fluxes in contrasting agroforestry systems

To the best of our knowledge, this study is the first to apply ¹⁵N₂OPD at different soil depths in contrasting agroforestry systems to directly quantify gross N₂O emissions and uptake in the field. Our results revealed significant differences in gross N₂O emissions and uptake

between the agroforestry systems in the topsoil (0 – 5 cm, $P \leq 0.03$) but not in the subsoil (40 – 60 cm, $P \geq 0.06$). Riparian tree buffer had higher gross N₂O fluxes in topsoil than the tree row of alley cropping due to higher substrate availability rather than microbial population size. The similar gross N₂O fluxes in subsoil between the two agroforestry systems were attributed to the very low and comparable mineral N availability. Although we found comparable gross N₂O fluxes between depths in each agroforestry system, a hot moment for gross N₂O emissions was observed in the topsoil of riparian tree buffer, i.e., a large N₂O source was detected in the early spring. Gross N₂O uptake in subsoil was affected by seasonal changes in soil temperature, indicating positive feedback of climate change on N₂O reduction to N₂ in subsoil. Our study highlights the importance of substrate availability in regulating gross N₂O fluxes and a greater capability of NO₃⁻-N reduction to N₂ due to N limitation in subsoil in the two agroforestry systems. This study also emphasizes the importance of the adoption of a relatively new technique (i.e. ¹⁵N₂OPD) to conduct field-based measurements since the complexity of ecosystems cannot be simulated under laboratory conditions.

4.2. Linking gross N₂O fluxes with functional gene abundance

According to results from Chapters 2 and 3, we did not find any relationships between gross N₂O emissions and denitrification gene abundance either across cropland agroforestry and monoculture or separately for each management system or across contrasting agroforestry systems at depths. These findings emphasize the importance of substrate availability and aeration status on regulating gross N₂O emissions and minimizing the role of denitrifier population size, which conflicts with the assumption that biogeochemical process rates, e.g. denitrification, can be predicted by the abundances of specific genes (Rocca et al., 2015). This suggests that denitrifier abundance may become a limiting factor for gross N₂O emissions when substrate levels and anaerobic conditions already prevail. However, both studies found that gross N₂O uptake was positively correlated with *nirK* gene abundance in the top-5 cm soil across the tree row of agroforestry systems or riparian tree buffer and tree row of alley cropping. This indicates a mineral N limitation under conditions of high available C and WFPS since denitrifiers could not gain enough energy from only NO₂⁻-to-N₂O reduction, and thus completed the final step of denitrification, N₂O-to-N₂ reduction. This reflects the interaction between substrates and denitrifier population size because such a relationship was not observed in crop row of agroforestry and monoculture where they received fertilizer inputs.

4.3. The relationships among gross N₂O emission, gross N₂O uptake, and net N₂O flux

In Chapter 2, we found that gross N₂O emissions were strongly correlated with net N₂O flux, especially in the crop row of agroforestry and monoculture ($R^2 \geq 0.97$) with high mineral N level ($\geq 13 \text{ mg N kg}^{-1}$), indicating that net N₂O emissions were mainly driven by gross N₂O emissions. In Chapter 3, although we did not find such a relationship in the riparian tree buffer and the tree row of alley cropping, gross N₂O emissions were highly correlated with gross N₂O uptake especially under the very low mineral N level ($< 5 \text{ mg N kg}^{-1}$) where net N₂O uptake was detected. This finding was in contrast with the studies from Yang et al. (2011; 2016b) who found a similar correlation in a managed grassland and cropland with high soil mineral N concentration but not in a salt marsh with low mineral N availability where net N₂O uptake occurred (Yang and Silver, 2016a). This is possible because the way we applied the ¹⁵N₂OPD technique was different from what Yang et al. did. Yang et al. applied the technique directly into a two-piece aluminum static flux chamber with a volume of 17 L while we took four intact 250-cm³ soil cores of the top 5-cm depth to incubate in a 6.6 L glass desiccator. Nonetheless, these findings highlight that mineral N levels could be an underlying controlling factor for regulating the relationships among gross N₂O emission, gross N₂O uptake, and net N₂O flux.

4.4. Net N₂O flux

Across the 1.5-year field measurement period, net N₂O flux measured by static chamber method from our previous study (Shao et al., unpublished data) was 1 to 3 times greater than those concurrently measured by the field soil core incubation (Table 4.1) in both management systems, indicating the contribution of N₂O emissions at lower depths. On the other hand, this finding supported the accuracy of the ¹⁵N₂OPD technique since we obtained reasonable net N₂O flux by using the field soil core incubation in agricultural soils. Net N₂O flux measured by soil core incubation was from top-5 cm soil while net N₂O flux measured by static chamber was from the whole soil profile. For example, tree rows of both agroforestry systems were sinks of N₂O using the field core incubation in top-5 cm soil whereas a source of N₂O using the static chamber method in the soil profile (Table 4.1). Because of this, we applied ¹⁵N₂OPD into two depths (i.e. 0 – 5 and 40 – 60 cm) in the tree row of agroforestry to investigate if subsoil contributed to more N₂O emissions during its upward diffusion. However, the results in Chapter 3 did not justify this assumption possibly because of missing

soil depths (e.g. 5 to 40 cm soil) and limited measurements that may not have captured the peak of N₂O emissions.

Table 4.1 Mean (\pm SE, $n = 4$ plots for the Phaeozem and Cambisol soils, $n = 8$ plots for the Arenosol soil) net N₂O fluxes, measured in the top 5-cm depth by field incubation of intact soil cores, and concurrent measurements on the soil surface by static chamber method from March 2018 to September 2019 at three sites of cropland agroforestry and cropland monocultures in Germany.

Soil type	Management system	Net N ₂ O flux from the top 5-cm cores (soil core incubation) ($\mu\text{g N m}^{-2} \text{h}^{-1}$)	Net N ₂ O flux from the soil surface (chamber method) ($\mu\text{g N m}^{-2} \text{h}^{-1}$)
Phaeozem (Dornburg)	Agroforestry		
	Tree row	-0.47 ± 1.08	1.58 ± 0.78
	1 m crop row	3.75 ± 0.85	6.14 ± 2.73
	7 m crop row	5.49 ± 3.14	12.10 ± 3.58
	24 m crop row	15.46 ± 5.41	33.40 ± 12.49
	Monoculture	9.45 ± 7.24	9.39 ± 5.19
Cambisol (Wendhausen)	Agroforestry		
	Tree row	-0.72 ± 0.68	0.51 ± 1.20
	1 m crop row	7.71 ± 5.08	11.99 ± 5.26
	7 m crop row	9.41 ± 5.12	13.13 ± 6.13
	24 m crop row	12.01 ± 6.28	14.60 ± 5.00
	Monoculture	13.71 ± 6.92	17.45 ± 8.85
Arenosol (Vechta)	Monoculture	5.45 ± 3.52	18.22 ± 8.75

Note. Soil net N₂O fluxes measured by static chamber method were from Shao et al. (unpublished data).

4.5. Outlook

Our research provides the first year-round quantification of gross N₂O emission and uptake using ¹⁵N₂O PD for cropland agroforestry and monoculture, with key implications for support

on GHG regulation function for policy implementation of agroforestry. Our results show for the first time that the combination of the $^{15}\text{N}_2\text{O}$ PD with modern molecular techniques can provide a new perspective on the mechanisms that control N_2O dynamics in temperate agricultural soils. Our findings emphasize the need for additional studies on gross N_2O emission and uptake to better quantify their magnitudes and mechanisms since the $^{15}\text{N}_2\text{O}$ PD technique is rarely applied in agroforestry systems. Regarding the process rates linking to microbial population size, efforts should not only focus on denitrifiers but also ammonia oxidizer bacteria since we cannot tell the source of N_2O from the $^{15}\text{N}_2\text{O}$ PD technique. We could not quantify the contribution of N_2O emissions in lower depths due to the missing depths and limited measurements. Thus, future studies should concentrate on long-term field studies that sample soil depth increments to better constrain the contribution of subsoils to ecosystem N loss. This thesis also emphasizes the importance of plant uptake on indirectly regulating gross N_2O emissions. Thus, future studies can investigate the effects of different plants (e.g., Legume vs. Non-legume) on gross N_2O fluxes, thereby fully understanding controls on N_2O dynamics from interactions among microbes, soils, and plants.

4.6. References

- Rocca, J.D., Hall, E.K., Lennon, J.T., Evans, S.E., Waldrop, M.P., Cotner, J.B., Nemergut, D.R., Graham, E.B., Wallenstein, M.D., 2015. Relationships between protein-encoding gene abundance and corresponding process are commonly assumed yet rarely observed. *The ISME Journal* 9, 1693–1699.
- Schmidt, M., Corre, M.D., Kim, B., Morley, J., Göbel, L., Sharma, A.S.I., Setriuc, S., Veldkamp, E., 2021. Nutrient saturation of crop monocultures and agroforestry indicated by nutrient response efficiency. *Nutrient Cycling in Agroecosystems* 119, 69–82.
- Yang, W.H., Silver, W.L., 2016a. Gross nitrous oxide production drives net nitrous oxide fluxes across a salt marsh landscape. *Global change biology* 22, 2228–2237.
- Yang, W.H., Silver, W.L., 2016b. Net soil–atmosphere fluxes mask patterns in gross production and consumption of nitrous oxide and methane in a managed ecosystem. *Biogeosciences* 13, 1705–1715.
- Yang, W.H., Teh, Y.A., Silver, W.L., 2011. A test of a field-based ^{15}N -nitrous oxide pool dilution technique to measure gross N_2O production in soil. *Global Change Biology* 17, 3577–3588.

Acknowledgment

What a great achievement of finishing my Ph.D. study in Germany! This is a milestone in my life. I am grateful to all people I met in Germany and I wouldn't have finished my study without them.

I would like to thank my Ph.D. supervisors, Dr. Marife Corre and Professor Edzo Veldkamp. Without your acceptance, I wouldn't come to Germany to study. Thanks for your patience when I was struggling with my English at the beginning, which gave me more courage and confidence to speak. Ed, thanks for your insightful advice and encouragement every time I gave a presentation and this made me feel more confident for myself and my work. Marife, your critical attitude towards science makes me impressive, and how I wish I could emulate your critical thinking. And you have been always my primary source of knowledge and expertise in science. Thanks for your critical comments on the manuscript and patience for several hours of explanation. Thanks for your role as a life tutor even though I did not agree with all of your opinions sometimes.

I sincerely appreciate the support from my thesis committee members: Professor Klaus Dittert and Dr. Guntars Martinson. Thank you for making time for my thesis committee meeting and those insightful and constructive comments and feedback.

I am so appreciative of the support from my friends and colleagues who helped me in the field and laboratory. A first special thank is given to Lukas Beule and Guodong Shao for their efficient cooperation in the fieldwork, which made me have a great time in the field for my first field experience. Many thanks to Julia Morley, Helena Römer, Selena Algermissen, Antje Sophie Makowski, and Vamsi for their field assistance. I would like to thank Dirk and Julian for their great help with soil depth sampling. Without you, I wouldn't have had such a wonderful field experience. Last but not least, my sincere thanks to our technicians: Andrea Bauer, Kerstin Langs, and Martina Knaust for all laboratory assistance.

I am indebted for the friendships from the PTS group. Special thanks to Dan, Guantao, and Guodong, for the hardship, joy, and fun we had, for their accompany to my life in Goettingen; and to Cecile, for the role as an oral English partner, for the discussions from our work to life, for our happiness and sadness, for our secrets and gossip in our office; and to Xenia, for the

translation of my work; and to Najeeb, for the assistance of my thesis; and to Oliver, Marcus, Leonie, Joost, Greta, Rodine, and Raphael, for their help from work and life.

I am especially grateful to all my Chinese friends. We had a great moment in Goettingen. We traveled together, laughed together, helped each other, shared our secrets, and imagined our future life. Thanks to all of you for making my Ph.D. life colorful, wonderful, and meaningful, which will be one of the best precious moments in my life.

I acknowledge China Scholarship Council for funding my life expense in Germany. Without this funding, I would not have had the opportunity to study abroad.

Lastly, I would like to thank all my family for their selfless support and love. Special thanks to my little brother for his company with my parents and this did not make my parents feel lonely. Hey bro, you will be the one to realize your dreams when I am back home with our parents. I would like to thank Mr. Peng for his encouragement and accompany when I felt down and frustrated. I believe that we will have a better life in the future.

DECLARATION OF ORIGINALITY AND CERTIFICATE OF AUTHORSHIP

I, Jie Luo, hereby declare that I am the sole author of this dissertation and that all references and data sources have been appropriately acknowledged. I furthermore declare that this work has not been submitted elsewhere in any form as part of another dissertation procedure. I certify that the manuscripts presented in chapters 2 and 3 have been written by myself as the first author.

Göttingen, February, 2022

(Jie Luo)